ISTANBUL TECHNICAL UNIVERSITY ★ GRADUATE SCHOOL OF SCIENCE ENGINEERING AND TECHNOLOGY

DESIGN OF VEHICULAR COMMUNICATION SYSTEMS EMPLOYING PHYSICAL LAYER NETWORK CODING OVER CASCADED FADING CHANNELS

Ph.D. THESIS

Serdar Özgür ATA

Electronics and Communication Engineering Department

Telecommunication Engineering Program

JANUARY 2017

ISTANBUL TECHNICAL UNIVERSITY ★ GRADUATE SCHOOL OF SCIENCE ENGINEERING AND TECHNOLOGY

DESIGN OF VEHICULAR COMMUNICATION SYSTEMS EMPLOYING PHYSICAL LAYER NETWORK CODING OVER CASCADED FADING CHANNELS

Ph.D. THESIS

Serdar Özgür ATA
(504102311)

Electronics and Communication Engineering Department

Telecommunication Engineering Program

Thesis Advisor: Prof. Dr. İbrahim ALTUNBAŞ

JANUARY 2017

İSTANBUL TEKNİK ÜNİVERSİTESİ ★ FEN BİLİMLERİ ENSTİTÜSÜ

KASKAD SÖNÜMLEMELİ KANALLARDA FİZİKSEL KATMAN AĞ KODLAMA YAPAN ARAÇLAR ARASI HABERLEŞME SİSTEMLERİNİN TASARIMI

DOKTORA TEZİ

Serdar Özgür ATA
(504102311)

Elektronik ve Haberleşme Mühendisliği Anabilim Dalı

Telekomünikasyon Mühendisliği Programı

Tez Danışmanı: Prof. Dr. İbrahim ALTUNBAŞ

OCAK 2017

Serdar Özgür ATA, a Ph.D. student of ITU Graduate School of Science Engineering and Technology 504102311 successfully defended the thesis entitled "DESIGN OF VEHICULAR COMMUNICATION SYSTEMS EMPLOYING PHYSICAL LAYER NETWORK CODING OVER CASCADED FADING CHANNELS", which he prepared after fulfilling the requirements specified in the associated legislations, before the jury whose signatures are below.

Thesis Advisor :	**Prof. Dr. İbrahim ALTUNBAŞ** Istanbul Technical University	.....
Jury Members :	**Prof. Dr. H. Ümit AYGÖLÜ** Istanbul Technical University	.....
	Prof. Dr. Oğuz KUCUR Gebze Technical University	.....
	Prof. Dr. M. Ertuğrul ÇELEBİ Istanbul Technical University	.....
	Prof. Dr. Erdal PANAYIRCI Kadir Has University	.....

Date of Submission : **24 November 2016**
Date of Defense : **17 January 2017**

To my beloved daughter,

FOREWORD

A decade off to studentship, the stressful professional career, three surgical operations due to three accidents and the responsibilities of being a little girl's father... Despite a rather tiring period, now I am happy to have come to the end of the doctorate studies with this thesis because of my desire and my motivation from the first day to the last day, which I never lost. I would like to express my gratitude to everyone who somehow stood by me within that period. I thank to my dear thesis supervisor Prof.Dr. İbrahim ALTUNBAŞ because of his support and instructing speeches during my studies. I also thank to dear Prof.Dr. Ümit AYGÖLÜ and Prof.Dr. Oğuz KUCUR having taken part in the thesis monitoring committee for their valuable feedback and contributions.

My daughter Ayşe İpek, who was born just at the beginning of my Ph.D. studentship, is nearly 6 years old. The moments during which I refused her wishes for playing with her father - a little child's most natural right - saying that I had to study and disappointed her were the most oppressive moments that put me in an awkward position during the time left behind. I would like to express my gratitude to my beloved daughter once more, who helped me with the mature sympathy she had beyond her years during such difficult moments, and I have been experiencing the endless happiness and pride of being her father. I hope this doctorate study will also be a good model for her within the years of her education.

November 2016 Serdar Özgür ATA

TABLE OF CONTENTS

Page

ABBREVIATIONS

AF	**:** Amplify and Forward
ANC	**:** Analog Network Coding
AWGN	**:** Additive White Gaussian Noise
BER	**:** Bit Error Rate
BPSK	**:** Binary Phase Shift Keying
CDF	**:** Cumulative Distribution Function
CF	**:** Compress and Forward
CSI	**:** Channel State Information
DF	**:** Decode and Forward
EGC	**:** Equal Gain Combining
EM	**:** Electro Magnetic
i.i.d.	**:** independent and identically distributed
i.n.i.d.	**:** independent but not identically distributed
LOS	**:** Line of Sight
M2M	**:** Mobile-to-Mobile
MGD	**:** Mixture Gamma Distribution
MGF	**:** Moment Generating Function
MIMO	**:** Multiple Input Multiple Output
MPSK	**:** M-ary Phase Shift Keying
MRC	**:** Maximum Ratio Combining
pdf	**:** Probability Density Function
PEP	**:** Pairwise Error Probability
PLNC	**:** Physical Layer Network Coding
PSK	**:** Phase Shift Keying
QAM	**:** Quadrature Amplitute Modulation
QPSK	**:** Quadrature Phase Shift Keying
SC	**:** Selection Combining
SER	**:** Symbol Error Rate
SNR	**:** Signal to Noise Ratio
SINR	**:** Signal Interference to Noise Ratio
STBC	**:** Space-Time Block Codes
STTC	**:** Space-Time Trellis Codes
TWRN	**:** Two-Way Relay Networks
V2X	**:** Vehicle-to-Things
V2I	**:** Vehicle-to-Infrastructure
V2V	**:** Vehicle-to-Vehicle

SYMBOLS

$f_X()$	: Probability density function
$F_X()$	: Cumulative distribution function
$M_X()$	: Moment generating function
$E[.]$	: Expectation value operator
σ^2	: Variance
$Q(.)$	: Gauss function
α_i	: i-th Gamma distribution's parameter
β_i	: i-th Gamma distribution's parameter
ζ_i	: i-th Gamma distribution's parameter
$\gamma(.,.)$	: Incomplete Gamma function
m	: Nakagami distribution's parameter
h	: Channel gain, fading coefficient
x	: Modulated signal
n	: Noise signal
G	: Power scaling factor
Ω	: Average power
N	: Cascading degree
E_s	: Symbol energy
N_0	: Noise power
P	: Signal power
γ	: Instantaneous signal to noise ratio
γ_0	: Average signal to noise ratio
γ_{e2e}	: End to end signal to noise ratio
$\Gamma(.)$	: Gamma function
$G_{\cdot,\cdot}^{\cdot,\cdot}[.\|_{\cdot,\cdot}^{\cdot,\cdot}]$	: Meijer's G function
K_v	: v-th order, second type modified Bessel function
P_e	: Error probability
P_{out}	: Service outage probability
P_b	: Bit error rate
P_s	: Symbol error rate
T_i	: i-th time slot
d_o	: Asymptotic diversity order
$\mathbf{X}$	: Transmitted symbol sequence
$\hat{\mathbf{X}}$	: Erroneous decoded symbol sequence
$P\left(\mathbf{X}, \hat{\mathbf{X}}\right)$	: Pairwise error probability
λ_i	: i-th eigenvalue of a matrix
$Tr(.)$	: Trace operator

LIST OF TABLES

Page

LIST OF FIGURES

Page

DESIGN OF VEHICULAR COMMUNICATION SYSTEMS EMPLOYING PHYSICAL LAYER NETWORK CODING OVER CASCADED FADING CHANNELS

SUMMARY

As a current state-of-the-art in wireless communications, Vehicle-to-Vehicle (V2V) communications is the core technology to build the intelligent transportation infrastructures promising the solutions to the issues such as traffic efficiency increasing, accident reduction and safety improvements. In comparison with the cellular wireless communication, there are some new challenges within the V2V communication. The statistical properties of the V2V communication channels differ from those of the cellular channels. Thereby, well known cellular channel models such as Rayleigh, Rician and Nakagami-*m* are not appropriate to simulate the fading in V2V communication channels. Field measurements reveal that V2V communication channels can be modeled by a class of channel models where the gain is obtained by multiplying the gains of virtual channels produced by each individual scattering group around that behaves as an independent signal source. Due to their multiplicativity nature, V2V communication channels are named as cascaded fading channels.

A major challenge in V2V communications is that the physical environment is unsettled due to the mobility of the wireless units and other vehicles around these units. Additionally, the vehicle antennas have relatively lower heights. Therefore, especially considering the traffic in urban areas, most of the time there will be no line-of-sight between the communicating vehicles. This makes cooperative communications inevitable for seamless and reliable communication among the moving vehicles. And yet, compared to non-cooperative communication, the cooperation protocols require more time slots, which results in a decrease in data transmission rate. A method to cope with this drawback is physical layer network coding (PLNC) providing the simultaneous data transmissions of the vehicles via the same relay. The PLNC method will play an important role in the design of the high performance V2V communication systems serving in the heavy traffic conditions when a large number of users need to be notified about suddenly changing situations.

Studies presented in this thesis can be divided into three categories. In the first category, a cooperative V2V communication system employing PLNC using fixed gain amplify-and-forward technique is proposed and its outage and error performance analysis is investigated. Analytic results are derived under the cascaded Nakagami-*m* fading channel model assumption covering double Rayleigh, cascaded Rayleigh, double Nakagami-*m*, generalized-K and conventional cellular channel models as well. Therefore, the results obtained by this work are also valid for all these channel models. In the error performance investigation of the proposed system, first, exact cumulative density function of the end to end signal to noise ratio is derived. Then, using this cumulative density function, the exact closed-form outage probability is obtained. Then the exact closed-form symbol error rate expression for various modulation types is derived. As a continuation of this work, the performance analysis of the same

system is investigated for not only cascaded but also fast fading Rayleigh channels in the presence of the self-interference. Thus the exact closed-form outage probability expression is obtained, and it is shown that the self-interference may cause the error floor in the performance of the network coded communication systems.

In the second category, a multiple input multiple output (MIMO) V2V communication system is proposed. In this proposed system, all source and relay vehicles have multiple antennas while the relays employ the PLNC method using variable gain amplify-and-forward technique. The analytic results are derived for the cascaded Nakagami-*m* fading channels, and therefore the result of this work are held for the cascaded and non-cascaded channels, as mentioned above. Furthermore, the performance of the system is evaluated in terms of joint outage probability of the sources, and the exact outage probability expression is obtained in a single integral form while the upper and the lower bounds of the outage probability are obtained in the closed-form. Moreover, asymptotic diversity order is quantified as a function of the number of the relays, the number of the antennas at the sources and the relays, and the channel parameters which are cascading degree and fading parameter values. Within this system, it is shown that the service outage probability performance can be enhanced by employing joint antenna and relay selection.

In the third category, PLNC and space-time trellis coding (STTC) techniques are combined to improve the error performance of a multi-antenna multi-relay V2V system. The upper bound expression of the pairwise error probability of the system is evaluated for double Rayleigh fading channels. Then using the upper bound expression, a novel code-design criterion is derived for cascaded fading channels. Then, by using this new criterion, a novel STTCs with 4 and 8 states are proposed for MIMO V2V PLNC systems.

KASKAD SÖNÜMLEMELİ KANALLARDA FİZİKSEL KATMAN AĞ KODLAMA YAPAN ARAÇLAR ARASI HABERLEŞME SİSTEMLERİNİN TASARIMI

ÖZET

İnsandan insana ses taşıma odaklı ikinci nesil (2nd Generation, 2G) mobil haberleşme teknolojilerinin kaydettiği başarıdan sonra telsiz iletişim alanındaki eğilimler insandan-makinaya olarak adlandırılan veri taşıma odaklı telsiz iletişim teknolojilerine (3rd Generation, 3G) doğru yönelmiştir. Bu veri taşıma odaklı iletişim konsepti ile birlikte son kullanıcılar multi-media mesajlaşma, internet erişimi, e-ticaret ve video paylaşımı gibi çok çeşitli telsiz iletişim servislerine kavuşma imkanı buldular. Telsiz iletişimdeki başarılı ve hızlı ilerlemenin bir sonucu olarak günümüzde bu alanda yapılan araştırma-geliştirme çalışmalarının yönü yüksek veri iletim hızları (>100Mb/s) ve daha yüksek bant-verimliliği (>10b/s) gerektiren makineden-makineye (Mactine-to-Machine, M2M) telsiz iletişime doğru yönelmiş bulunmaktadır. M2M telsiz iletişiminde bir araştırma/uygulama alanı araçtan-nesnelere (Vehicle-to-things, V2X) haberleşmedir. Araçtan araca (Vehicle-to-Vehicle, V2V) ve araçtan yol kenarındaki baz istasyonuna (Vehicle-to-Infrastructure, V2I) olmak üzere iki haberleşme sistemini birlikte içeren V2X haberleşme sistemleri günümüzde özellikle büyük metropollerde günlük hayatı pek çok yönden olumsuz etkileyen trafik kaynaklı problemlere karşı getirdiği çözüm önerileri nedeniyle üniversitlerde teorik çalışmalar yapan araştırmacıların yanı sıra, resmi kurumların, standartları belirleyen organizasyonların ve özellille otomotiv ve bilişim endüstrisindeki şirketlerin gittikçe artan dikkatini çekmeyi başarmıştır. Araçlar arası haberleşme teknolojilerinin gelişimine ivme kazandıran önemli gelişmelere bakılacak olursa; 1999 yılında ABD'de Federal Communication Comission (FCC) 5.9GHz frekans bandında 75MHz'lik bir frekans bandının V2X haberleşme için kullanımını onaylamıştır. 2008 yılında ise Avrupa haberleşme standardları enstitüsü (European Telecommunication Standards Institute) yine 5.9GHz frekans bandında 30Mhz'lik bir bandın bu amaçla kullanılmasını önermiştir. FCC'nin 2003 yılında ITS (Intelligent Transportation Systems) uygulamalarında kullanılacak haberleşme birimleri için yayımladığı rapor ve talebin ardından DSRC (Dedicated Short Range Communication) olarak adlandırılan V2X haberleşme sistemlerinin standardizasyonu için çalışmalar başlamış ve 2004 yılında IEEE 802.11standardı temel alınarak geliştirilen IEEE 802.11p standardı WAVE (Wireless Access in Vehicular Environments) olarak da bilinen adıyla 2010 yılında kabul edilmiştir. Bugün artık pek çok üniversitede çeşitli araştırma grupları V2X haberleşme üzerine akademik çalışmalar yürütürken endüstriyel seviyede ise Avrupa'da örneğin büyük ölçekli Avrupa Birliği projeleri olarak CAR2CAR Communication Corsortium, Secure Vehicular Communication ve NEARCTIS yürütülmektedir. Amerika'da ise ulaştırma bakanlığının desteklediği IntelliDrive projesi ile güvenlik, mobil iletişim ve çevre koruma amaçlı hedefler doğrultusunda trafik altyapısı, araçlar ve yolcuların mobil haberleşme cihazları arasında haberleşmeyi sağlayacak bir telsiz iletişim ağı alt yapısı kurma çalışmaları sürdürülmektedir. Benzer

çalışmalar Japon Otomobil Teknolojileri Araştırma Enstitüsü JARI tarafından da yapılmaktadır. Yine V2V haberleşmenin trafik güvenliğini arttırmadaki öneminin anlaşılmasından sonra lider otomobil üreticisi firmalar "Crash Avoidance Metrics Partnership" adını verdikleri proje için ortak çatı altında biraraya gelmişlerdir. Kısaca belirtilmek istenirse, telsiz iletişim alanında V2X haberleşme yeni ama oldukça önemli bir çalışma alanı olarak görülmektedir.

Günümüz telsiz haberleşme teknolojilerinden biri olan araçtan araca haberleşme, trafik verimliliğini arttırma, kazaların azaltılması ve trafikte güvenli sürüş konulara çözümler sağlayacak akıllı taşıma sistemlerinin gerçeklenmesinde çekirdek teknoloji konumundadır. Hücresel haberleşme ile karşılaştırıldığında, V2V haberleşme bazı yeni zorlukları içerir. V2V haberleşme kanallarının istatistiksel özellikleri hücresel telsiz haberleşme kanallarının istatistiksel özelliklerinden farklıdır. Bu nedenle, Rayleigh, Rician ve Nakagami-*m* gibi iyi bilinen hücresel haberleşme kanal modelleri V2V haberleşme kanallarındaki sönümlemeyi modellemek için uygun değildir. Yapılan saha ölçümlerinden görüldüğü üzere, V2V haberleşme kanallarında kanal kazancı, hareketli kaynaklar etrafında, her biri ayrı bir işaret kaynağı gibi davranan birbirinden bağımsız saçıcı gupların oluşturduğu sanal kanalların kanal kazançlarının çarpımından meydana gelmektedir. Kanal kazancının bu çarpımsallık niteliğinden dolayı V2V haberleşme kanalları kaskad sönümlemeli kanal modeli olarak adlandırılan bir grup kanal modeli ile modellenmelidirler.

V2V haberleşmede karşılaşılan zorlukların bir nedeni, gerek haberleşen araçların gerekse onların etrafındaki diğer araçların yüksek hızlardaki hareketliliği nedeniyle haberleşme ortamının çevresel olarak çok hızlı değişmesidir. Bunun yanısıra araç antenlerinin görece düşük yükseklikte olmasının da etkisiyle, özellikle yerleşim birimleri içindeki yoğun trafik şartları düşünüldüğünde, haberleşen araçlar arasında çoğu zaman doğrudan görüş olmayacaktır. Bu da iletişimin sürekliliği ve güvenilirliği açısından işbirlikli haberleşmeyi kaçınılmaz kılmaktadır. Ancak doğrudan haberleşmeye nazaran daha fazla zaman dilimi gereksinimi işbirlikli sistemlerin temel dezavantajıdır. Veri iletim hızında kayba neden olan bu dezavantajı yok etmenin bir yolu, iki haberleşme biriminin aynı zaman aralığında aynı röle üzerinden veri aktarmasına imkan tanıyan fiziksel katman ağ kodlama (Physical Layer Network Coding, PLNC) tekniğidir. Ani gelişen durumların çok sayıda kullanıcıya kısa sürede bildirilmesini gerektirecek trafik içi haberleşmede PLNC tekniği yüksek başarımlı V2V haberleşme sistemlerinin tasarımında önemli bir rol oynayacaktır.

Bu tezde sunulan çalışmalar üç grupta ele alınabilir. Birinci gruptaki ilk çalışmada tek antenli tek röleli ve röle üzerinde sabit kazançlı kuvvetlendir-ve-aktar tekniği kullanılarak PLNC yapılan bir işbirlikli V2V haberleşme sistemi tasarlanmıştır. Sistemin performans analizleri kaskad Nakagami-*m* kanal modeli varsayımı altında yapılmış olup bu kanal modeli, araçlar arası haberleşmeye uygun olan çift Rayleigh, kaskad Rayleigh, çift Nakagami-*m* ve genelleştirilmiş-K kanal modellerinin yanı sıra geleneksel hücresel haberleşme kanal modellerini de kapsamaktadır. Dolayısıyla bu çalışmada elde edilen sonuçlar bu kanal modelleri için de geçerlidir. Sistemin hata performans analizleri yapılırken öncelikle uçtan-uca işaret gürültü oranına ait birikimsel olasılık dağılım fonksiyonu kapalı formda elde edilmiş, ardından bu dağılım fonksiyonu kullanılarak sistemin servis kesinti olasılığı ve çeşitli modülasyon tipleri için sembol hata olasılığı ifadeleri kapalı formda bulunmuştur. Bu analizlerin bir devamı olarak, birinci grupta yapılan ikinci çalışmada ise, kaynaklarda öz-girişim

işaretinin tam olarak yok edilemediği durumlar için yine tek antenli tek röleli rölede sabit kazançlı kuvvetlendir-ve-aktar tekniği kullanılarak PLNC yapılan sistemin performans analizi kaskad ve hızlı sönümlemeli Rayleigh kanal varsayımı altında yapılmış ve sisteme ait servis kesinti olasılığı ifadesi kapalı formda elde edilerek öz girişimin sistem performansına etkileri incelenmiştir.

Tezde yer alan ikinci grup çalışmada, çok girişli çok çıkışlı (multiple input multiple output, MIMO) bir V2V haberleşme sistemi tasarlanmıştır. Sistemde birden çok röle olup kaynaklar ve tüm röleler çok antenlidir. Ayrıca röleler değişken kazançlı kuvvetlendir-ve-aktar tekniği uygulayarak PLNC yapmaktadır. Bu çalışmada da kaskad Nakagami-*m* kanal modeli kullanıldığından elde edilen sonuçlar yukarıda bahsedilen diğer kaskad veya kaskad olmayan kanal modelleri için de geçerlidir. Burada yapılan analizler ile tüm sistemin servis kesinti performansı kaynakların ortak servis kesinti olasılıkları cinsinden ifade edilerek bu olasılık tek katlı integral formunda bulunmuştur. Ardından servis kesinti olasılığı için alt ve üst sınır ifadeleri kapalı formda elde edilmiştir. Bulunan sınır ifadeleri aracılığıyla sistemde elde edilebilecek çeşitleme derecesi, röle sayısı, kaynak ve rölelerde kullanılan anten sayıları ve kanalların kaskadlık dereceleri ve sönümleme parametrelerinin aldığı değerlere bağlı olarak sistem parametreleri cinsinden ifade edilmiştir. Tasarlanan bu sistem ile ortak anten ve röle seçimi yapılarak V2V haberleşme sistemlerinin performansının daha da iyileştirilebileceği gösterilmiştir.

Tezde yapılan üçüncü çalışmada PLNC yapılan bir çok antenli çok röleli V2V haberleşme sisteminde uzay-zaman kafes kodlama tekniği kullanılarak sistem performansının daha da iyileştirilmesi sağlanmıştır. Bu amaçla öncelikle sistemin çiftsel hata olasılığı için bir üst sınır ifadesi çift Rayleigh sönümlemeli kanal varsayımı için elde edilmiştir. Daha sonra bu olasılığı en küçük yapacak kodların inşaası için yeni bir kod tasarım ölçütü türetilmiş ve bu ölçüt kullanılarak çift Rayleigh sönümlemeli kanallarda PLNC tekniği kullanan MIMO V2V haberleşme sistemler için 4 ve 8 durumlu yeni uzay-zaman kafes kodları bulunmuştur.

1. INTRODUCTION

After the successful employment of 2G technologies providing human-to-human mobile communications based on voice transmission, the focus of the studies in wireless communications tended to data-centric machine-to-man type mobile communication technologies. This new concept resulted in the successor generation of the cellular standards called 3G. 3G technologies have enabled many communication services such as multi-media messaging, world wide web, e-commerce, video sharing, etc. As a consequence of innovative and ground breaking progresses in mobile communications, research and development efforts in this field have been directed to machine-to-machine/mobile-to-mobile (M2M) wireless communication technologies, which require higher data transmission rate and higher bandwidth efficiency. One of the research topics in M2M wireless communications is vehicle-to-things (V2X) communications including both vehicle-to-vehicle (V2V) and vehicle-to-infrastructure (V2I) communications. Since V2X communications offer many benefits such as the management of the traffic density, reducing accidents, accessing to accident scenes in shorter times, driver-friendly services like convoy-driving and self-driving, etc., it attracts the increasing attention of the researchers, standardization institutions, industrial companies and government bodies. Accordingly, the Federal Communications Commission (FCC) of the U.S. approved the use of a bandwidth of 75 MHz at 5.9 GHz band for V2X communications [1]. Then, the European Telecommunications Standards Institute (ETSI) allowed the usage of a bandwidth of 30 MHz at 5.9 GHz band for inter-vehicle communications [2]. Having revealed the requirements for equipments in the intelligent transportation systems by the FCC in 2003, standardization studies of the V2X systems have been started in 2004 under the name of Dedicated Short Range Communication [3]. Then, in 2010, IEEE 802.11p standard has been released as an approved amendment to the IEEE 802.11 standard to add wireless access in vehicular environments (WAVE), which is a vehicular communication system. Today, a lot of research groups in academic area work on vehicular communications topics. Moreover, large-scale EU

projects have been carried out by the industry, such as CAR2CAR Communication Consortium, Secure Vehicular Communication (SeVeCom), and NEARCTIS. In the U.S., a wireless communication network infrastructure has been designed for communications among the traffic infrastructure, vehicles and mobile user equipments, and the IntelliDrive project has been supported by the Department of Transportation for security, mobile communications and environmental protection issues. Similar studies have been continued by the Japan Automotive Research Institute. As a promising technology, V2X communications also become an area of interest for the automotive industry, therefore, leading automotive manufacturers all over the world have started a collaboration under the name of "Crash Avoidance Metrics Partnership". Consequently, the design of the robust and reliable V2X communication systems will be at the center in building the intelligent transportation infrastructures of the smart cities in the near future. This makes the V2X communications an attractive area for researchers in universities and engineers in industry.

It has been observed that the fading effect in the V2V communication channels is worse than those in the cellular communication channels [4–12]. Therefore, well-known channel models, i.e. Rayleigh, Rician and Nakagami-m, are insufficient in case of vehicular communications. It is shown that each independent scattering group surrounding the mobile units acts as an individual signal source and produces an independent channel gain [13–15]. Therefore, the overall fading gain in V2V communication channels is obtained by multiplying these virtual channels' gains. Due to the multiplicative property of the channel gain, inter-vehicle channels are modeled by a new class of the channel models which are called cascaded fading channel models in general [15–27] .

Since communicating units in the V2X wireless communication systems are mobile, the transmission medium is unsettled. Especially considering the traffic in urban areas, most of the time there will be no line-of-sight (LOS) between the communicating units. This makes cooperative communications inevitable for seamless and reliable communications [28, 29]. In cooperative communication, the intermediate units called relays are used to support reliable and robust communication channels for the terminal units. Moreover, in case of multi-hop communication, which is the simplest form of cooperative communications, the coverage area may be expanded significantly by

making use of the relay chains. However cooperative systems require more time slots compared to peer-to-peer communications. This is the main disadvantage of the cooperative systems leading a degradation in the data transmission rate. In order to tackle this problem, a technique called network coding is proposed [30–32]. The conventional network coding is implemented by performing XOR operation on data bits of the different users. After that, a new type of cooperation method called physical layer network coding (PLNC) [33, 34] has been proposed by applying the network coding idea at the electrical signal domain on relays by exploiting the additivity property of the electromagnetic (EM) waves. PLNC reduces the required number of the time slots in cooperative communications by allowing multiple users to transmit their signals through the same relay simultaneously. It is obvious that PLNC can play an important role to improve the performance of the cooperative V2V communication systems when a large number of users need to be notified about suddenly changing situations in the traffic.

1.1 Purpose of the Thesis

In the wireless communications literature, there are few studies on the cooperative communications over cascaded fading channel models while the literature on physical layer network coded V2X communications are at their infancy even for single antenna systems. The aim of this thesis is to design cooperative V2V communication systems enabling high data transmission rates by making use of PLNC while cascaded fading channel models will be used in conformity with the vehicular communication channels. Then, error performance analysis associated with these systems will be investigated. After that, V2V systems employing PLNC at the multi-antenna relay will be designed to obtain higher error performance by using antenna selection techniques. Furthermore, it is targeted to enhance the system performance by making use of multi-relay/multi-antenna PLNC methods with joint relay and antenna selection techniques. Thus, performance superiority will be provided as compared to the single-relay/single-antenna systems. Aftermost, space-time coded PLNC techniques over cascaded fading channels will be studied to improve the error performance of the V2V communication systems.

1.2 Literature Review

As a current state-of-the-art in wireless communications, V2V communications is expected to be a key technology to build intelligent transportation infrastructures, due to promising increased traffic efficiency, accident reduction and safety improvements. Therefore, the V2V communications attract the increasing notice of researchers in several engineering disciplines. From a communication engineering's point of view, there are several new challenges within the V2V communications in comparison with the cellular wireless communications because of the reasons such as mobility of communicating vehicles, rapid changes in physical communication environment around these vehicles, low heights of vehicle antennas, and frequent obstructions of the line-of-sight between transmitting and receiving ends due to the surrounding vehicles and buildings. In [5–12], it is shown that statistical properties of the V2V channels differ from those of the cellular channels and fading conditions in vehicular channels are much hostile. Thereby, well-known conventional fading models, i.e. Rayleigh, Rician and Nakagami-*m* fading models, are insufficient in vehicular communications. It has been revealed in [13–15] that the cascaded fading model, in which the channels' fading gain is produced by multiplying the channel gains of independent scattering groups around mobile units, provides an accurate statistical model for V2V communications. These studies have motivated the investigations of new cascaded fading models and then double Rayleigh and its generalized form, cascaded Rayleigh fading models are examined in [17, 24] and [18], respectively. Double Nakagami-*m* channel model in [21, 22] and cascaded Nakagami-*m* channel model in [19] are studied. Generalized-K fading model allows the investigation of the fading and shadowing effects within a unified framework [16], and it is shown in [27] that double Nakagami-*m* and generalized-K are equivalent channel models. Therefore generalized-K fading model can also be used to model vehicular channels if its distribution parameters are selected in a proper fashion. In addition, [7] offers to use Weibull channel model in V2V communications. Cascaded generalized-K and cascaded Weibull channel models are investigated in [23, 26] and [20], respectively. Furthermore, it is shown that an arbitrarily close approximation to the statistical properties of double Nakagami-*m* and generalized-K fading models can be obtained by a novel approach called mixture gamma distribution model [35], which simplifies

the analysis associated with the complicated or intractable performance expressions by exploiting the opportunity to express any probability density function (pdf) in terms of a weighted sum of the gamma distributions.

Another difficulty in V2V communications stems from the mobility of communicating vehicles at high speeds. The communication environment around the vehicles changes rapidly and by this reasoning, most of the time direct-link between these vehicles is absent where multi-path fading becomes a major concern. At this point, spatial diversity has been an effective tool to cope with this problem [36, 37]. The spatial diversity, also called as antenna diversity, is one of the most popular diversity techniques to tackle the problems caused by the destructive nature of wireless channels. The basic idea behind the diversity is that a transmitter transmits the signal through several independent paths to receive independent signal replicas at the receiver where multiple inputs are provided so that the fading effects among these inputs are uncorrelated. Thus, if one or more paths suffer from deep fading at a certain time, the other independent paths may have a strong signal at that input. One of the methods to obtain the spatial diversity is to use multiple antennas on the transmitter and/or receiver. In this case, the equivalent channel is called multiple input multiple output (MIMO) channel. Nowadays, MIMO technology becomes mature for wireless communications and it is incorporated into current wireless broadband standards [38,39]. However, deploying multiple antennas requires more RF chains and increases hardware complexity, cost and power consumptions and therefore may not be feasible for some practical applications [40]. This drawback is compensated through antenna selection techniques [41–49], which can be implemented at the transmitter [44,47,49], at the receiver [41–43], or at both sides [46, 50, 51]. These techniques offer a trade-off between complexity and performance. In the literature, several studies point out that the enhancement of the performance of V2X communication systems can be achieved by employing antenna diversity and selection methods [24, 52–59].

Although the placement of the multiple antennas on a wireless unit is a smart way to obtain diversity to effectively combat the deleterious effects of fading in wireless channels, a class of methods called cooperative communications, also known as relay-assisted communications, are proposed to obtain the spatial diversity even in case of single antenna units when the multiple antennas are not available. It has been

shown in [13] that the channels in communications via relays can also be modeled in a cascaded manner. The cooperative communication enables single-antenna users in a multi-user environment to share their antennas and generate a virtual multiple antenna transmitter that allows them to achieve antenna diversity [60–62]. In relay-assisted communication, a source sends its messages directly and/or over the relays, which are mostly the other users around, to a destination. Because the fading paths from the source to the relays, and the relays to the destination are statistically independent, this situation generates an antenna diversity at the receiver. In cooperative communications, the relays can employ several cooperation methods such as amplify-and-forward (AF) and decode-and-forward (DF) [63]. In the AF method, relays simply amplify the received signal and retransmit it to the destination nodes. Due to its computational simplicity and ease in practical implementation, the AF method has become more attractive than the other ones. The AF method can be divided into two categories, which are variable gain relaying [64] and fixed gain relaying [65]. In the variable gain relaying, the relay must have the full channel state information (CSI) of the channels between communicating terminals. This requires to track the statistics of the channels continuously by frequently sending pilot signals. Thus the variable gain relaying causes spectral inefficiency and needs complex structures in hardware implementation. In the fixed gain relaying, knowledge of the average statistics of the channels is used, so less number of pilot signals are required and better spectral efficiency can be obtained. On the other hand, it is obvious that the variable gain relaying has much better error performance, therefore, it may be preferred in mission critical applications, such as alerting the vehicles approaching to an accident scene at very high speeds. Furthermore, in order to overcome the bandwidth inefficiency problem resulted from cooperation among multiple nodes, relay selection techniques based on working with a single relay or a certain relay groups maximizing the instantaneous SNR at the destination can be used, instead of using all of the relays within the system. With these techniques, it is shown that the error performance can be enhanced and the system complexity can be reduced, without loss of diversity gain [66–72].

Besides the spatial diversity, time diversity, frequency diversity, polarization diversity and space-time diversity are the mostly used diversity techniques to improve signal quality in wireless channels. Furthermore, by combining the channel coding and

antenna diversity methods, a special type of antenna diversity called space-time coding [73–75] can be implemented to enhance the error performance of the wireless communication systems. Space time coding can be grouped under two main category which are space-time block coding (STBC) and space-time trellis coding (STTC). Both improve the error performance significantly by providing lower error rates in comparison with the uncoded systems [76–79].

On the other hand, studies in the literature on cooperative communications targeted the vehicular channel models is not rich as those for the cellular communications. Bit error rate (BER) performance bounds and optimum power allocation strategies are studied for double Rayleigh channels in [80]. [81] investigates the impact of imperfect channel estimation on the performance of an inter-vehicular system with AF relaying over double Rayleigh fading channels. In [82] and [83], outage probability performance is analyzed for double Rayleigh channels. The performance of a V2X system with multiple relays employing the distributed equal gain combining technique is studied for double Rayleigh and double Rician channels in [25] and [84], respectively. The performance of distributed generalized low-density codes for double Rayleigh fading channels is investigated for a V2I cooperative relay networks in [85]. BER performance analysis is investigated for the relay selection in a distributed AF relay network for cascaded Rayleigh fading channels in [86]. The performance of the relay selection is examined in [87] for a dual-hop V2X system employing DF technique over double Rayleigh channels. The outage probability and error performance analysis of the AF relaying cooperative systems with relay selection over double Rayleigh fading channels are investigated in [88]. Outage probability and power optimization problem of multi-hop inter-vehicular communication systems are studied in [89] for the cases of AF and DF relaying over cascaded Rayleigh fading channels. Antenna diversity order, error performance and optimum power allocation issues are investigated for cascaded Nakagami-m channels in [90]. Symbol error rate (SER) analysis is studied for the V2V systems with single antenna units and single relay employing the AF method over double Nakagami-m channels in [91] and over cascaded Nakagami-m channels in [92]. [79] proposes a new distributed STTC for the systems employing the AF method over double Rayleigh channels. Relay selection performance of a dual hop multi-relay system employing the AF method over composite fading channels is

examined in [93]. The performance of a multi-hop system is investigated for the DF and AF methods in [94] and [95], respectively, over generalized-K channels. The symbol error performance analysis of a multi-relay cooperative system performing selection combining at the receiver is examined in [96] for generalized-K channels.

The increasing number of users and/or relays in communication networks has inevitably accelerated studies for network capacity enhancement. In recent years, one of the most important studies proposed for this subject is the network coding technique [30–32]. This technique depends on the XOR operation of users' data bits at the network layer. The demand for capacity increasing and higher data transmission rate in the upper layers of the communication systems obviously have a counterpart in the physical layer. Compared to the non-cooperative communications, the cooperation of the multiple users consumes more time slots for signaling, which results in a decrease in data transmission rate. A method to cope with this drawback is PLNC providing simultaneous data transmissions for users via the same relay by exploiting the additive property of the EM waves [33,34]. PLNC is also known as analog network coding, bidirectional relaying, or two-way relaying. This method takes two time slots for exchanging information between two users and thus provides better bandwidth efficiency [97] than the conventional cooperative communication systems, where two sources communicate with the help of a relay. Especially in dense traffic conditions, PLNC can take an important role to increase the data transmission rate in emergency cases, which must be reported to many users in a short period of time. Some of the studies on PLNC are listed in [98–105]. Besides the enhancement of capacity and data transmission rate obtained within PLNC systems, error performance of these systems can be improved by using various cooperation techniques originally proposed for classical cooperative communication systems [106–116]. For example, [106–108] use the antenna selection techniques to enhance the error performance in multi-antenna PLNC systems while the impact of relay selection techniques on error performance for multi-relay PLNC system is investigated in [109–112]. Furthermore, space-time coding techniques are employed to improve the error performance of multi-relay [113, 114] and multi-antenna [115, 116] PLNC systems.

On the other hand, most of the studies on PLNC have used cellular channel models. In case of vehicular channel models where PLNC is employed, the number of studies

is very limited. The symbol error and service outage probabilities are investigated for cascaded Nakagami-*m* fading channels in [117] and [118], while the performance analysis of two-way AF relaying has been worked for generalized-K and Weibull fading channels in [119] and [120], respectively. The relay selection in a multi-relay PLNC system with single antenna nodes has been studied for double Rayleigh fading channels in [121], double Nakagami-*m* fading channels in [122]. [123] examines the outage probability and SER performance of a multi-relay PLNC system employing the relay selection. In [124], a partial relay selection method is used to improve the performance of a roadside-based PLNC system having multiple relays employing the AF method over mixed Nakagami-*m* and double Nakagami-*m* fading conditions.

1.3 Original Contributions

In this thesis, for the first time in the literature, a cooperative V2V communication system employing PLNC using fixed gain AF method over cascaded Nakagami-*m* channels is designed, the performance analysis of this system is examined, and closed-form expressions of the exact service outage and the exact symbol error probabilities are derived. As a continuation of this work, the performance analysis of the proposed system is investigated for cascaded and fast fading Rayleigh channels in the presence of the self-interference, and the exact outage probability expression is obtained in the closed-form. In the PLNC literature, this work is the only one in which the channel is modeled as not only cascaded but also fast fading channel. In addition to this, for the first time in this thesis, in a MIMO PLNC system with multiple relays employing variable gain AF method over cascaded Nakagami-*m* channels, it is shown that the service outage probability performance can be enhanced by employing joint antenna and relay selection. In this work, the exact outage probability expression is obtained as a single integral form while the upper and the lower bounds of the outage probabilities are obtained in closed-forms. Moreover, asymptotic diversity order is quantified as a function of the number of the relays, the number of the antennas placed on the sources and relays, and the cascading degrees and fading parameter values of the channels. Another original contribution of the thesis is that a novel design criterion for STTCs is found for cascaded fading channels. Then, by using this new criterion, novel STTCs with 4 and 8 states are proposed for MIMO V2V PLNC systems.

List of the journal and conference publications presenting the original contributions of this thesis to the wireless communication literature is given below.

- Serdar Özgür Ata, İbrahim Altunbaş (2016). Fixed gain AF PLNC over cascaded Nakagami-m fading channels for vehicular communications, *AEU - International Journal of Electronics and Communications*, 70(4), 510-516. http://dx.doi.org/doi:10.1016/j.aeue.2016.01.003

- Serdar Özgür Ata, İbrahim Altunbaş (2017). Joint relay and antenna selection in MIMO PLNC inter-vehicular communication systems over cascaded fading channels, *Wireless Personal Communication*, 90(2), 901-923. http://dx.doi.org/10.1007/s11277-016-3584-2

- Serdar Özgür Ata, İbrahim Altunbaş (2015). Relay antenna selection for V2V communications using PLNC over cascaded fading channels, *IEEE Int. Wireless Commun. and Mobile Computing Conf.*, 1336-1340, Dubrovnik, Croatia. http://dx.doi.org/doi:10.1109/IWCMC.2015.7289276

- Serdar Özgür Ata, İbrahim Altunbaş (2015). Relay antenna selection for V2V PLNC system, *IEEE 23rd Signal Proc. and Commun. App. Conf.*, Malatya, Turkey. http://dx.doi.org/doi:10.1109/SIU.2015.7129958

- Serdar Özgür Ata, İbrahim Altunbaş (2016). Analog network coding over cascaded fast fading Rayleigh channels in the presence of self-interference, *IEEE 24th Signal Proc. and Commun. App. Conf.*, Zonguldak, Turkey. http://dx.doi.org/doi:10.1109/SIU.2016.7495725

- Serdar Özgür Ata, İbrahim Altunbaş (2016). STTC design for MIMO V2V PLNC systems over cascaded fading channels, Submitted to the journal of Transaction on Emerging Telecommunication Technologies.

2. FADING CHANNEL MODELS AND COOPERATIVE COMMUNICATION TECHNIQUES IN WIRELESS COMMUNICATIONS

2.1 Fading Channel Models

In wireless communications, EM waves transmitted by the source are subject to three main destructive effects while traveling in the medium occupied by various obstacles. These effects are called as reflection, scattering and diffraction. When EM waves impinge to an object that has a size larger than EM's wavelength, the reflection occurs, whereas the scattering occurs if the obstacle size is less than EM's wavelength. The effect of the diffraction is occurred when EM waves interact with sharp edged objects on their path. Due to these destructive effects, received signal by destination is a superposition of the multiple copies of the transmitted signal. Each signal copy reaches the receiving antenna from a different path and therefore has different amount of phase and amplitude distortion. The superposition of these signals is received as a single combined signal by the receiver. Rapid fluctuations on the amplitude of the combined signal is called fading [4]. Beside the fading effect, path loss and shadowing are another destructive phenomena to bring about an attenuation at the signal strength. Path loss is caused by the distance between the transmitter and the receiver. Shadowing also causes signal power fluctuates. These fluctuations are experienced on local-mean powers, that is, the fluctuations from shadowing is not as fast as those from fading effect, but it is faster than those caused by path-loss. Another characteristic parameter in a wireless communication channel is Doppler spread which is produced by the motion of the transmitter and/or the receiver. Doppler spread is a measure of the spectral broadening or reducing of the incoming signal. In wireless communication systems, path loss, shadowing, fading and Doppler spread make the error performance much worse than the performance of Gaussian noise channel.

2.1.1 Additive Noise

Thermal noise in hardware components for communication systems appears as additive noise at the received signal. This noise is modeled as a Gaussian random process and called the additive white Gaussian noise (AWGN). Amplitude of a Gaussion signal at a certain time is a random variable and its pdf and cumulative distribution function (CDF) are given by

$$f_X(x) = \frac{1}{\sqrt{2\pi}\sigma_x} e^{-\frac{(x-m_x)^2}{2\sigma_x^2}} \tag{2.1a}$$

$$F_X(x) = 1 - Q\left(\frac{x-m_x}{\sigma_x}\right) \tag{2.1b}$$

where m_x and σ_x are the expected value and the standard deviation, respectively. $Q(.)$ is the Gaussian function [4] which is stated as

$$Q(x) = \frac{1}{\sqrt{2\pi}} \int_x^\infty e^{-\frac{t^2}{2}} dt. \tag{2.2}$$

The power spectral density of the AWGN signal, $S_x(f)$ is defined as the Fourier transform of the autocorrelation function of the process and one-sided and two-sided power spectral densities remain constant as N_0 and $N_0/2$ for all frequencies f as illustrated in Figure 2.1(a) and (b), respectively. The value of N_0 depends on the temperature and it is formulated as $N_0 = \kappa T$, where $\kappa = 1.38064852x10^{-23} \frac{Joule}{Kelvin}$ is Boltzman constant and T is the temperature in Kelvin.

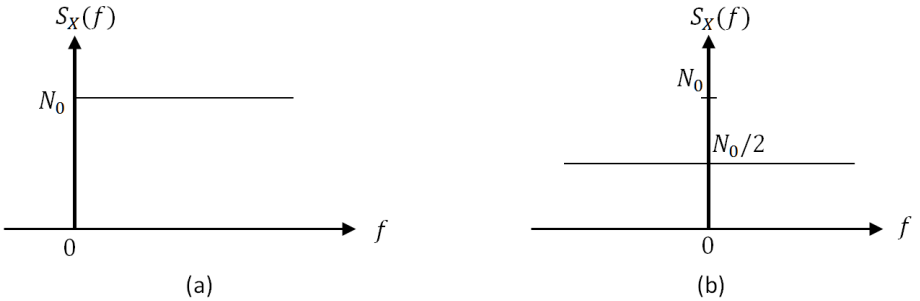

Figure 2.1 : (a) Single-sided (b) two-sided power spectral density of AWGN.

2.1.2 Fading Channel Model

A fading wireless communication channel impulse response model can be represented as in Figure 2.2 in terms of bandpass signals. In the figure, $g(t,\tau)$ is the impulse

response of the channel given by

$$g(t,\tau) = \sum_{n=1}^{N} C_n e^{j2\pi\left(f_{D,n}t - \left(f_c + f_{D,n}\right)\tau_n\right)} \delta(\tau - \tau_n), \tag{2.3}$$

where f_c is the carrier frequency while C_n, $f_{D,n}$, and τ_n represent the attenuation factor, Doppler shift and the time delay of the n-th component, respectively [4]. Apparently, the impulse response depends on the time instant t that the signal was sent, and the duration τ elapsed until the observation moment of the signal at the receiver. Therefore the channel in wireless communications is not the time-invariant channel. If the maximum value of the delay among the received signals is defined as

$$\tau_{max} = \max_{i,j} |\tau_i - \tau_j|, \tag{2.4}$$

when $\tau_{max} << T_s$ where T_s is the modulation duration, we can assume that delay of the each EM wave reaching the receiver is a constant as $\hat{\tau}$. In this case, the impulse response of the channel can be written as

$$g(t,\tau) = g(t)\delta(\tau - \hat{\tau}). \tag{2.5}$$

So, the channel transfer function, which is the Fourier transform of $g(t,\tau)$ becomes

$$T(t,f) = \mathscr{F}\{g(t,\tau)\} = g(t)e^{-j2\pi f\hat{\tau}}. \tag{2.6}$$

Hence, amplitude response of the transfer function, i.e., $|T(t,f)| = |g(t)|$, does not depend on frequency. The channels in which the amplitude response is frequency invariant are called frequency non-selective or flat channels. In a generalized view, $g(t)$ is a complex-valued function and named as channel gain or fading coefficient, and explicitly expressed as

$$g(t) = g_I(t) + jg_Q(t) = |g(t)|e^{j\angle g(t)} = he^{j\angle g(t)} \tag{2.7}$$

where $g_I(t)$ and $g_Q(t)$ represent the in-phase and the quadrature components, respectively [4]. Also, $h = |g(t)|$ is the envelope and $\angle g(t)$ denotes the phase.

In classification of the wireless communication channels, the effective measures are delay spread, coherence bandwidth, Doppler spread and the coherence time of the

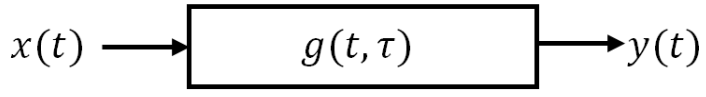

Figure 2.2 : Bandpass channel impulse response model.

channel. In order to state that a channel is frequency non-selective channel, the condition of $\tau_{max} << T_s$ must be satisfied. This can equivalently be formulated as follows: Let the coherence bandwidth of the channel be represented by $B_c \approx \frac{1}{\tau_{max}}$ and bandwidth of the modulated signal be represented by $B_s \approx \frac{1}{T_s}$. If the condition

$$B_c >> B_s \tag{2.8}$$

is satisfied, then such fading channels are frequency non-selective ones. Otherwise, if $B_c \approx B_s$ or $B_c < B_s$, then the transmitted signal is faded in frequency domain through the channel. In this case, the channel is named as frequency selective. Some of the frequency components of the signal are not allowed to pass in the frequency selective channel, therefore, the bandwidth of the signal is reduced. This causes a time spread in the signal and results in inter-symbol interference (ISI).

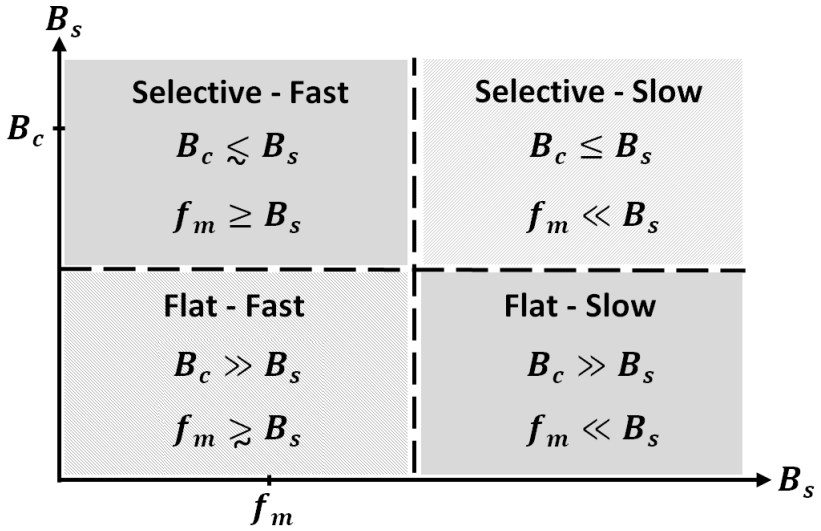

Figure 2.3 : Classification of fading channels.

By using Doppler shift causing a spread in the signal bandwidth, the channels can also be classified according to the variation of their impulse responses. The maximum value of the Doppler shift is given by

$$f_m = \frac{v}{c} f_c \tag{2.9}$$

where v is the receiver's speed, c is the speed of the light, and f_c is the carrier frequency. The channel coherence time depending on the Doppler shift is defined as

$$T_c \approx \frac{1}{f_m}. \tag{2.10}$$

Thus, the fading channels can be classified depending on both of these parameters. If $T_c >> T_s$ or $f_m << B_s$, then the channel changes slowly in time, and thus the channel

is called slow-fading channel. In this case, consecutive symbols sent by the transmitter in a T_c-length duration are affected by the same fading coefficient. On the contrary, for $T_c \leq T_s$ or $f_m \geq B_s$, the channel is described as a fast fading channel. Figure 2.3 summarizes the channel classification depending on the relations between the values of B_c, B_s and f_m [4].

2.1.3 Rayleigh Channel Model

If there is no dominant component among the EM waves reaching the receiver in multi-path propagation, $g_I(t)$ and $g_Q(t)$ in (2.7) are the Gauss random processes with zero mean and σ^2 variance. In this case, the envelope of $g(t)$ at a certain time, h, is a random variable with Rayleigh distribution whose pdf and CDF are given by [4]

$$f_h(h) = \frac{h}{\sigma^2} e^{-\frac{h^2}{2\sigma^2}}, \qquad h \geq 0 \tag{2.11a}$$

$$F_h(h) = 1 - e^{-\frac{h^2}{2\sigma^2}} \tag{2.11b}$$

and the average power for this random variable is $\Omega = E[h^2] = 2\sigma^2$. In Figure 2.4, the pdf plots of Rayleigh distribution are presented for various Ω values.

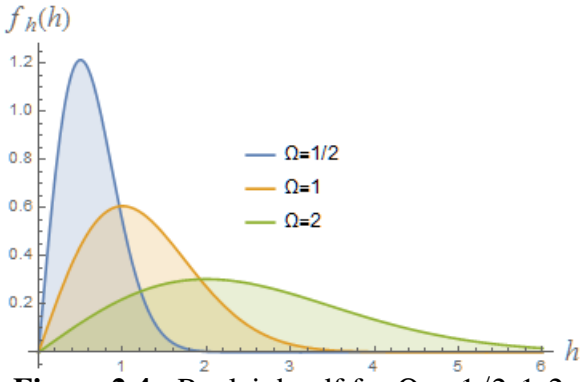

Figure 2.4 : Rayleigh pdf for $\Omega = 1/2, 1, 2$.

2.1.4 Nakagami-m Channel Model

The Nakagami-m distribution is used to model the attenuation of the signals traversing multiple paths. The pdf and CDF of Nakagami-m distribution are given by [4]

$$f_h(h) = \frac{2m^m}{\Gamma(m)\Omega^m} h^{2m-1} e^{-\frac{m}{\Omega}h^2}, \qquad h \geq 0 \tag{2.12a}$$

$$F_h(h) = \frac{\gamma\left(m, \frac{m}{\Omega}h^2\right)}{\Gamma(m)} \tag{2.12b}$$

where $\Gamma(.)$ is the gamma function [125, 8.310/1], $\gamma(.,.)$ is the lower incomplete gamma function defined as $\gamma(\alpha,\rho)=\int_0^\rho t^{\alpha-1}e^{-t}dt$ [125, 8.350/1], m is the Nakagami parameter of the distribution defined as $m=\frac{E^2[h^2]}{E[(h-E[h])^2]}$ and $\Omega=E[h^2]=2m\sigma^2$ is the average power. For $m=1$, the Nagakami-m distribution recovers the Rayleigh distribution. In Figure 2.5, the pdf plots of Nakagami-m distribution are shown for various m and Ω values.

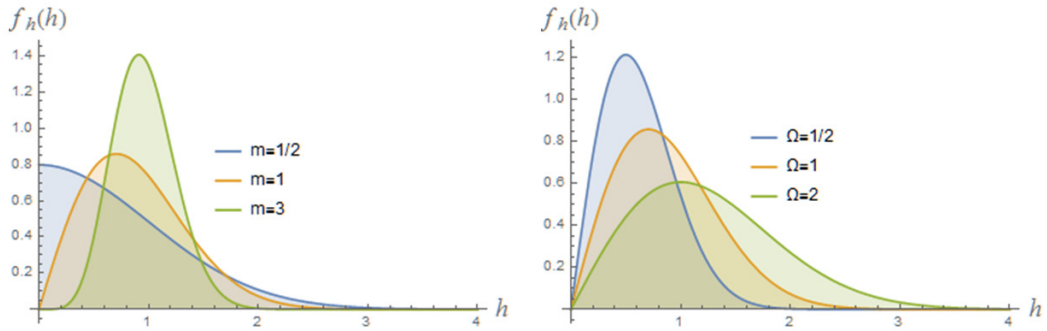

Figure 2.5 : Nakagami-m pdf for (a) $m=1/2,1,3$ and $\Omega=1$ (b) $m=1$ and $\Omega=1/2,1,3$.

2.1.5 Cascaded Fading Channel Model

As mentioned in the literature survey, it is known that the statistical properties of the V2V channels differ from those of the cellular channels [11–13]. Thereby, well-known conventional fading models, i.e. Rayleigh, Rician and Nakagami-m fading models, are insufficient in case of vehicular communications. It has been revealed in [13, 15] that the cascaded fading model, in which the channels' fading gain is produced by multiplying the channel gains of the independent scattering groups around mobile units, provides an accurate statistical model for V2V communications.

In order to evaluate the statistical model of the fading at the cascaded channels, we should derive a statistical model for a random variable produced by multiplying the gain of each independent path where the signal is traveling. This means that, the end-to-end channel gain between the transmitter and the receiver is

$$h=\prod_{n=1}^{N}h_n, \tag{2.13}$$

where h_n is the n-th channel's gain while N is the cascading degree of the channel. The distributions of h_n coefficients determine the distribution of h. For example, if each h_n

has Nakagami-m distribution, then h is the cascaded Nakagami-m distributed random variable. If we define the instantaneous SNR at the receiver as

$$\gamma = h^2 \frac{E_s}{N_0} \tag{2.14}$$

where E_s is the energy per symbol, then the pdf of γ for the cascaded channels is given as [19]

$$f_\gamma(\gamma) = \frac{1}{\gamma \prod_{n=1}^{N} \Gamma(m_n)} G_{0,N}^{N,0} \left[\frac{\gamma}{\gamma_s} \prod_{n=1}^{N} \frac{m_n}{\Omega_n} \middle|_{m_1, m_2, \ldots, m_N}^{-} \right] \tag{2.15}$$

and its CDF is

$$F_\gamma(\gamma) = \frac{1}{\prod_{n=1}^{N} \Gamma(m_n)} G_{1,N+1}^{N,1} \left[\frac{\gamma}{\gamma_s} \prod_{n=1}^{N} \frac{m_n}{\Omega_n} \middle|_{m_1, m_2, \ldots, m_N, 0}^{1} \right] \tag{2.16}$$

where $\gamma_s = \frac{E_s}{N_0}$ and $G_{p,q}^{m,n}\left[. \middle| \begin{matrix} a_1, \ldots, a_n, a_{n+1}, \ldots, a_p \\ b_1, \ldots, b_m, b_{m+1}, \ldots, b_p \end{matrix} \right]$ is the Meijer's G-function [125, 9.301]. Substituting $m_n = 1$ in (2.15) and (2.16), the pdf and CDF of the cascaded Rayleigh fading channel are obtained.

In case of error performance analysis over cascaded channels, if the conditional SER in a communication system is a function of the instantaneous SNR as follows

$$P_e(\gamma) = AQ\left(\sqrt{2B\gamma}\right), \tag{2.17}$$

then the average error probability in this system can be obtained by

$$\bar{P}_e(\gamma) = \frac{A\sqrt{B}}{2\sqrt{\pi}} \int_0^\infty \frac{e^{-B\gamma}}{\sqrt{\gamma}} F_\gamma(\gamma) d\gamma \tag{2.18}$$

where A and B are modulation-specific constants like that $A = 1$, $B = 2$ for BPSK $A = 1, B = 1$ for coherent BFSK, $A = 2(M-1)/M$, $B = 6/(M^2-1)$ for M-ASK. Note that $A = 4(1 - 1/\sqrt{M})$ and $B = 3/(M-1)$ for M-QAM and $A = 2$, $B = \sin^2(\pi/M)$ for M-PSK in case of high SNR regime [126]. Hence, the average error probability for the cascaded Nakagami-m channel is

$$\begin{aligned} \bar{P}_e(\gamma) &= \frac{A\sqrt{B}}{2\sqrt{\pi}} \int_0^\infty \frac{e^{-B\gamma}}{\sqrt{\gamma}} \frac{1}{\prod_{n=1}^{N} \Gamma(m_n)} G_{1,N+1}^{N,1} \left[\frac{\gamma}{\gamma_s} \prod_{n=1}^{N} \frac{m_n}{\Omega_n} \middle|_{m_1, m_2, \ldots, m_N, 0}^{1} \right] d\gamma \\ &= \frac{A}{2\sqrt{\pi} \prod_{n=1}^{N} \Gamma(m_n)} G_{2,N+1}^{N,2} \left[\frac{1}{B\gamma_s} \prod_{n=1}^{N} \frac{m_n}{\Omega_n} \middle|_{m_1, m_2, \ldots, m_N, 0}^{\frac{1}{2}, 1} \right]. \end{aligned} \tag{2.19}$$

In Figure 2.6, average bit error rate plots of QPSK modulation, $A = 2$ and $B = \sin^2(\pi/4)$, are given for various values of m and N. As it is seen from the figure, the error probability is worsen when the cascading degree of the channel increases.

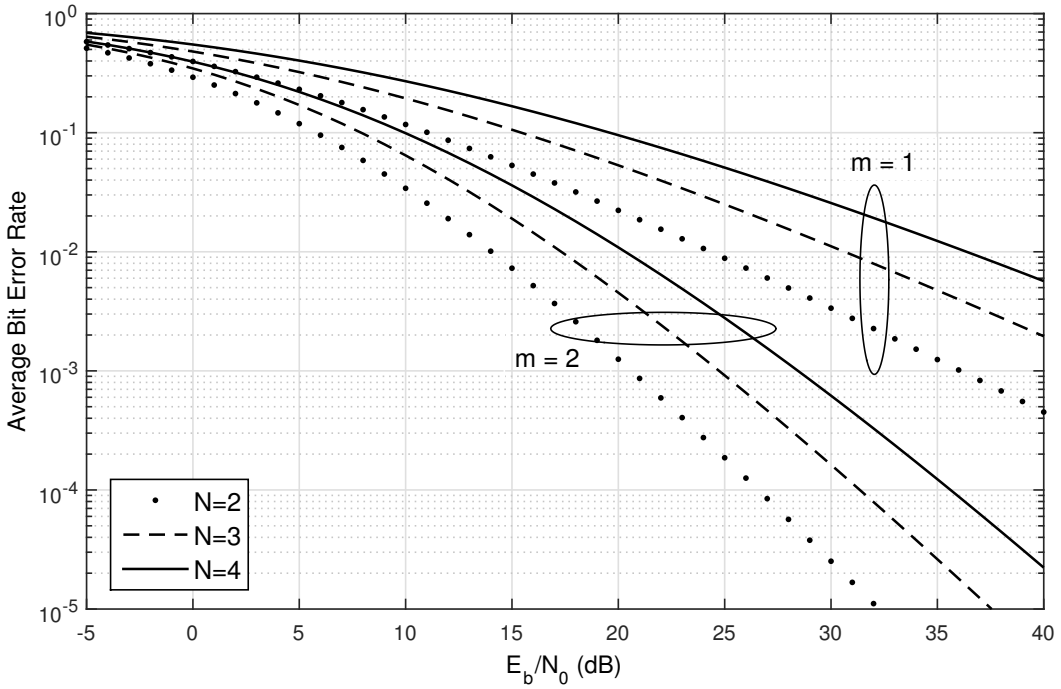

Figure 2.6 : Average bit error rate for QPSK modulation scheme over the cascaded Nakagami-*m* fading channel for various values of *m* and *N*.

Another benchmark for the performance of a wireless communication system is outage probability, which is the probability of the instantaneous SNR's falling below a certain γ_{th} threshold value. Therefore, it can be determined by the value of the CDF of instantaneous SNR at the point of γ_{th} and given by

$$P_{out} = \int_0^{\gamma_{th}} f_\gamma(\gamma) d\gamma = F_\gamma(\gamma_{th}). \tag{2.20}$$

Hence, the outage probability for cascaded Nakagami-*m* channels is

$$P_{out} = \frac{1}{\prod_{n=1}^{N} \Gamma(m_n)} G_{1,N+1}^{N,1} \left[\frac{\gamma_{th}}{\gamma_s} \prod_{n=1}^{N} \frac{m_n}{\Omega_n} \Bigg|_{m_1, m_2, \ldots, m_N, 0}^{1} \right]. \tag{2.21}$$

2.1.6 Mixture Gamma Distribution

Due to the special mathematical functions used in the composite fading models, the performance analysis of the wireless systems may be complicated or intractable. In order to avoid these problems and to support a simpler framework, the mixture Gamma distribution is proposed [35]. By this method, an arbitrarily close approximation to any pdf of the instantaneous SNR can be obtained by a weighted sum of gamma pdfs as follows

$$f_\gamma(x) = \sum_{k=1}^{K} w_k f_k(x) = \sum_{k=1}^{K} \alpha_k x^{\beta_k - 1} e^{-\zeta_k x} \tag{2.22}$$

where K is the number of terms, $f_k(x) = \frac{\zeta_k^{\beta_k} x^{\beta_k - 1} e^{-\zeta_k x}}{\Gamma(\beta_k)}$ is the pdf of the standard Gamma distribution with the parameters α_k, β_k and ζ_k while $w_k = \frac{\alpha_k \Gamma(\beta_k)}{\zeta_k^{\beta_k}}$ is the weighting coefficient of the k-th Gamma component satisfying $\sum_{k=1}^{K} w_k = 1$. In that case, CDF of the instantaneous SNR becomes

$$F_\gamma(x) = \sum_{k=1}^{K} \alpha_k \zeta_k^{-\beta_k} \gamma(\beta_k, \zeta_k x). \tag{2.23}$$

In addition, the moment generating function (MGF) [127] of γ can be given as

$$M_\gamma(s) = E[e^{-s\gamma}] = \sum_{k=1}^{K} \frac{\alpha_k \Gamma(\beta_k)}{(\zeta_k + s)^{\beta_k}} \tag{2.24}$$

and the n-th moment of γ becomes

$$m_\gamma(n) = E[\gamma^n] = \sum_{k=1}^{K} \alpha_k \Gamma(\beta_k + n) \zeta_k^{\beta_k + n}. \tag{2.25}$$

2.2 Cooperative Communication Techniques

Cooperative communication is one of the most attractive research topics in wireless communications due to being a key enabling technology to tackle the fading effects in wireless channels. The simplest form of the cooperative communication systems is multi-hop communication where the source and destination communicate with the help of two or more nodes, which are acting as the relay nodes [95]. As well known, in wireless communications, power of the transmitted signals is significantly attenuated by distance. Therefore, multi-hop cooperative communication technique is used when peer-to-peer communications is not feasible. In this technique, a long distance communication is realized by using consecutive short-distance communication links provided by the help of the intermediate nodes called as relays. On the other hand, it is not possible to obtain antenna diversity in multi-hop communication systems with single antenna relays. In [28], the lower and upper bounds of the channel capacity are investigated for a three-node relay channel model, which constitutes the fundamentals of the studies on cooperative communications. The results of this work have been substantially improved further in [29] where the capacity of the Gaussian relay channel is evaluated and an achievable lower bound to the capacity of the general relay channel is established. Multi-antenna systems [36, 37], advances in channel coding, the improvement of the space-time coding techniques [73], and

Table 2.1 : Cooperative communication protocols.

	T_1	T_2
P-I	$S \rightarrow R, D$	$S, R \rightarrow D$
P-II	$S \rightarrow R$	$S, R \rightarrow D$
P-III	$S \rightarrow R, D$	$R \rightarrow D$
P-IV	$S \rightarrow R$	$R \rightarrow D$

the studies on the analysis of the fading channels in relayed communication systems [64, 128, 129] lead to investigation of several cooperative communication techniques used in wireless communications. The basic model for cooperative communications is the relay-assisted channel model including three nodes. Figure 2.7 illustrates this model. Here, the source (S) sends its signal x to the both destination (D) and relay (R). The relay processes the noisy-form of x by using several techniques [63] and sends the obtained signal x_r to the destination. By using this signaling scheme, different forms of the same signal suffering independent destructive effects reach the receiver antenna, and thus, the antenna diversity is obtained. The protocols P-I, P-II, P-III and P-IV which can be used for the message flow among the nodes in two time slots (T_1 and T_2) are shown in Table 2.1. Since information is carried in one direction, from source to destination, by the relay using these protocols, this type of relay-assisted communication systems is called one-way relaying systems. While P-I is the most general form of the relaying communication, P-II and P-III are proposed to tackle the mathematical difficulties in P-I [63, 130]. P-IV corresponds to the aforementioned multi-hop (here, dual-hop) cooperative communications.

In cooperative communications, the relay uses several methods to process the received signal from the source. Mostly used methods are amplify-and-forward (AF) [63, 64] and decode-and-forward (DF) [63, 94] methods. In the AF method, the relay amplifies

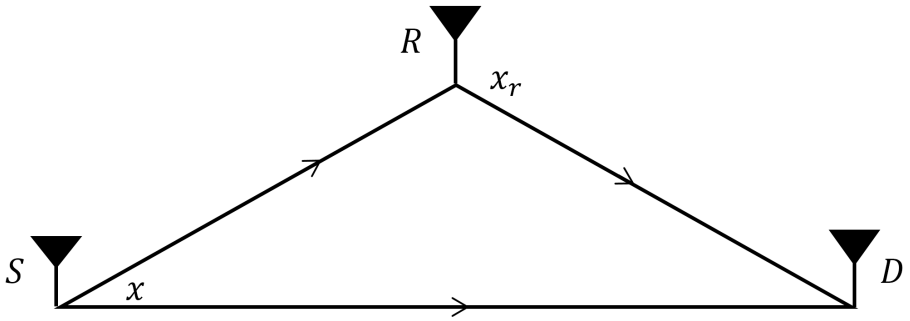

Figure 2.7 : Three-node-relay channel model.

Table 2.2 : Protocols used in two-way relaying cooperative communications.

	T_1	T_2	T_3	T_4
P-V	$S_a \rightarrow R$	$R \rightarrow S_b$	$S_b \rightarrow R$	$R \rightarrow S_a$
P-VI	$S_a \rightarrow R$	$S_b \rightarrow R$	$R \rightarrow S_a, S_b$	

the received noisy signal by a power scaling ratio to normalize it, then forwards this scaled signal to the destination. When amplifying the signal received from the source, the noise is also amplified at the relay as a drawback of the AF method. And yet, the diversity can be achieved, since the destination receives the two independent faded forms of the source's signal that one is from the source and the other is through the relay. Furthermore, in order to allow the receiver to do the best estimation from the received signal, CSIs between the sources and the relay must be known. In the DF method, the relay first decodes the received signal to reconstruct the original signal, and forwards this decoded signal to the destination. To this end, if the relay makes an error in decoding, then the error propagation occurs, and therefore the cooperation may lead worse results. Hence, CSIs between all the nodes must be known for the optimum decoding at the receiver in the DF method, too.

When cooperative and V2X communications are considered together, the cooperative communication techniques can easily be applied in the V2X communications without significant infrastructure investment because the vehicles in the traffic would also behave as relays in addition to relay units to be placed on the roadside.

2.3 Physical Layer Network Coding

Since relay operates in one direction, from source to destination, in classical relaying systems, the message exchange takes two time slots which means that the communication is completed in twice the amount of time compared to direct communication, and the data transmission rate is reduced in half. One way of overcoming this disadvantage is to use the two-way relays. In this case, the units at both ends of the communication behave as a source and a destination. If it is assumed that there is no LOS between the sources S_a and S_b, the messaging can be accomplished in three or four time slots by using two-way relays, as presented in Table 2.2. When using P-V, two symbols are transmitted in four time slots, so the transmission rate is the same as that in the one-way relaying cooperation. If P-VI is used in the system, the

realized cooperation scheme is called network coding [30, 31]. Figure 2.8 presents the two-way relaying structure for network coding.

In the network coding technique, the source S_a sends x_a message to R in the first time slot T_1 while the source S_b sends x_b message to R in the second time slot T_2. Then R typically employs XOR operation, which is denoted by $\oplus$ operator, on the sources' bits and obtains the network coded message x_r as

$$x_r = x_a \oplus x_b \tag{2.26}$$

and forwards it to both S_a and S_b in the third time slot T_3. When S_a and S_b receive x_r, S_a decodes x_b by using network coding operation as follows

$$x_a \oplus x_r = x_a \oplus (x_a \oplus x_b) = x_b. \tag{2.27}$$

and S_b obtains x_a by executing $x_b \oplus x_r = x_a$. By employing this protocol, two source symbols are exchanged by the sources using three time slots, thus the transmission rate of the network coding system is increased by 33% compared to the systems using P-V.

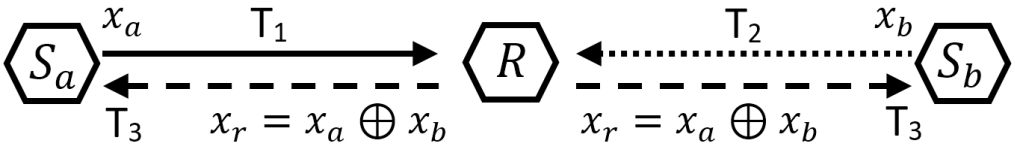

Figure 2.8 : Network coding in two-way relaying cooperative communications.

By Inspiring from the network coding idea, a new cooperation technique called physical layer network coding (PLNC) is proposed [33]. This technique exploits the additivity property of EM waves, which is a natural correspondence of the bits' being XOR, and allows both sources to transmit their signals simultaneously by using the same relay. The signaling sequence in PLNC is presented in Table 2.3. The PLNC technique may be explained in the best way by making use of two-way relay network in Figure 2.9. In the figure, h_a and h_b denote the fading coefficients of the channels between the sources and the relay. The sources send their messages, $x_a(t)$ and $x_b(t)$,

Table 2.3 : PLNC communication protocol.

	T_1	T_2
PLNC	$S_a, S_b \rightarrow R$	$R \rightarrow S_a, S_b$

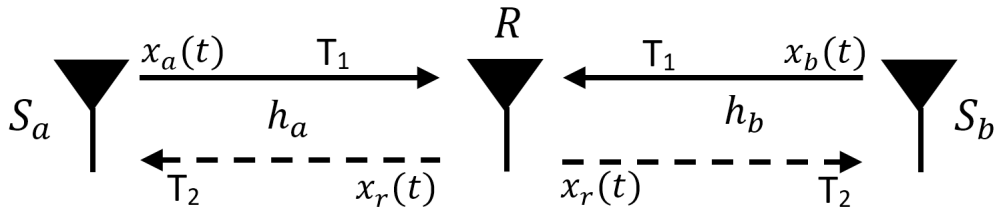

Figure 2.9 : Physical layer network coding system.

simultaneously in the first time slot T_1. At the end of this time slot, the relay receives the distorted versions of these signals as follows

$$x_r(t) = h_a x_a(t) + h_b x_b(t) + n_r(t) \tag{2.28}$$

where $n_r(t)$ is the AWGN. By assuming that the AF method is used, the relay amplifies $x_r(t)$ with a power scaling factor denoted by G, then forwards the scaled signal to the sources in the second time slot T_2. The received signals at the sources are

$$x_{a,r}(t) = h_a G h_a x_a(t) + h_a G h_b x_b(t) + h_a G n_r(t) + n_a(t), \tag{2.29a}$$

$$x_{b,r}(t) = h_b G h_a x_a(t) + h_b G h_b x_b(t) + h_b G n_r(t) + n_b(t)). \tag{2.29b}$$

If the sources are assumed to have complete CSI, they can extract their self-interference signals from the received signals, and thus, obtain the signals below

$$\tilde{x}_{a,r}(t) = h_a G h_b x_b(t) + h_a G n_r(t) + n_a(t), \tag{2.30a}$$

$$\tilde{x}_{b,r}(t) = h_b G h_a x_a(t) + h_b G n_r(t) + n_b(t). \tag{2.30b}$$

These signals are processed by miscellaneous signal processing methods such as maximum-likelihood decision rule [76], and the messages of the sources are obtained. As it is seen that two messages can be transmitted in two slots in PLNC, therefore transmission rate is increased by 100% compared to P-V.

2.4 Space Time Coding

Space-time coding is a technique that greatly improves the performance of a wireless communication system by using multiple antennas at the transmitter and receiver [73]. A type of space-time coding is STBC [74] which can provide the maximum possible antenna diversity by using simple receiver structures and decoding algorithms. On the other hand, STBC does not provide any coding gain. Another space-time coding technique is STTC [75] which is able to provide both coding gain and diversity gain.

However, STTC requires more complex transmitter and receiver structures than STBC. STTCs are based on trellis codes, therefore a STTC encoder performs a kind of trellis coded modulation scheme on multi-antenna transmitter structures while decoding of the STTCs can be done via Viterbi decoder at the receiver.

Encoder structure of a STTC using $M-$PSK modulation with n_T transmit antennas is can be modeled in Figure 2.10. The encoder consists of $n = \log_2 M$ shift registers. The memory order of the k-th branch, denoted by v_k for $k = 1,2,...,n$, is determined as $v_k = \left\lfloor \frac{v+k-1}{\log_2 M} \right\rfloor$, where $v = \sum_{k=1}^{n} v_k$ is the total memory order of the encoder. For $j = 1,2,...,v_k$ and $i = 1,2,...,n_T$, $g_{j,i}^k$ coefficients are the multiplication coefficients of the k-th encoder branch. The n multiplication coefficient set sequences are called generator sequences which fully describe the encoder. The generator sequence of the k-th branch is

$$\mathbf{g}^k = \left[\left(g_{0,1}^k, g_{0,2}^k, \cdots, g_{0,n_T}^k \right), \left(g_{1,1}^k, g_{1,2}^k, \cdots, g_{1,n_T}^k \right), \ldots, \left(g_{v_k,1}^k, g_{v_k,2}^k, \cdots, g_{v_k,n_T}^k \right) \right]. \tag{2.31}$$

Further, assume that the data stream to be sent is

$$\mathbf{c} = (\mathbf{c}_0, \mathbf{c}_1, \ldots, \mathbf{c}_t, \ldots) \tag{2.32}$$

where $\mathbf{c}_t$ is the $n-$bits input message given by

$$\mathbf{c}_t = \left(c_t^1, c_t^2, \ldots, c_t^n \right) \tag{2.33}$$

to be fed to the encoder at the t-th modulation interval. The encoder maps the input binary stream to the output symbol stream by generating the M-PSK modulated x_t^i

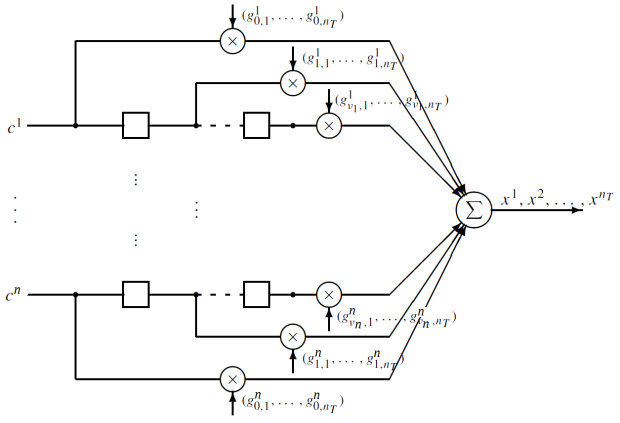

Figure 2.10 : Space-time trellis encoder.

symbols as

$$x_t^i = \sum_{k=1}^{n} \sum_{j=0}^{v_k} g_{j,i}^k c_{t-j}^k \ modulo\ M. \tag{2.34}$$

Each x_t^i symbol is transmitted via the i-th antenna at time t. The n_T-length modulated symbol stream, $\mathbf{x}_t$ is given by

$$\mathbf{x}_t = \left(x_t^1, x_t^2, ..., x_t^{n_T}\right)^T \tag{2.35}$$

and called as the "space-time symbol". The elements of $\mathbf{x}_t$ are transmitted simultaneously through n_T transmit antennas.

At the receiver with n_R antennas, the received symbols are decoded by performing the maximum-likelihood decision rule by the Viterbi Algorithm. If the receiver has complete CSI, the branch metrics are calculated as follows

$$\sum_{j=1}^{n_R} \left| r_t^j - \sum_{i=1}^{n_T} h_{j,i}^t x_t^i \right|^2 \tag{2.36}$$

where r_t^j is the received signal at the j-th antenna at time t and $h_{j,i}^t$ is the gain of the channel between the i-th transmitter and j-th receiver antennas. The Viterbi Algorithm makes a decision of the decoded sequences by selecting the path which has the minimum path metric on the trellis.

We can analyze the performance of the STTC by investigating the pairwise error probability (PEP). The PEP, denoted by $P(\mathbf{X}, \hat{\mathbf{X}})$ is the probability that the decoder selects as its estimate an erroneous sequence $\hat{\mathbf{X}} = \left(\hat{\mathbf{x}}_t^1, ..., \hat{\mathbf{x}}_t^L\right)$ when the transmitted sequence has been in fact $\mathbf{X} = \left(\mathbf{x}_t^1, ..., \mathbf{x}_t^L\right)$, where L is the transmitted data frame length in symbol for each antenna. In the analysis of STTC, a codeword difference matrix is defined as

$$\mathbf{B}\left(\mathbf{X}, \hat{\mathbf{X}}\right) = \mathbf{X} - \hat{\mathbf{X}}. \tag{2.37}$$

Then, the $n_T \times n_T$ codeword distance matrix $\mathbf{A}\left(\mathbf{X}, \hat{\mathbf{X}}\right)$ is constructed as

$$\mathbf{A}\left(\mathbf{X}, \hat{\mathbf{X}}\right) = \mathbf{B}\left(\mathbf{X}, \hat{\mathbf{X}}\right) \mathbf{B}\left(\mathbf{X}, \hat{\mathbf{X}}\right)^H \tag{2.38}$$

where $(.)^H$ is the Hermitian (transpose conjugate) operator. Let the channels between the transmitter and the receiver be the quasi-static Rayleigh channels and the receiver has CSI. Then, the pairwise error probability is upper bounded by

$$P\left(\mathbf{X}, \hat{\mathbf{X}}\right) \leq \left(\frac{E_s}{4N_0}\right)^{r n_R} \prod_{i=1}^{r} \lambda_i^{-n_R} \tag{2.39}$$

where r denotes the rank of matrix $\mathbf{A}\left(\mathbf{X},\hat{\mathbf{X}}\right)$ and $\lambda_1,\lambda_2,...,\lambda_r$ are the nonzero eigenvalues of the matrix $\mathbf{A}\left(\mathbf{X},\hat{\mathbf{X}}\right)$ [73,76]. At this point, it should be said that (2.39) is valid for the small number of n_r [75]. Depending on r and $\lambda_1,\lambda_2,...,\lambda_r$, the following design criteria, rank and determinant criteria, for STTCs are defined.

Rank criterion: In a MIMO system with n_T transmitting and n_R receiving antennas, the maximum possible diversity gain to be achieved is $n_T\,n_R$. Therefore, in order to obtain the maximum diversity order, the condition $r = n_T$ should be satisfied. That means, the matrix $\mathbf{A}\left(\mathbf{X},\hat{\mathbf{X}}\right)$ must have full rank for all the pairs of the distinct codewords. In other words, if $r \geq r_{min}$ for any pair of the distinct codewords, the minimum diversity order to be gained in a $n_T \times n_R$ MIMO system is $r_{min}\,n_R$.

Determinant criterion: The value of $\prod_{i=1}^{r}\lambda_i$ is the absolute value of the sum of the determinants of all the principal $r \times r$ cofactors of the matrix $\mathbf{A}\left(\mathbf{X},\hat{\mathbf{X}}\right)$. Therefore, in order to maximize the achievable coding gain, the determinant of the matrix $\mathbf{A}\left(\mathbf{X},\hat{\mathbf{X}}\right)$ should be maximized for all the pairs of the distinct codewords.

On the other hand, it is shown that rank and determinant criteria are held if $r\,n_R < 4$, otherwise, the upper bound for the PEP can be further approximated as

$$P\left(\mathbf{X},\hat{\mathbf{X}}\right) \leq \frac{1}{4}\,exp\left[-n_R\frac{E_s}{4N_0}\sum_{i=1}^{n_T}\lambda_i\right], \tag{2.40}$$

and by using this upper bound, an improved design criterion called trace criterion is obtained [75].

Trace criterion: Note that term $\sum_{i=1}^{n_T}\lambda_i$ in (2.40) is equal to trace of the matrix $\mathbf{A}\left(\mathbf{X},\hat{\mathbf{X}}\right)$, $Tr\left(\mathbf{A}\left(\mathbf{X},\hat{\mathbf{X}}\right)\right) = \sum_{i=1}^{n_T}\lambda_i$. Therefore, minimizing the PEP can be accomplished by maximizing the trace of the matrix $\mathbf{A}\left(\mathbf{X},\hat{\mathbf{X}}\right)$. To this end, it can be indicated that the trace of the matrix $\mathbf{A}\left(\mathbf{X},\hat{\mathbf{X}}\right)$ is equivalent to the squared Euclidean distance between the codewords $\mathbf{X}$ and $\hat{\mathbf{X}}$ as

$$Tr\left(\mathbf{A}\left(\mathbf{X},\hat{\mathbf{X}}\right)\right) = \sum_{i=1}^{n_T}\sum_{t=1}^{L}\left|x_t^i - \hat{x}_t^i\right|^2. \tag{2.41}$$

Therefore, maximizing the minimum trace of the matrix $\mathbf{A}\left(\mathbf{X},\hat{\mathbf{X}}\right)$ is equivalent to maximizing the minimum Euclidean distance between all the pairs of the distinct codewords.

3. DESIGN OF V2V COMMUNICATION SYSTEMS EMPLOYING FIXED GAIN AF PLNC

As it is mentioned in the literature review, the knowledge of the average statistics of the channels is enough for the fixed gain relaying which requires less number of pilot signals and therefore has better spectral efficiency. It is also more practical in terms of implementation than the systems using variable gain AF method.

3.1 Fixed-Gain AF PLNC over Cascaded Nakagami-m Fading Channels for Vehicular Communications

In this section, we propose an inter-vehicle communication system employing PLNC with the fixed gain AF method on the relay and investigate its performance. Analytic results are derived for the cascaded Nakagami-m fading channel model covering cascaded Rayleigh, double Nakagami-m, generalized-K and conventional cellular channel models as well. As we investigate the performance of the system, first we derive the exact CDF of the end-to-end SNR. Using this CDF, we obtain the exact closed-form outage probability. Then we derive the exact closed-form SER expression for various modulation types. At the end of this section, we present the numerical results.

3.1.1 System Model

As illustrated in Figure 3.1 we investigate an inter-vehicle communication system in which two source vehicles V_a and V_b are communicating with the help of a relay V_r employing PLNC with fixed gain AF relaying because of the shortness of the LOS between the sources. All nodes in the system are mobile, therefore the channel between V_i and V_r is modeled as a cascaded Nakagami-m fading channel with the cascading degree of N_i, for $i \in \{a,b\}$. Thus, the channel's fading coefficient h_i and its average

power are

$$h_i = \prod_{n=1}^{N_i} h_{i,n} \tag{3.1a}$$

$$E[h_i^2] = \Omega_i = \prod_{n=1}^{N_i} \Omega_{i,n} \tag{3.1b}$$

respectively, where $h_{i,n}$ random variables are independent and non-identically Nakagami-m distributed with the distribution parameter $m_{i,n}$ and the average power $E[h_{i,n}^2] = \Omega_{i,n}$.

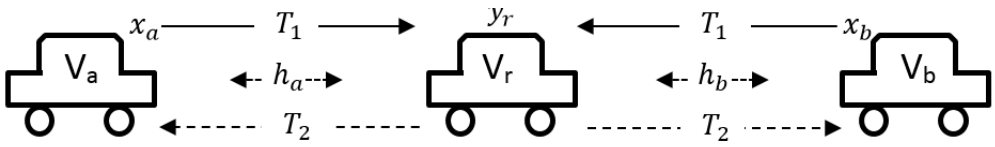

Figure 3.1 : Inter-vehicle communication using PLNC with the AF method.

In the system, we assume that all nodes know the average statistics of the CSI for all channels while the sources know their own information-bearing symbols. Thus, the source vehicles are able to cancel self-interference [106, 107, 111]. We also assumed that all the nodes transmit with equal power of $P_a = P_b = P_r = P$ and all the additive noises at the nodes are Gaussian random variables with zero mean and two-sided power spectral density of $N_0/2$. The communication between the sources is accomplished by using two time slots PLNC with the fixed gain AF method employed at the relay. Therefore, V_a and V_b send their messages x_a and x_b simultaneously to V_r and the signal

$$y_r = h_a\sqrt{P}x_a + h_b\sqrt{P}x_b + n_r \tag{3.2}$$

is received at the relay in the first time slot T_1. In the second time slot T_2, the relay amplifies y_r with a fixed power scaling factor G, such that,

$$G^2 = \frac{\gamma_0}{C} \tag{3.3}$$

where $\gamma_0 = \frac{P}{N_0}$ and $C = \gamma_0\Omega_a + \gamma_0\Omega_b + 1$ [65], then forwards it to the sources. After cancelling the self-interference, the received signals at the source nodes are

$$\tilde{y}_a = h_a G h_b\sqrt{P}x_b + h_a G n_r + n_a, \tag{3.4a}$$

$$\tilde{y}_b = h_b G h_a\sqrt{P}x_a + h_b G n_r + n_b \tag{3.4b}$$

where n_r, n_a and n_b are additive noises. Then the instantaneous E2E-SNR at V_a and V_b can be written as

$$\gamma_{a,e2e} = \frac{\gamma_a \gamma_b}{\gamma_a + C}, \tag{3.5a}$$

$$\gamma_{b,e2e} = \frac{\gamma_a \gamma_b}{\gamma_b + C} \tag{3.5b}$$

where $\gamma_a \triangleq h_a^2 \gamma_0$ and $\gamma_b \triangleq h_b^2 \gamma_0$ are the instantaneous SNR of the channels between the sources and the relay [65]. With the help of (2.15) and (2.16), and for $i \in \{a,b\}$, the pdf of γ_i becomes

$$f_{\gamma_i}(\gamma) = \frac{1}{\gamma \prod_{n=1}^{N_i} \Gamma(m_{i,n})} G_{0,N_i}^{N_i,0} \left[\frac{\gamma}{\gamma_0} \prod_{n=1}^{N_i} \frac{m_{i,n}}{\Omega_{i,n}} \middle|_{m_{i,1},\ldots,m_{i,N_i}}^{-} \right] \tag{3.6}$$

and the CDF of γ_i is

$$F_{\gamma_i}(\gamma) = \frac{1}{\prod_{n=1}^{N_i} \Gamma(m_{i,n})} G_{1,N_i+1}^{N_i,1} \left[\frac{\gamma}{\gamma_0} \prod_{n=1}^{N_i} \frac{m_{i,n}}{\Omega_{i,n}} \middle|_{m_{i,1},\ldots,m_{i,N_i},0}^{1} \right]. \tag{3.7}$$

By setting the fading parameter values in (3.7) and (3.6) to unit, $m_{i,l} = 1$, the pdf and the CDF of the instantaneous SNR for cascaded Rayleigh channels are obtained. Double Nakagami-m and generalized-K are the special cases of the cascaded Nakagami-m, in which the cascading degrees of the channels are set as $N_i = 2$. Also, one can reach non-cascaded channel conditions used in cellular communication by setting the cascading degrees to unit, $N_i = 1$.

3.1.2 Performance Analysis

In order to analyze the performance of the system we first examine the CDF of $\gamma_{a,e2e}$ or $\gamma_{b,e2e}$. By using (3.6) and (3.7) and for $i, j \in \{a,b\}$ and $i \neq j$, we state the CDF of $\gamma_{i,e2e}$ as follows

$$
\begin{aligned}
F_{\gamma_{i,e2e}}(\gamma) &= P\left(\gamma_{i,e2e} \leq \gamma\right) \\
&= P\left(\frac{\gamma_i\gamma_j}{\gamma_i + C} \leq \gamma\right) \\
&= \int_0^\infty P\left(\frac{\gamma_i\gamma_j}{\gamma_i + C} \leq \gamma \middle| \gamma_i\right) f_{\gamma_i}(\gamma_i) d\gamma_i \\
&= \int_0^\infty P\left(\gamma_j \leq \left(1 + \frac{C}{\gamma_i}\right)\gamma \middle| \gamma_i\right) f_{\gamma_i}(\gamma_i) d\gamma_i \\
&= \int_0^\infty F_{\gamma_j}\left(\left(1 + \frac{C}{\gamma_i}\right)\gamma \middle| \gamma_i\right) f_{\gamma_i}(\gamma_i) d\gamma_i \\
&= \left(\prod_{n=1}^{N_i} \Gamma(m_{i,n})\right)^{-1} \left(\prod_{n=1}^{N_j} \Gamma(m_{j,n})\right)^{-1} I_0
\end{aligned} \tag{3.8}
$$

where I_0 is

$$
\begin{aligned}
I_0 \;=\; & \int_0^\infty G_{1,N_j+1}^{N_j,1}\left[\frac{\left(1+\frac{C}{\gamma_i}\right)\gamma}{\gamma_0}\prod_{n=1}^{N_j}\frac{m_{j,n}}{\Omega_{j,n}}\,\middle|\,{}^{1}_{m_{j,1},\ldots,m_{j,N_j},0}\right] \\
& \times\frac{1}{\gamma_i}G_{0,N_i}^{N_i,0}\left[\frac{\gamma_i}{\gamma_0}\prod_{n=1}^{N_i}\frac{m_{i,n}}{\Omega_{i,n}}\,\middle|\,{}^{-}_{m_{i,1},\ldots,m_{i,N_i}}\right] d\gamma_i.
\end{aligned} \tag{3.9}
$$

Using $\gamma_i = 1/\xi$ transformation, (3.9) has the form of

$$
I_0 = \int_0^\infty \xi^{-1} G_{1,N_j+1}^{N_j,1}\left[\beta + \beta C\xi\,\middle|\,{}^{1}_{m_{j,1},\ldots,m_{j,N_j},0}\right] G_{0,N_i}^{N_i,0}\left[\frac{\zeta}{\xi}\,\middle|\,{}^{-}_{m_{i,1},\ldots,m_{i,N_i}}\right] d\xi \tag{3.10}
$$

where $\beta = \frac{\gamma}{\gamma_0}\prod_{n=1}^{N_j}\frac{m_{j,n}}{\Omega_{j,n}}$ and $\zeta = \frac{1}{\gamma_0}\prod_{n=1}^{N_i}\frac{m_{i,n}}{\Omega_{i,n}}$. Then, using the transformation and the argument simplification properties [131, 07.34.16.0002.01] of the Meijer's G-function and applying $\tau = \beta C\xi$ transformation, I_0 is written in the form of

$$
I_0 = \int_0^\infty \tau^{-1} G_{1,N_j+1}^{N_j,1}\left[\beta + \tau\,\middle|\,{}^{1}_{m_{j,1},\ldots,m_{j,N_j},0}\right] G_{N_i,0}^{0,N_i}\left[\omega\tau\,\middle|\,{}^{1-m_{i,1},\ldots,1-m_{i,N_i}}_{-}\right] d\tau \tag{3.11}
$$

where $\omega = \frac{1}{\beta C\zeta}$. Finally, the integral in (3.11) can be solved by using the integral property [131, 07.34.21.0082.01] of the Meijer's G-function with the shifted arguments

and thus we obtain $F_{\gamma_{i,e2e}}(\gamma)$ in the closed-form as

$$F_{\gamma_{i,e2e}}(\gamma) = \left(\prod_{n=1}^{N_i}\Gamma(m_{i,n})\right)^{-1}\left(\prod_{n=1}^{N_j}\Gamma(m_{j,n})\right)^{-1}\sum_{t=0}^{\infty}\frac{(-1)^t}{t!}\left(\frac{\gamma}{\gamma_0}\right)^t\left(\prod_{n=1}^{N_j}\frac{m_{j,n}}{\Omega_{j,n}}\right)^t \times G_{N_i+N_j+2,2}^{1,N_i+N_j+1}\left[\frac{\gamma_0^2}{C\gamma}\left(\prod_{n=1}^{N_i}\frac{\Omega_{i,n}}{m_{i,n}}\right)\left(\prod_{n=1}^{N_j}\frac{\Omega_{j,n}}{m_{j,n}}\right)\middle|\begin{matrix}\underline{u}\\ \underline{v}\end{matrix}\right] \quad (3.12)$$

where $\underline{u} \triangleq 1,\ 1-m_{i,1},\ ...,\ 1-m_{i,N_i},\ t+1-m_{j,1},...,\ t+1-m_{j,N_j},\ t+1$ and $\underline{v} \triangleq t,\ t+1$.

3.1.2.1 Outage probability

With the help of (2.20) and (2.21), and by using the CDF in (3.12), the individual outage probabilities of the source vehicles, V_a and V_b, are obtained as

$$P_{out,i} = P\left(\gamma_{i,e2e} \leq \gamma_{th}\right) = F_{\gamma_{i,e2e}}(\gamma_{th}) \quad (3.13)$$

for $i \in \{a,b\}$ in closed-form. γ_{th} in (3.13) denotes the threshold SNR value for $\gamma_{i,e2e}$.

3.1.2.2 Symbol error rate

With the help of (2.18), by using the CDF in (3.12), and then doing some arrangements, the average SER becomes

$$\bar{P}_{i,se} = \frac{A\sqrt{B}}{2\sqrt{2\pi}}\left(\prod_{n=1}^{N_i}\Gamma(m_{i,n})\right)^{-1}\left(\prod_{n=1}^{N_j}\Gamma(m_{j,n})\right)^{-1}\sum_{t=0}^{\infty}\frac{(-1)^t}{t!}\gamma_0^{-t}\left(\prod_{n=1}^{N_j}\frac{m_{j,n}}{\Omega_{j,k}}\right)^t I_1 \quad (3.14)$$

where I_1 is

$$I_1 = \int_0^{\infty}\gamma^{t-\frac{1}{2}}e^{-\frac{\lambda}{2}\gamma}G_{N_i+N_j+2,2}^{1,N_i+N_j+1}\left[\frac{\Phi}{\gamma}\middle|\begin{matrix}\underline{u}\\ \underline{v}\end{matrix}\right]d\gamma \quad (3.15)$$

for $\Phi = \frac{\gamma_0^2}{C}\left(\prod_{n=1}^{N_i}\frac{\Omega_{i,n}}{m_{i,n}}\right)\left(\prod_{n=1}^{N_j}\frac{\Omega_{j,n}}{m_{j,n}}\right)$. Performing some algebraic manipulation and using the transformation and the argument simplification properties of the Meijer's G-function [131, 07.34.16.0002.01], I_1 is written in the form of

$$\begin{aligned} I_1 &= \int_0^{\infty}\Phi^{t-\frac{1}{2}}\left(\frac{\gamma}{\Phi}\right)^{t-\frac{1}{2}}e^{-\frac{\lambda}{2}\gamma}G_{N_i+N_j+2,2}^{1,N_i+N_j+1}\left[\frac{\Phi}{\gamma}\middle|\begin{matrix}\underline{u}\\ \underline{v}\end{matrix}\right]d\gamma \\ &= \int_0^{\infty}\Phi^{t-\frac{1}{2}}\left(\frac{\gamma}{\Phi}\right)^{t-\frac{1}{2}}e^{-\frac{\lambda}{2}\gamma}G_{2,N_i+N_j+2}^{N_i+N_j+1,1}\left[\frac{\gamma}{\Phi}\middle|\begin{matrix}1-\underline{v}\\ 1-\underline{u}\end{matrix}\right]d\gamma \\ &= \Phi^{t-\frac{1}{2}}\int_0^{\infty}e^{-\frac{\lambda}{2}\gamma}G_{2,N_i+N_j+2}^{N_i+N_j+1,1}\left[\frac{\gamma}{\Phi}\middle|\begin{matrix}\frac{1}{2},-\frac{1}{2}\\ \underline{w}\end{matrix}\right]d\gamma \end{aligned} \quad (3.16)$$

where $\underline{w} \triangleq t-\frac{1}{2}, m_{i,1}+t-\frac{1}{2}, ..., m_{i,N_i}+t-\frac{1}{2}, m_{j,1}-\frac{1}{2}, ..., m_{j,N_j}-\frac{1}{2}, -\frac{1}{2}$. This integral can be solved by using the integral property of the Meijer's G-function [131, 07.34.21.0088.01] and the average SER expression is obtained in the closed-form as

$$\begin{aligned}\bar{P}_{i,se} &= \frac{A\sqrt{B}}{2\sqrt{2\pi}}\left(\prod_{n=1}^{N_i}\Gamma(m_{i,n})\right)^{-1}\left(\prod_{n=1}^{N_j}\Gamma(m_{j,n})\right)^{-1}\sum_{t=0}^{\infty}\frac{(-1)^t}{t!}\gamma_0^{-t} \\ &\quad\times\left(\prod_{n=1}^{N_j}\frac{m_{j,n}}{\Omega_{j,n}}\right)^{t}\left(\frac{\gamma_0^2}{C}\left(\prod_{n=1}^{N_i}\frac{\Omega_{i,n}}{m_{i,n}}\right)\left(\prod_{n=1}^{N_j}\frac{\Omega_{j,n}}{m_{j,n}}\right)\right)^{t-\frac{1}{2}}\frac{2}{B} \\ &\quad\times G_{3,N_i+N_j+2}^{N_i+N_j+1,2}\left[\frac{2C}{B\gamma_0^2}\left(\prod_{n=1}^{N_i}\frac{m_{i,n}}{\Omega_{i,n}}\right)\left(\prod_{n=1}^{N_j}\frac{m_{j,n}}{\Omega_{j,n}}\right)\middle|\begin{matrix}0,\frac{1}{2},-\frac{1}{2}\\ \underline{w}\end{matrix}\right].\end{aligned} \tag{3.17}$$

3.1.3 Numerical Results

We present computer simulations to verify the analytical results in this section. The assumptions in the simulations are that the average powers of the channels fading parameters are equal as $\Omega_a = \Omega_b = 1$, and all vehicles transmit with the unit power, $P_a = P_b = P_r = 1$. We assume that the channels from a source to the relay and the relay to this source are symmetrical, that means, fading coefficients from one of the sources (V_a or V_b) to the relay and the relay to this source are the same.

Figure 3.2 reveals the impact of the cascading degrees of the channels on the outage probability while the threshold SNR is chosen as $\gamma_{th} = 5$ dB. In order to picture only the effect of the cascading degrees, the values of the fading parameters for both channels are assumed as equal, $m_a = m_b = 2$. During the simulations and the analytic calculations, the cascading degrees of the channels are set to $N_a = N_b = 1$, 2, 3 and 4. It is seen from the plots that the increasing cascading degree leads to degradation in the outage performance of the system, that means, the outage probability increases with the increasing cascading degree. For example, in order to obtain $P_{out} = 10^{-2}$, approximately extra 7 dB SNR is required in double Nakagami-m channels, where $N_a = N_b = 2$, in comparison with the classic Nakagami-m channels, where $N_a = N_b = 1$.

In Figure 3.3, we present the impact of the fading parameter values (m_a, m_b) of the channels on the outage probability for the threshold SNR $\gamma_{th} = 5$ dB. We choose the cascading degrees of the channels as equal as $N_a = N_b = 3$ to only show the effect of the fading parameters which are set as $m_a = m_b = 1.5$, 2, 3 and 4 in the simulations

and the analytic calculations. As shown in Figure 3.3, the outage probability decreases with the increasing values of the parameter m.

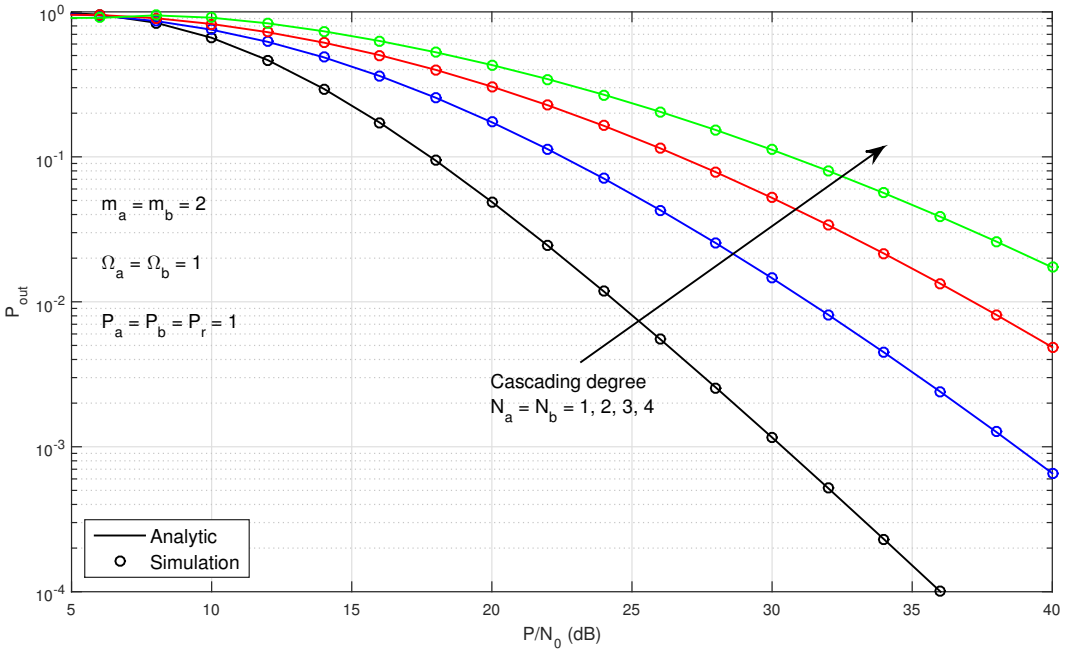

Figure 3.2 : Impact of the cascading degrees on the outage probability for $\gamma_{th} = 5$ dB.

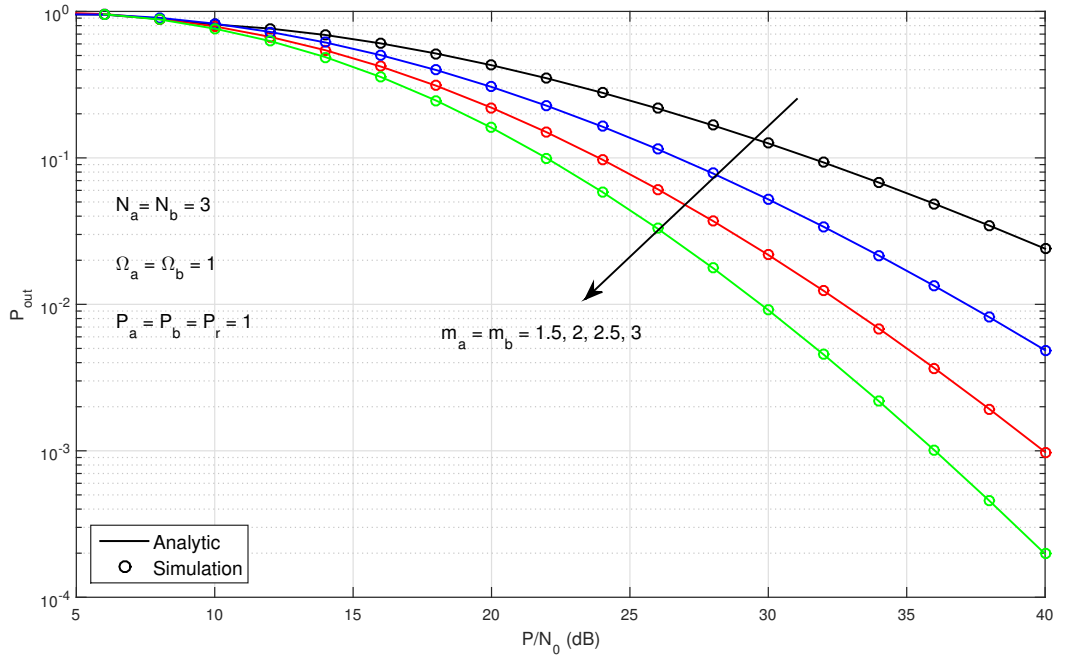

Figure 3.3 : Impact of m parameters on the outage probability for $\gamma_{th} = 5$ dB.

In Figure 3.4, we present the plots for the outage performance of the system in miscellaneous channel conditions with the asymmetric fading parameters and the cascading degrees for $\gamma_{th} = 5$ dB. Being compatible with Figure 3.2 and Figure 3.3, it is seen that the increasing values of the fading parameters in the channels have improving

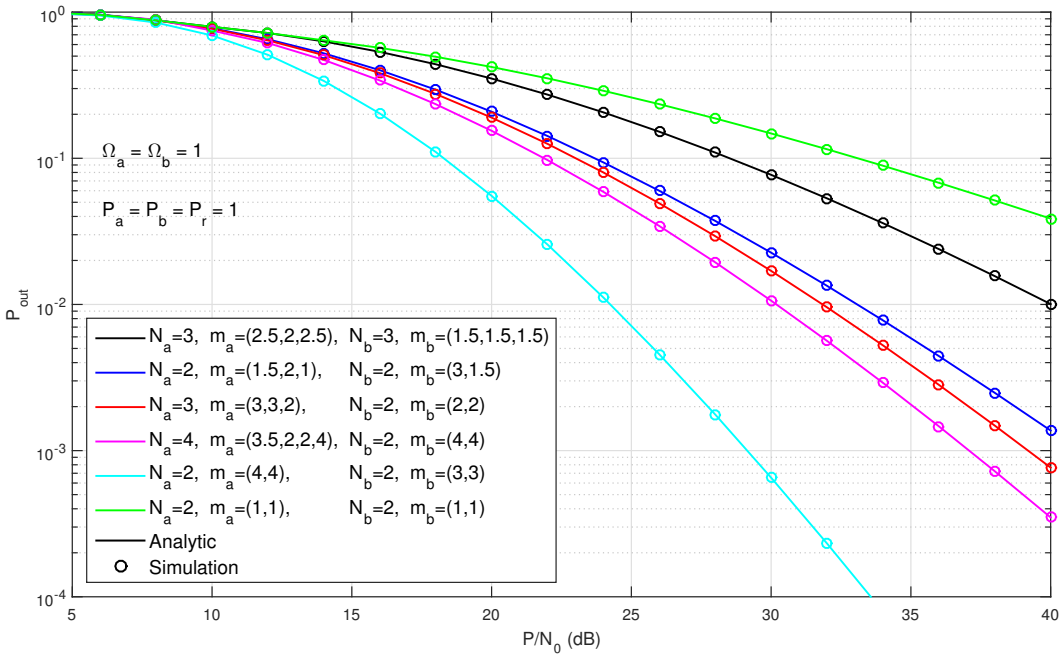

Figure 3.4 : The outage performance over miscellaneous channel conditions with the asymmetric fading parameters and the cascading degrees. $\gamma_{th} = 5$ dB.

effect on the outage probability while the increasing cascading degree is aggravating the outage probability performance.

In Figure 3.5 and Figure 3.6, we present the SER performance of the system for BPSK and 4-ASK modulation schemes, respectively. As it is expected, the increasing cascading degrees of the channels make the SER performance worse for both modulation types. For example, for BPSK modulation, the system provides SER values of 1.3×10^{-2}, 3.4×10^{-2} and 5.9×10^{-2} at SNR $= P/N_0 = 20$ dB for the cascading degrees $N_a = N_b = 2$, 3 and 4, respectively. On the other hand, we see from the figures that BPSK modulation offers significant amount of SNR gains over 4-ASK modulation for the same SER performance. It is also seen that the performance difference between BPSK and 4-ASK modulations is getting bigger when the cascading degrees of the channels increase.

In Figure 3.7 we provide the plots for the SER performance of the system in miscellaneous channels' conditions with the asymmetric fading parameters and the cascading degrees for BPSK modulation. As it is expected and in consistent with the results presented in Figure 3.5 and Figure 3.6, the SER performance of the system improves with the increasing values of the fading parameters, on the contrary, the increasing cascading degrees result in degradation in the SER performance.

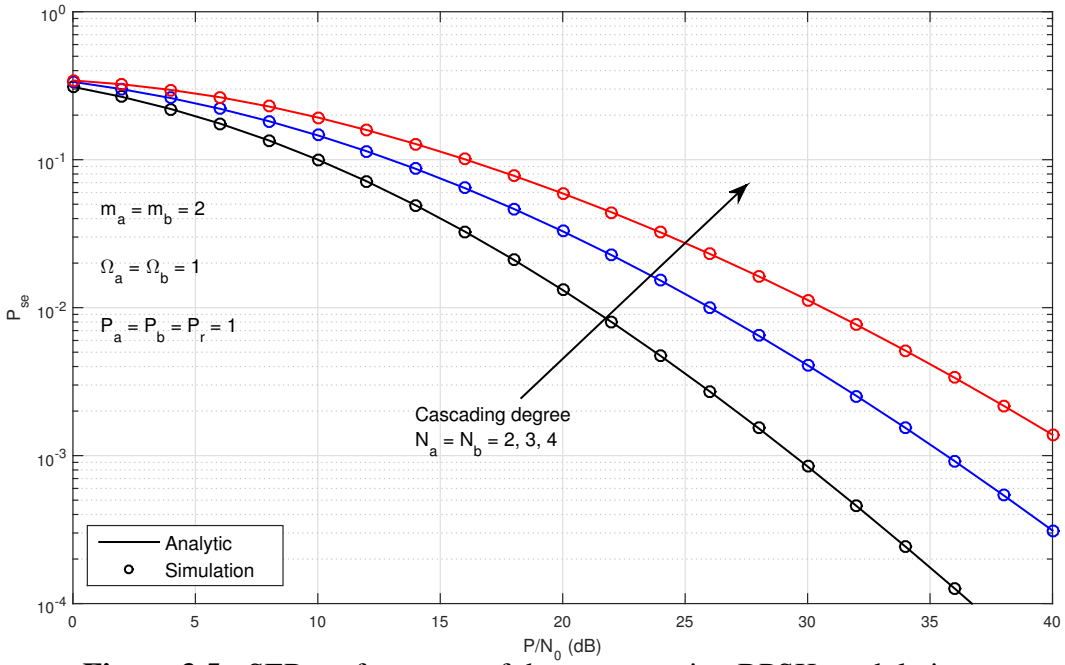

Figure 3.5 : SER performance of the system using BPSK modulation.

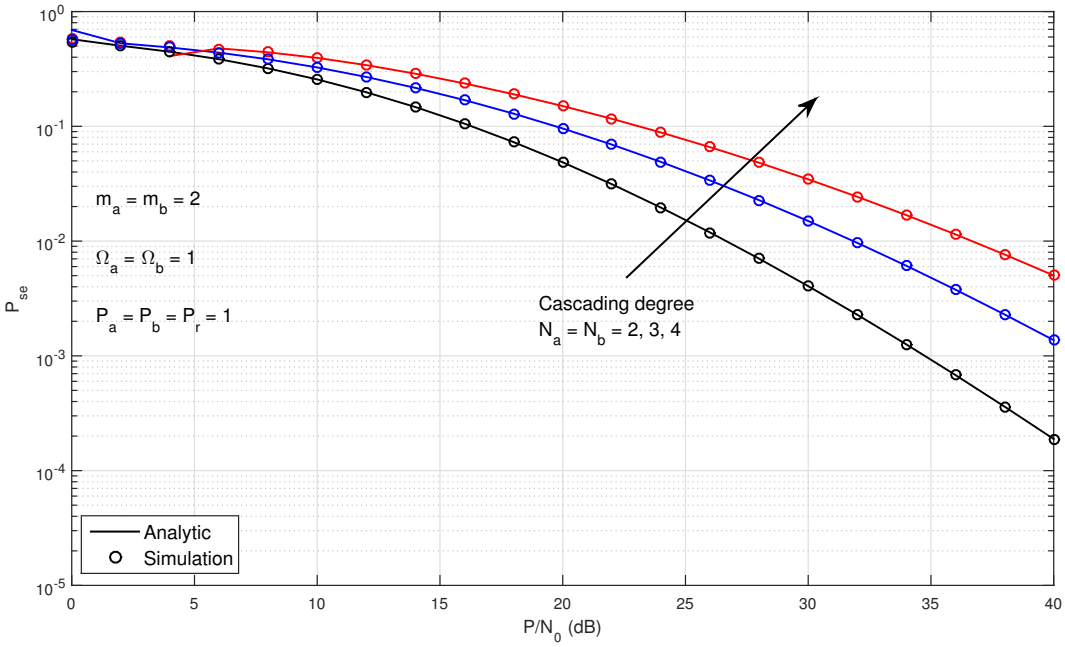

Figure 3.6 : SER performance of the system using 4-ASK modulation.

Notice also that all the derived analytic results for both the outage probability and the SER performances of the V2V communication system employing PLNC with the fixed gain AF method at relay over the cascaded Nakagami-*m* channels have perfect match with the simulation results.

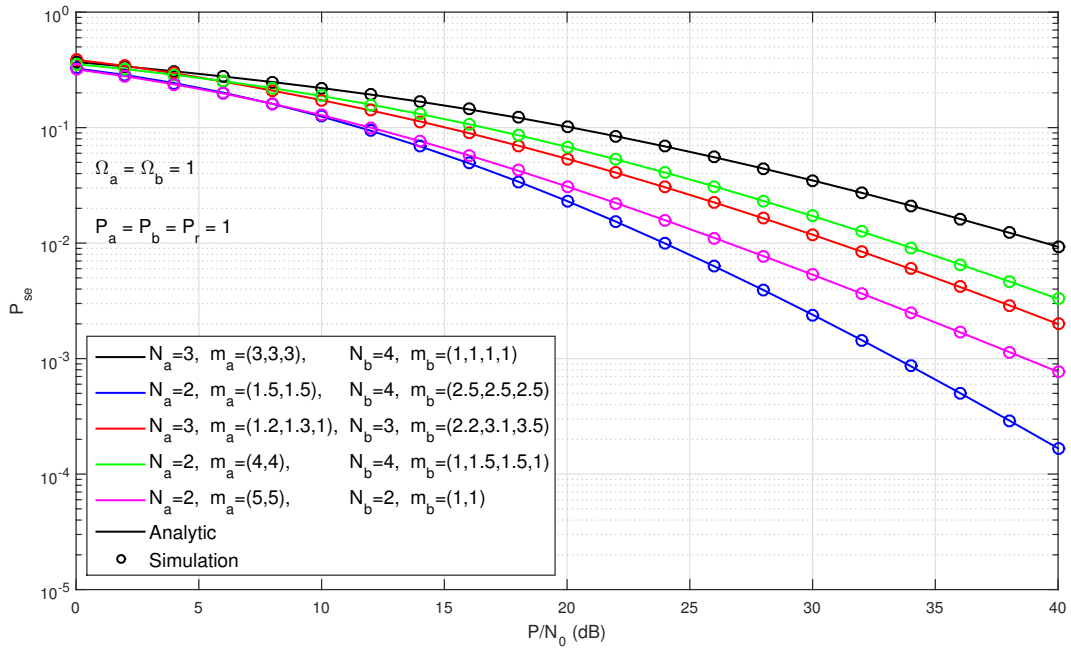

Figure 3.7 : SER performance of the system using BPSK modulation over miscellaneous channel conditions with the asymmetric fading parameters and the cascading degrees.

3.2 Fixed Gain AF PLNC over Cascaded Fast Rayleigh Fading Channels in the Presence of Self-Interference

V2V communication systems is an application field of M2M communications. In the known literature on the V2V/M2M communication, it is assumed that the channels are quasi-static fading channels. On the other hand, due to high-speed sources and even surrounding objects, physical environment changes so fast and therefore the fast fading channel model may be more realistic in practice. Secondly, it is also assumed in the literature on PLNC that all nodes have full CSI and they can cancel self-interference perfectly. However it is very difficult to reach this ideal situation in practice, because of the using limited-length pilot signals to avoid the high cost of the channel estimation in terms of spectral efficiency. Therefore, a design of the V2V/M2M communication system that takes into consideration of both fast fading and the existence of the self-interfering signals may be more reasonable for the realistic.

In this section, the outage performance analysis of a PLNC V2V/M2M communication system using fixed gain AF method at relay is performed in the presence of the self-interference over the cascaded and fast fading Rayleigh channels. As we

investigate the performance of the system, we derive the exact CDF of the end-to-end signal-to-interference-noise ratio (SINR) and obtain the exact closed-form outage probability by using this CDF. The numerical results are presented at the end of the section.

3.2.1 System Model

For the communication system in Figure 3.8, two source terminal V_a ve V_b are communicating with the help of V_r operates as a two-way relay, due to the absence of the LOS between the sources. We assume that all nodes in the system are mobile.

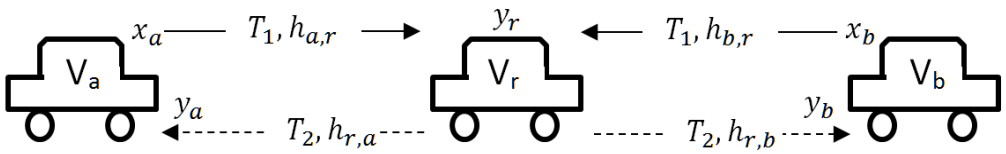

Figure 3.8 : V2V/M2M communication using PLNC over cascaded and fast fading channels.

So, the channels between V_a, V_b and V_r can be modeled as cascaded Rayleigh fading channels. Thus, for $\{i, j\} \in \{a, b, r\}$ and $i \neq j$, the fading coefficient $h_{i,j}$ of the channel between V_i and V_j is

$$h_{i,j} = \prod_{n=1}^{N_{i,j}} h_{i,j,n} \tag{3.18}$$

as the product of independent and non-identically Rayleigh distributed random variables denoted by $h_{i,j,n}$ with the average power $\Omega_{i,j,n} = E[h_{i,j,n}^2]$, $n = 1, ..., N_{i,j}$. Here $N_{i,j}$ is the cascading degree of the channel. The average power of the cascaded fading coefficient $h_{i,j}$ is

$$E[h_{i,j}^2] = \Omega_{i,j} = \prod_{n=1}^{N_{i,j}} \Omega_{i,j,n}. \tag{3.19}$$

In the system, it is also assumed that V_a, V_b and V_r transmit with unit power as $P_a = P_b = P_r = 1$. The additive noise signals at the nodes are assumed to be Gaussian random variables with zero mean and two-sided power spectral density of $N_0/2$. The channels are assumed as fast fading channels and therefore all $h_{i,j}$ coefficients stay constant in only one time slot during signaling. This is especially reasonable for V2V/M2M applications such as inter-vehicle networks where physical environment changes fast and continuously. Due to the fast fading nature of the channels, it is also assumed that none of the sources in the system has complete CSI. On the other hand,

it may be said that the sources and the relay know the average statistics of the CSI for the channels. That may be achieved by using the pilot signals in a single handshake phase to be initiated among the sources and the relay before the communication starts. Furthermore, messaging between the sources is accomplished in two time slots by using PLNC with the fixed gain AF method. Therefore, V_a and V_b simultaneously send their messages x_a and x_b to V_r and the relay receives the composite signal

$$y_r = h_{a,r}x_a + h_{b,r}x_b + n_r \tag{3.20}$$

at the end of the first time slot T_1. Here n_r is the additive noise at the antenna of V_r. In the second time slot T_2, the relay amplifies y_r with the fixed power scaling factor G, such that

$$G^2 = C^{-1} \tag{3.21}$$

for $C = \Omega_{i,r} + \Omega_{j,r} + N_0$, then forwards it to the sources. For $i, j \in \{a,b\}$ and $i \neq j$, after the self-interference cancellation is employed, the received signal at the source V_i is

$$y_i = \sqrt{\eta}h_{r,i}Gh_{i,r}x_i + h_{r,i}Gh_{j,r}x_j + h_{r,i}Gn_r + n_i \tag{3.22}$$

where n_i is additive noise. The first term on the right-side of (3.22), $\sqrt{\eta}h_{r,i}Gh_{i,r}x_i$, denotes the remaining part of the information-bearing signal belongs to V_i after employing the self-interference cancellation procedure. The constant η, $0 < \eta \leq 1$, points the success degree of the cancellation algorithm used by V_i. $\eta \to 0$ means that whole self-interference is successfully removed from the incoming signal. $\eta = 1$ means that the self-interference cancellation is not performed. This may be preferable due to the reasons for avoiding the receiver complexity, cost, power and time consumption affords. Any other values of η in (0,1) correspond to partially success in performing self-interference cancellation. Therefore, the instantaneous end-to-end SINR γ_i at the source node V_i is obtained as

$$\gamma_i^{SINR} = \frac{h_{r,i}^2 h_{j,r}^2}{\eta h_{r,i}^2 h_{i,r}^2 + h_{r,i}^2 N_0 + CN_0} \tag{3.23}$$

by dividing the desired signal power by the total power of the interference and the noise.

3.2.2 Performance Analysis

We start the analysis by investigating the CDF of γ_i which is

$$\begin{aligned} F_{\gamma_i^{SINR}}(\gamma) &= P\left(\gamma_i^{SINR} \leq \gamma\right) \\ &= P\left(\frac{h_{r,i}^2 h_{j,r}^2}{h_{r,i}^2 h_{i,r}^2 \eta + h_{r,i}^2 N_0 + C N_0} \leq \gamma\right). \end{aligned} \tag{3.24}$$

For $\gamma_i \triangleq h_{i,r}^2$, $\gamma_j \triangleq h_{j,r}^2$ and $\gamma_r \triangleq h_{r,i}^2$, (3.24) can be expressed in the form of

$$\begin{aligned} F_{\gamma_i^{SINR}}(\gamma) &= P\left(\gamma_j \leq \gamma\left(\eta\gamma_i + N_0 + \frac{CN_0}{\gamma_r}\right)\right) \\ &= \int_0^\infty \int_0^\infty F_{\gamma_j}\left(\gamma\left(\eta\gamma_i + N_0 + \frac{CN_0}{\gamma_r}\right)\right) f_{\gamma_r}(\gamma_r)\, d\gamma_r f_{\gamma_i}(\gamma_i)\, d\gamma_i. \end{aligned} \tag{3.25}$$

With the help of (2.15) and (2.16), the pdf and the CDF of γ_s become

$$f_{\gamma_s}(\gamma) = \gamma^{-1} G_{0,N_{s,d}}^{N_{s,d},0}\left[\gamma\Omega_{s,d}^{-1}\middle|\begin{matrix} - \\ 1,\ldots,1 \end{matrix}\right], \tag{3.26a}$$

$$F_{\gamma_s}(\gamma) = G_{1,N_{s,d}+1}^{N_{s,d},1}\left[\gamma\Omega_{s,d}^{-1}\middle|\begin{matrix} 1 \\ 1,\ldots,1,0 \end{matrix}\right] \tag{3.26b}$$

respectively, where $s \in \{i,j,r\}$, $d = r$ if $s \in \{i,j\}$ or $d = i$ if $s = r$. Thus, the inner integral of (3.25) is written as

$$\begin{aligned} I_0 &= \int_0^\infty F_{\gamma_j}\left(\gamma\left(\eta\gamma_i + N_0 + \frac{CN_0}{\gamma_r}\right)\right) f_{\gamma_r}(\gamma_r)\, d\gamma_r \\ &= \int_0^\infty G_{1,N_{j,r}+1}^{N_{j,r},1}\left[\gamma\left(\eta\gamma_i + N_0 + \frac{CN_0}{\gamma_r}\right)\Omega_{j,r}^{-1}\middle|\begin{matrix} 1 \\ 1,\ldots,1,0 \end{matrix}\right] \gamma_r^{-1} G_{0,N_{r,i}}^{N_{r,i},0}\left[\gamma_r\Omega_{r,i}^{-1}\middle|\begin{matrix} - \\ 1,\ldots,1 \end{matrix}\right] d\gamma_r \end{aligned} \tag{3.27}$$

Applying $\tau = \frac{\gamma CN_0}{\Omega_{j,r}}\gamma_r^{-1}$ transformation, then, using the transformation and argument simplification property of the Meijer's G-function [131, 07.34.16.0002.01], (3.27) has the form of

$$I_0 = \int_0^\infty \tau^{-1} G_{N_{r,i},0}^{0,N_{r,i}}\left[\frac{\Omega_{j,r}\Omega_{r,i}}{\gamma CN_0}\tau\middle|\begin{matrix} 0,\ldots,0 \\ - \end{matrix}\right] G_{1,N_{j,r}+1}^{N_{j,r},1}\left[\tau + \frac{\gamma}{\Omega_{j,r}}\left(\eta\gamma_i + N_0\right)\middle|\begin{matrix} 1 \\ 1,\ldots,1,0 \end{matrix}\right] d\tau \tag{3.28}$$

By using the integral property with the shifted arguments [131, 07.34.21.0082.01] and the transformation and argument simplification property [131, 07.34.16.0002.01] of the Meijer's G-function, I_0 can be solved as

$$I_0 = \sum_{t=0}^{\infty} \frac{(-1)^t}{t!} \left(\frac{\gamma N_0}{\Omega_{j,r}}\right)^t \left(\frac{\eta\gamma_i}{N_0}+1\right)^t G_{N_{r,i}+N_{j,r}+2,2}^{1,N_{r,i}+N_{j,r}+1}\left[\frac{\Omega_{j,r}\Omega_{r,i}}{CN_0}\gamma\middle|_{t,t+1}^{1,0,...,0,t,...,t,t+1}\right] \tag{3.29}$$

Substituting (3.29) in (3.25), and using $(x+y)^t = \sum_{n=0}^{t}\binom{t}{n}x^n y^{t-n}$ binom expansion, $F_{\gamma_i^{SINR}}(\gamma)$ becomes

$$F_{\gamma_i^{SINR}}(\gamma) = \sum_{t=0}^{\infty} \frac{(-1)^t}{t!} \left(\frac{\gamma N_0}{\Omega_{j,r}}\right)^t G_{N_{r,i}+N_{j,r}+2,2}^{1,N_{r,i}+N_{j,r}+1}\left[\frac{\Omega_{j,r}\Omega_{r,i}}{CN_0}\gamma\middle|_{t,t+1t}^{1,0,...,0,t,...,t,t+1}\right] \times \sum_{n=0}^{t}\binom{t}{n}\left(\frac{\eta}{N_0}\right)^{t-n} I_1 \tag{3.30}$$

where I_1 is

$$I_1 = \int_0^{\infty} \gamma_i^{t-n-1} G_{0,N_{i,r}}^{N_{i,r},0}\left[\gamma_i\Omega_{i,r}^{-1}\middle|_{1,...,1}^{-}\right] d\gamma_i. \tag{3.31}$$

I_1 is solved by using the integral property of the Meijer's G-function [131, 07.34.21.0009.01] as

$$I_1 = \Omega_{i,r}^{t-n}\Gamma(t-n+1)^{N_{i,r}}. \tag{3.32}$$

By substituting (3.32) in (3.30), we obtain the CDF of γ_i as

$$F_{\gamma_i^{SINR}}(\gamma) = \sum_{t=0}^{\infty}\left(-\frac{\gamma N_0}{\Omega_{j,r}}\right)^t G_{N_{r,i}+N_{j,r}+2,2}^{1,N_{r,i}+N_{j,r}+1}\left[\frac{\Omega_{j,r}\Omega_{r,i}}{CN_0}\gamma\middle|_{t,t+1}^{1,0,...,0,t,...,t,t+1}\right] \times \sum_{n=0}^{t}\left(\frac{\eta\Omega_{i,r}}{N_0}\right)^{t-n}\frac{\Gamma(k-n+1)^{N_{i,r}}}{(t-n)!n!} \tag{3.33}$$

in the closed-form. Therefore, the outage probability of the source node V_i is obtained as

$$P_{out,i} = P\left(\gamma_i^{SINR} \le \gamma_{th}\right) = F_{\gamma_i^{SINR}}(\gamma_{th}). \tag{3.34}$$

in the closed-form for the threshold SINR γ_{th}.

3.2.3 Numerical Results

We present computer simulations to verify analytical results in this section. In the simulations, it is assumed that the fading coefficients of the channels have unit average power, $\Omega_{a,r} = \Omega_{r,a} = \Omega_{b,r} = \Omega_{r,b} = 1$. In Figure 3.9, the impact of the interfering signal power on the outage probability is presented in association with the various values of η. We choose the threshold SINR as $\gamma_{th} = 5$ dB and the cascading degrees between the sources and the relay as $N_{a,r} = N_{r,a} = 2$. The figure shows that error floors occur for -13 dB and -20 dB attenuations at the interference signal power. On the other hand, self-interference effect does not cause an error floor on the outage probability when the attenuation falls to the level of -30 dB.

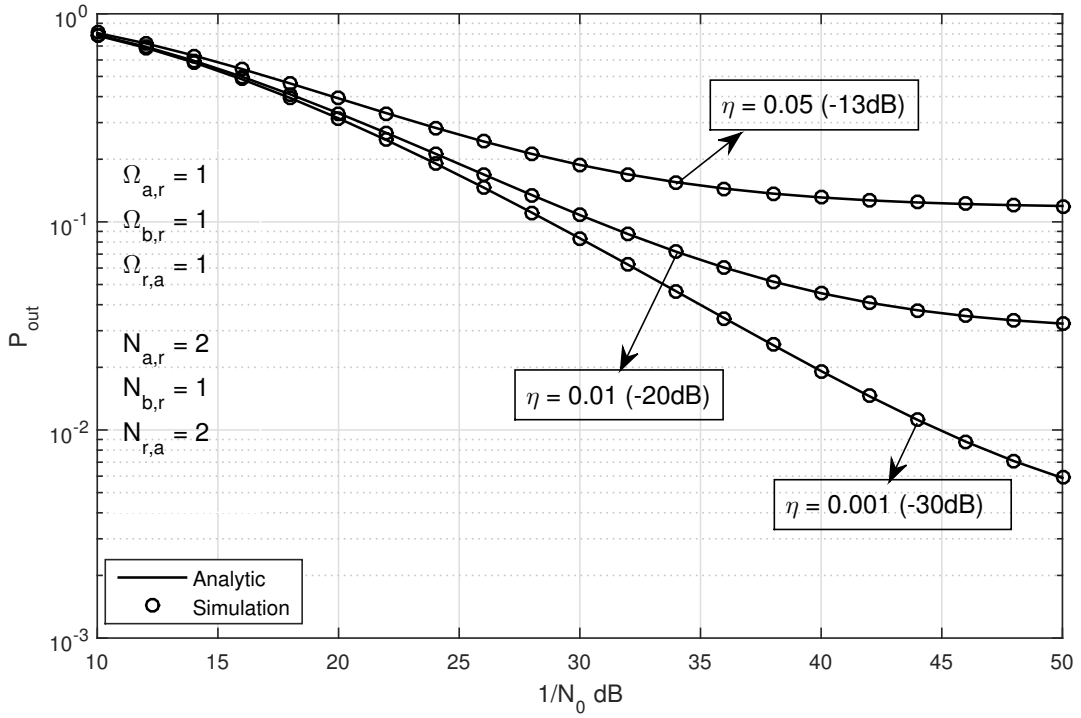

Figure 3.9 : Impact of the interference power on the outage probability for $\gamma_{th} = 5$ dB.

Figure 3.10 reveals the impact of the cascading degrees of the channels on the outage probability while the threshold SNR is chosen as $\gamma_{th} = 5$ dB. It is seen from the plots that the increasing cascading degree leads to degradation in the outage performance of the system.

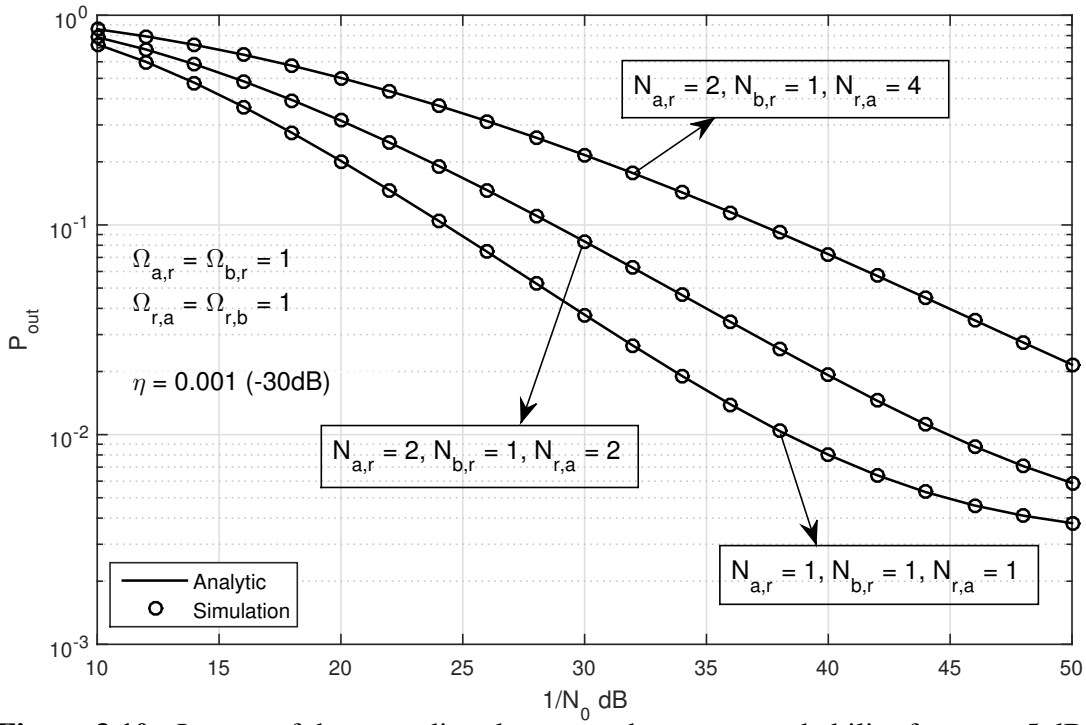

Figure 3.10 : Impact of the cascading degree on the outage probability for $\gamma_{th} = 5$ dB.

4. DESIGN OF MULTI-ANTENNA V2V COMMUNICATION SYSTEMS EMPLOYING VARIABLE GAIN AF PLNC

The PLNC technique can provide higher data transmission rates to be required in case of emergency situations which must be reported to many vehicles in a short period of time in urban traffic. While using PLNC technique, it is possible to improve the error performance and enhance the data transmission rates by using more than one relay or antenna. On the other hand, instead of using all of the relays or antennas, an improved performance can be achieved by selecting one or a group of them according to certain selection criteria. In this way, the transmission rate of the system can also be increased.

4.1 Relay Antenna Selection for V2V Communications using PLNC over Cascaded Fading Channels

In this section, we propose a V2V communication system employing PLNC with variable gain AF method at the relay which has multiple antennas and focuses on the antenna selection problem at the relay for double-Nakagami-m fading channel model.

4.1.1 System Model

Due to no LOS between V_a and V_b vehicles in the V2V PLNC system shown in Figure 4.1, they are communicating via V_r acting as a relay having M_r antennas. The fading coefficients of the channels among the source nodes (V_a, V_b) and the k-th antenna of the relay are independent and non-identically distributed random variables which are denoted by $h_{a,k}$ and $h_{b,k}$, respectively. For $i \in \{a,b\}$,

$$h_{i,k} = h_{i,k,1}\, h_{i,k,2} \tag{4.1}$$

where $h_{i,k,1}$ and $h_{i,k,2}$ are independent Nakagami-m distributed random variables which make the channel between the source vehicle V_i and the k-th antenna of the relay double-Nakagami-m distributed. The pdf of the channel fading coefficient $h_{i,k}$ is given

by

$$f_{h_{i,k}}(h) = \frac{4h^{m_{i,k,1}+m_{i,k,2}-1}}{\prod_{n=1}^{2}\Gamma(m_{i,k,n})(\Omega_{i,k,n}/m_{i,k,n})^{(m_{i,k,1}+m_{i,k,2})/2}} K_{m_{i,k,1}-m_{i,k,2}}\left(2h\sqrt{\prod_{n=1}^{2}\frac{m_{i,k,n}}{\Omega_{i,k,n}}}\right) \tag{4.2}$$

where $m_{i,k,n}$ and $\Omega_{i,k,n} = E[h_{i,k,n}^2]$ are fading parameter and average power of $h_{i,k,n}$ in (4.1), respectively [19]. For simplicity, V_a, V_b and V_r are assumed to have equal transmitting power as $P_a = P_b = P_r = P$. We assume perfect channel estimation, the source nodes and the relay have full CSI, and are able to cancel the self-interference. In the system, the relay employs PLNC using AF method and therefore message transaction between V_a and V_b is accomplished in two time slots. In the first time slot, V_a and V_b send their messages x_a and x_b simultaneously to the V_r. The k-th antenna of V_r receives the signal y_k as

$$y_k = h_{a,k}\sqrt{P}x_a + h_{b,k}\sqrt{P}x_b + n_k \tag{4.3}$$

where n_k is the additive Gaussian noise with zero-mean and two-sided power spectral density of $N_0/2$. The relay amplifies y_k with the power scaling factor

$$G = \sqrt{\frac{P}{Ph_{a,k}^2 + Ph_{b,k}^2 + N_0}} \tag{4.4}$$

and forwards it to the sources in the second time slot. For $\{i, j\} \in \{a, b\}$ and $i \neq j$, the received signal at V_i is

$$y_{i,k} = h_{i,k}Gh_{i,k}\sqrt{P}x_i + h_{i,k}Gh_{j,k}\sqrt{P}x_j + h_{i,k}Gn_k + n_i. \tag{4.5}$$

After cancelling the self-interference, the remaining signal becomes

$$\tilde{y}_{i,k} = h_{i,k}Gh_{j,k}\sqrt{P}x_j + h_{i,k}Gn_k + n_i \tag{4.6}$$

where n_i is assumed to be zero-mean Gaussian random variable with two-sided power spectral density of $N_0/2$. Let the instantaneous SNR of the channels between the source

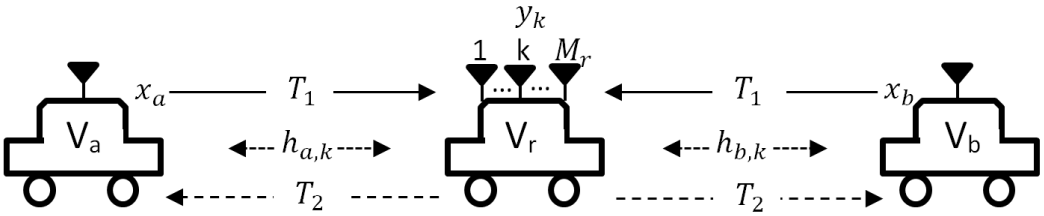

Figure 4.1 : V2V Communication using PLNC with multi-antenna relay.

nodes and the relay be

$$\gamma_{i,k} \triangleq h_{i,k}^2 \frac{P}{N_0} \quad \text{and} \quad \gamma_{j,k} \triangleq h_{j,k}^2 \frac{P}{N_0} \tag{4.7}$$

then the instantaneous E2E-SNR at V_i represented by $\Upsilon_{i,k}$ can be written approximately [102] as

$$\Upsilon_{i,k} \cong \frac{\gamma_{i,k}\gamma_{j,k}}{2\gamma_{i,k}+\gamma_{j,k}}. \tag{4.8}$$

Antenna selection on the relay is performed by $\max-\min$ criterion [132, 133] over the E2E-SNR values of the channels, and the index of selected antenna K is determined as follows

$$K = \underset{1\le k\le M_r}{\arg\max}\Big\{\Upsilon_k = \min\{\Upsilon_{a,k}, \Upsilon_{b,k}\}\Big\}. \tag{4.9}$$

For this purpose, an antenna selection phase is initiated. In this phase, the source nodes respectively send the pilot signals to the relay before they start to transmit their data messages. The overall SNR of V2V PLNC system with antenna selection can be defined as

$$\Upsilon_{(K)} = \max_{1\le k\le M_r}\Big\{\Upsilon_k = \min\{\Upsilon_{a,k}, \Upsilon_{b,k}\}\Big\}. \tag{4.10}$$

4.1.2 Performance Analysis

In order to analyze the performance of the V2V PLNC system with antenna selection, the pdf of $\Upsilon_{i,k}$ should be derived first. However, to the best of our knowledge, a closed-form solution for this pdf is not available. On the other hand, we can easily show that the following inequalities are satisfied for $\Upsilon_{i,k}$,

$$\begin{aligned}
\gamma_{j,k} \ge 2\gamma_{i,k} \quad &\Rightarrow \quad \frac{\gamma_{i,k}\gamma_{j,k}}{2\gamma_{i,k}+\gamma_{j,k}} \le \frac{\gamma_{i,k}\gamma_{j,k}}{\gamma_{j,k}} \Rightarrow \Upsilon_{i,k} \le \gamma_{i,k} \\
\gamma_{j,k} \le 2\gamma_{i,k} \quad &\Rightarrow \quad \frac{\gamma_{i,k}\gamma_{j,k}}{2\gamma_{i,k}+\gamma_{j,k}} \le \frac{\gamma_{i,k}\gamma_{j,k}}{2\gamma_{i,k}} \Rightarrow \Upsilon_{i,k} \le \frac{\gamma_{j,k}}{2} \\
\gamma_{j,k} \ge \gamma_{i,k} \quad &\Rightarrow \quad \frac{\gamma_{i,k}\gamma_{j,k}}{2\gamma_{i,k}+\gamma_{j,k}} \ge \frac{\gamma_{i,k}\gamma_{j,k}}{3\gamma_{j,k}} \Rightarrow \Upsilon_{i,k} \ge \frac{\gamma_{i,k}}{3} \\
\gamma_{j,k} \le \gamma_{i,k} \quad &\Rightarrow \quad \frac{\gamma_{i,k}\gamma_{j,k}}{2\gamma_{i,k}+\gamma_{j,k}} \ge \frac{\gamma_{i,k}\gamma_{j,k}}{3\gamma_{i,k}} \Rightarrow \Upsilon_{i,k} \ge \frac{\gamma_{j,k}}{3}
\end{aligned}$$

Hence an upper and a lower bound for $\Upsilon_{i,k}$ can be

$$\begin{aligned}
\Upsilon_{i,k} &\le \frac{1}{2}\min(2\gamma_{i,k}, \gamma_{j,k}) = \Upsilon_{i,k}^U \\
\Upsilon_{i,k} &\ge \frac{1}{3}\min(\gamma_{i,k}, \gamma_{j,k}) = \Upsilon_{i,k}^L
\end{aligned} \tag{4.11}$$

respectively [134]. Therefore we first derive the CDF of $\Upsilon_{i,k}^{U}$ as

$$\begin{aligned} F_{\Upsilon_{i,k}^{U}}(\gamma) &= 1 - P\left(\gamma_{i,k} > \gamma, \gamma_{j,k} > 2\gamma\right) \\ &= F_{\gamma_{i,k}}(\gamma) + F_{\gamma_{j,k}}(2\gamma) - F_{\gamma_{i,k}}(\gamma) F_{\gamma_{j,k}}(2\gamma) \end{aligned} \tag{4.12}$$

then we obtain the CDF of $\Upsilon_{i,k}^{L}$ as

$$\begin{aligned} F_{\Upsilon_{i,k}^{L}}(\gamma) &= 1 - P\left(\gamma_{i,k} > 3\gamma, \gamma_{j,k} > 3\gamma\right) \\ &= F_{\gamma_{i,k}}(3\gamma) + F_{\gamma_{j,k}}(3\gamma) - F_{\gamma_{i,k}}(3\gamma) F_{\gamma_{j,k}}(3\gamma). \end{aligned} \tag{4.13}$$

At this point, with the help of (2.16), and for $v \in \{i, j\}$, ($\{i, j\} \in \{a, b\}$ and $i \neq j$), using the definitions $\bar{\gamma}_{v,k} \triangleq E[\gamma_{v,k}]$, $C_{v,k} \triangleq \left(\Gamma(m_{v,k,1})\Gamma(m_{v,k,2})\right)^{-1}$ and $K_{v,k} \triangleq m_{v,k,1} m_{v,k,2} / \bar{\gamma}_{v,k}$, the CDFs of $\gamma_{i,k}$ and $\gamma_{j,k}$ becomes

$$F_{\gamma_{v,k}}(\gamma) = C_{v,k} G_{1,3}^{2,1}\left[\gamma K_{v,k}\Big|_{m_{v,k,1}, m_{v,k,2}, 0}^{1}\right]. \tag{4.14}$$

Substituting this CDF into (4.12) and (4.13), we obtain the CDF of $\Upsilon_{i,k}^{U}$ as

$$\begin{aligned} F_{\Upsilon_{i,k}^{U}}(\gamma) &= C_{i,k} G_{1,3}^{2,1}\left[\gamma K_{i,k}\Big|_{m_{i,k,1}, m_{i,k,2}, 0}^{1}\right] + C_{j,k} G_{1,3}^{2,1}\left[2\gamma K_{j,k}\Big|_{m_{j,k,1}, m_{j,k,2}, 0}^{1}\right] \\ &\quad - C_{j,k} G_{1,3}^{2,1}\left[2\gamma K_{j,k}\Big|_{m_{j,k,1}, m_{j,k,2}, 0}^{1}\right] C_{i,k} G_{1,3}^{2,1}\left[\gamma K_{i,k}\Big|_{m_{i,k,1}, m_{i,k,2}, 0}^{1}\right] \end{aligned} \tag{4.15}$$

and the CDF of $\Upsilon_{i,k}^{L}$ as

$$\begin{aligned} F_{\Upsilon_{i,k}^{L}}(\gamma) &= C_{i,k} G_{1,3}^{2,1}\left[3\gamma K_{i,k}\Big|_{m_{i,k,1}, m_{i,k,2}, 0}^{1}\right] + C_{j,k} G_{1,3}^{2,1}\left[3\gamma K_{j,k}\Big|_{m_{j,k,1}, m_{j,k,2}, 0}^{1}\right] \\ &\quad - C_{j,k} G_{1,3}^{2,1}\left[3\gamma K_{j,k}\Big|_{m_{j,k,1}, m_{j,k,2}, 0}^{1}\right] C_{i,k} G_{1,3}^{2,1}\left[3\gamma K_{i,k}\Big|_{m_{i,k,1}, m_{i,k,2}, 0}^{1}\right]. \end{aligned} \tag{4.16}$$

The CDF of $\Upsilon_k = \min\{\Upsilon_{a,k}, \Upsilon_{b,k}\}$ approximately becomes

$$F_{\Upsilon_k}(\gamma) \cong F_{\Upsilon_{a,k}}(\gamma) + F_{\Upsilon_{b,k}}(\gamma) - F_{\Upsilon_{a,k}}(\gamma) F_{\Upsilon_{b,k}}(\gamma). \tag{4.17}$$

Thus the CDF of $\Upsilon_{(K)}$ in (4.10) is obtained as

$$F_{\Upsilon_{(K)}}(\gamma) = \prod_{k=1}^{M_r} F_{\Upsilon_k}(\gamma). \tag{4.18}$$

Substituting (4.15) and (4.16) into (4.17) and (4.18) we can obtain the upper and the lower bound expressions of $F_{\Upsilon_{(K)}}(\gamma)$ in the closed-form.

4.1.2.1 Outage probability

The outage probability for the proposed V2V PLNC system is given as

$$P_{out} = F_{\Upsilon_{(K)}}(\gamma_{th}) \tag{4.19}$$

where γ_{th} denotes the threshold value for $\Upsilon_{(K)}$. Using $\Upsilon_{i,k}^{U}$ and $\Upsilon_{i,k}^{L}$ in (4.17) - (4.19) we obtain the lower and the upper bounds of P_{out}, respectively.

4.1.2.2 Asymptotic diversity order

Asymptotic diversity order of the proposed system can be obtained by applying the method in [135], which examines the behavior of the system in high SNR regime. Accordingly the pdf of $\Upsilon_{(K)}$ for $\zeta = \gamma/\bar{\gamma}$ can be written

$$f_{\Upsilon_{(K)}}(\zeta) = \alpha\zeta^{d_o} + O(\zeta^{d_o+1}) \tag{4.20}$$

as a function of ζ, then as $\zeta \to 0^{+}$ the asymptotic diversity order becomes d_o. By deriving (4.12) with respect to γ, the pdf of the upper bound of $\Upsilon_{i,k}$ is found as

$$f_{\Upsilon_{i,k}^{U}}(\gamma) = f_{\gamma_{i,k}}(\gamma) + 2f_{\gamma_{j,k}}(2\gamma) - f_{\gamma_{i,k}}(\gamma)F_{\gamma_{j,k}}(2\gamma) - 2f_{\gamma_{j,k}}(2\gamma)F_{\gamma_{i,k}}(\gamma). \tag{4.21}$$

Using (4.17), the pdf of the upper bound of Υ_k becomes

$$f_{\Upsilon_k^{U}}(\gamma) = f_{\Upsilon_{a,k}^{U}}(\gamma) + f_{\Upsilon_{b,k}^{U}}(\gamma) - f_{\Upsilon_{a,k}^{U}}(\gamma)F_{\Upsilon_{b,k}^{U}}(\gamma) - f_{\Upsilon_{a,k}^{U}}(\gamma)F_{\Upsilon_{b,k}^{U}}(\gamma) \tag{4.22}$$

and using (4.18), the pdf of the upper bound of $\Upsilon_{(K)}$ becomes

$$f_{\Upsilon_{(K)}^{U}}(\gamma) = M_r f_{\Upsilon_k^{U}}(\gamma)F_{\Upsilon_k^{U}}(\gamma)^{M_r-1}. \tag{4.23}$$

For the CDF in (4.14), the pdf of $\gamma_{v,k}$ is

$$f_{\gamma_{v,k}}(\gamma) = \frac{1}{\gamma}C_{v,k}G_{0,2}^{2,0}\left[\gamma K_{v,k}\Big|_{m_{v,k,1},\, m_{v,k,2}}^{-}\right],\ v \in \{i,j\},\ \{i,j\} \in \{a,b\}, i \neq j. \tag{4.24}$$

Using the series representation property [131, 07.34.06.0006.01] of the Meijer's G-function, for $\zeta \to 0^{+}$,

$$\begin{aligned} f_{\gamma_{v,k}}(\zeta) \;\cong\; & \frac{1}{\bar{\gamma}_{v,k}}\frac{\Gamma(m_{v,k,2}-m_{v,k,1})}{\Gamma(m_{v,k,1})\Gamma(m_{v,k,2})}\left(m_{v,k,1}m_{v,k,2}\right)^{m_{v,k,1}}\zeta^{m_{v,k,1}-1} \\ & + \frac{1}{\bar{\gamma}_{v,k}}\frac{\Gamma(m_{v,k,1}-m_{v,k,2})}{\Gamma(m_{v,k,1})\Gamma(m_{v,k,2})}\left(m_{v,k,1}m_{v,k,2}\right)^{m_{v,k,2}}\zeta^{m_{v,k,2}-1} \end{aligned} \tag{4.25}$$

and

$$F_{\gamma_{v,k}}(\zeta) \cong \frac{\Gamma(m_{v,k,2}-m_{v,k,1})}{\Gamma(1+m_{v,k,1})\Gamma(m_{v,k,2})}\left(m_{v,k,1}m_{v,k,2}\right)^{m_{v,k,1}}\zeta^{m_{v,k,1}} + \frac{\Gamma(m_{v,k,1}-m_{v,k,2})}{\Gamma(m_{v,k,1})\Gamma(1+m_{v,k,2})}\left(m_{v,k,1}m_{v,k,2}\right)^{m_{v,k,2}}\zeta^{m_{v,k,2}}. \tag{4.26}$$

We assume that all channels have equal average SNR, i.e., $\bar{\gamma}_{v,k} = \bar{\gamma}$. Then, by substituting (4.25) and (4.26) into (4.21) and following (4.22) and (4.23), we can obtain $f_{\Upsilon^U_{(K)}}(\beta)$, and then by rearranging the expression of $f_{\Upsilon^U_{(K)}}(\beta)$ in the form of (4.20), the asymptotic diversity order of the system can be expressed as follows

$$d_o = M_r \min_{1\leq k\leq M_r}(m_{a,k,1}, m_{a,k,2}, m_{b,k,1}, m_{b,k,2}) \tag{4.27}$$

as a function of the number of relay antennas and channel parameters. Similarly by evaluating the same analysis for the lower bound of $\Upsilon_{(K)}$, it is seen that the same asymptotic diversity order in 4.27 is obtained.

4.1.3 Numerical Results

In this section, we present computer simulations to verify the analysis on the theoretical outage probability and asymptotic diversity order expression derived in the previous section for the proposed V2V PLNC system with antenna selection. In the simulations, we assume that the fading coefficients of the double-Nakagami-*m* channels have unity average power, i.e., $E[h^2_{a,k}] = E[h^2_{b,k}] = 1$. The relay and the vehicles are assumed to transmit with the average power of $P = 1$.

Figure 4.2 presents the impact of the number of the relay antennas on the outage probability in the V2V PLNC system with antenna selection. $\gamma_{th} = 3$ dB, and the number of the relay antennas are chosen as $M_r = 2$, 4 and 6. Here m parameter values in all cascaded channels are assumed to be the same as $m = 2.5$. As shown on the graph, the increasing number of relay antennas decreases the outage probability of the system. As it is seen, the lower bound of the outage probability derived in this paper is very tight. The diversity orders $(5, 10, 15)$ obtained by using the simulations are consistent with those obtained by the analytical expression given in (2.6).

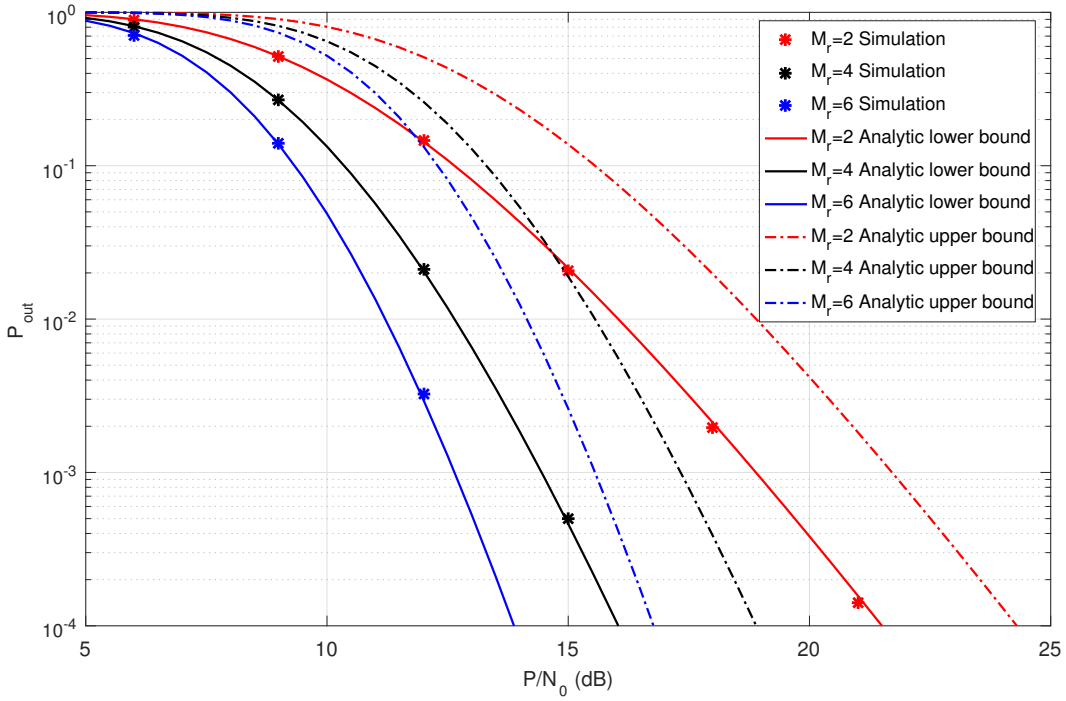

Figure 4.2 : Impact of the number of the relay antennas on the outage probability.

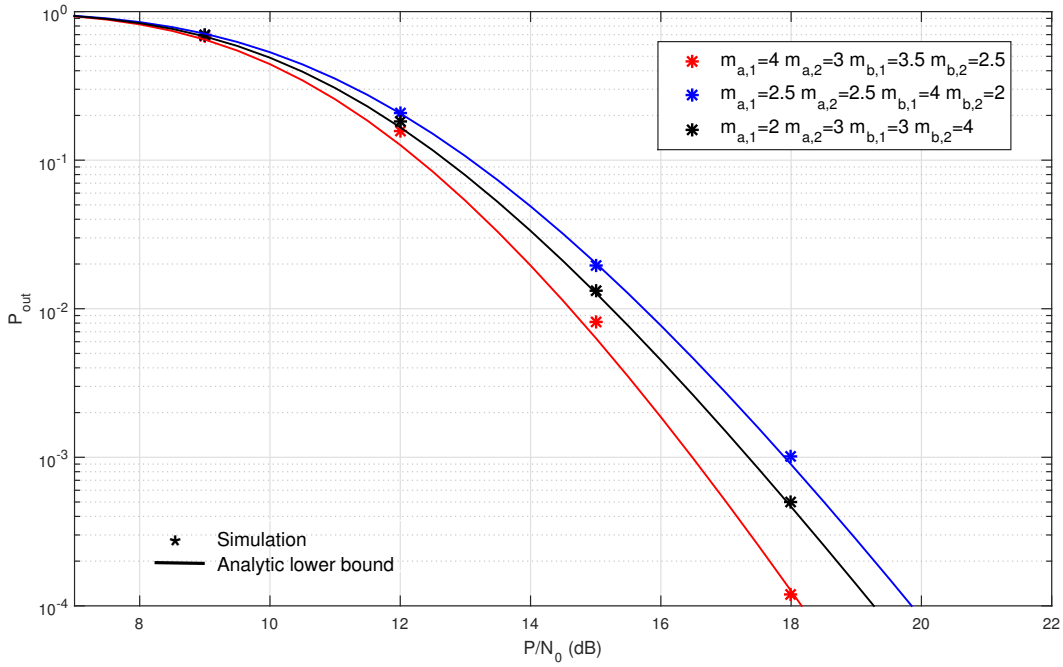

Figure 4.3 : Impact of m parameter values of the channel coefficients on the outage probability.

The impact of m parameter values of the channel coefficients on the outage probability is shown in Figure 4.3 where threshold SNR and the number of the relay antennas are chosen as $\gamma_{th} = 5$ dB and $M_r = 3$, respectively. As the value of m increases, the outage

probability decreases. Similarly the diversity orders $(7.5, 6, 6)$ obtained by using the simulations are consistent with those obtained by the analytical expression in (2.6).

4.2 Joint Relay and Antenna Selection in MIMO PLNC Inter-Vehicular Communication Systems over Cascaded Fading Channels

In this section, we investigate the joint relay and antenna selection performance in a multiple input multiple output V2V communication system employing PLNC with variable gain AF method at the relay antenna.

4.2.1 System Model

As illustrated in Figure 4.4, we consider an inter-vehicular communication system in which V_a and V_b are the source vehicles to communicate. We assume that the direct link between V_a and V_b is absent which is a realistic scenario for V2V communications where two sources are located far away from each other on a motorway or subjected to heavy shadowing by surrounding vehicles and buildings in dense city traffic in a street. Therefore, the sources try to transmit their messages through an intermediate vehicle acting as a relay which has direct link with both ends. In the system, the number of the possible vehicles playing the relay role is R and each of them is denoted by V_r for $r = 1, ..., R$. The numbers of the installed antennas on the sources and the r-th intermediate vehicle are M_a, M_b and M_r, respectively. Before the sources start to

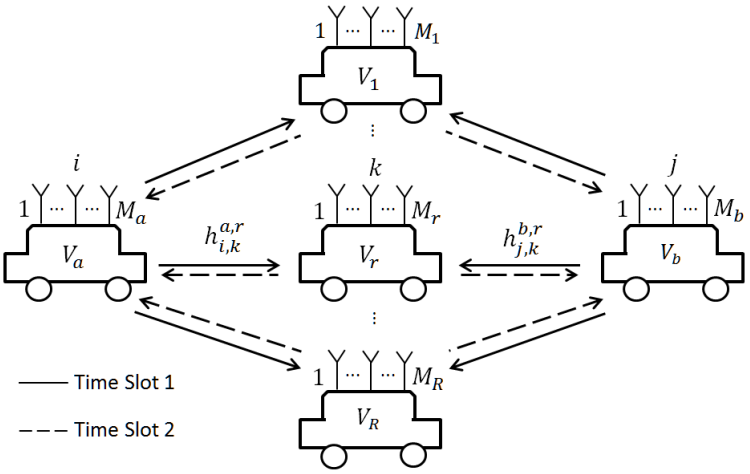

Figure 4.4 : MIMO V2V communication systems employing AF PLNC. V_a and V_b are source nodes, and V_r denotes r-th relay vehicle, for $r = 1, ..., R$. V_a, V_b and V_r have M_a, M_b and M_r antennas, respectively. Fading coefficients of the channels between the sources and relays are $h_{i,k}^{a,r}$ and $h_{j,k}^{b,r}$. Straight and dashed lines denote two consecutive time slots used in PLNC.

transmit their data messages, a joint antenna and relay selection phase is initiated in the system. In this phase, the source nodes successively send pilot signals to the relays by using each TX/RX antenna pair.

For the given system, the channel between each pair of the transmitter and receiver antennas is modeled by cascaded Nakagami-m fading channel. In this model, the fading coefficient of the channel is the product of Nakagami-m random variables. The number of these random variables give the cascading degree of the channel. In the system, the fading coefficient of the channel between the i-th antenna of V_a and the k-th antenna of V_r is represented by $h_{i,k}^{a,r}$ with the cascading degree of $N_{i,k}^{a,r}$, while the fading coefficient of the channel between the j-th antenna of V_b and the k-th antenna of V_r is represented by $h_{j,k}^{b,r}$ with the cascading degree of $N_{j,k}^{b,r}$. Thus, $h_{i,k}^{a,r}$ and $h_{j,k}^{b,r}$ are

$$h_{i,k}^{a,r} = \prod_{n=1}^{N_{i,k}^{a,r}} h_{i,k,n}^{a,r}, \tag{4.28a}$$

$$h_{j,k}^{b,r} = \prod_{n=1}^{N_{j,k}^{b,r}} h_{j,k,n}^{b,r} \tag{4.28b}$$

where $h_{i,k,n}^{a,r}$ and $h_{j,k,n}^{b,r}$ are independent and non-identically Nakagami-m distributed random variables with the fading parameters $m_{i,k,n}^{a,r}$ and $m_{j,k,n}^{b,r}$ and the average powers of $\Omega_{i,k,n}^{a,r} = E[(h_{i,k,n}^{a,r})^2]$ and $\Omega_{j,k,n}^{b,r} = E[(h_{j,k,n}^{b,r})^2]$, respectively. The average powers of the cascaded fading coefficients, $\Omega_{i,k}^{a,r}$ and $\Omega_{j,k}^{b,r}$, are

$$\Omega_{i,k}^{a,r} = E\left[(h_{i,k}^{a,r})^2\right] = \prod_{n=1}^{N_{i,k}^{a,r}} \Omega_{i,k,n}^{a,r}, \tag{4.29a}$$

$$\Omega_{j,k}^{b,r} = E\left[(h_{j,k}^{b,r})^2\right] = \prod_{n=1}^{N_{j,k}^{b,r}} \Omega_{j,k,n}^{b,r}. \tag{4.29b}$$

For the given system, we assume that all nodes know the fading statistics of all channels. Furthermore, the sources are able to cancel the self-interference, and additive noises at all nodes are assumed to be Gaussian random variables with zero mean and two-sided power spectral density of $N_0/2$. It is assumed that all nodes operate in half-duplex mode and transmit with equal power of $P_a = P_b = P_r = P$. The relays employ PLNC using the AF method, hence a message transaction between the sources is accomplished in two consecutive time slots. Therefore, V_a and V_b send their messages x_a and x_b simultaneously to the relay V_r and the signal received by k-th

antenna of V_r is

$$y_k^r = h_{i,k}^{a,r}\sqrt{P}x_a + h_{j,k}^{b,r}\sqrt{P}x_b + n_k^r \tag{4.30}$$

in the first time slot. Here, n_k^r denotes the additive noise. In the second time slot, V_r amplifies the y_k^r with the power scaling factor,

$$G = \sqrt{\frac{P}{P(h_{i,k}^{a,r})^2 + P(h_{j,k}^{b,r})^2 + N_0}} \tag{4.31}$$

then forwards it to the sources by using the k-th antenna. After canceling the self-interference, the received signals at the source nodes are

$$\tilde{y}_i^a = h_{i,k}^{a,r} G h_{j,k}^{b,r}\sqrt{P}x_b + h_{i,k}^{a,r} G n_k^r + n_i^a, \tag{4.32a}$$

$$\tilde{y}_j^b = h_{j,k}^{b,r} G h_{i,k}^{a,r}\sqrt{P}x_a + h_{j,k}^{b,r} G n_k^r + n_j^b \tag{4.32b}$$

where n_i^a and n_j^b are additive noises at the receiver antennas of sources. Then instantaneous end-to-end signal-to-noise ratio (E2E-SNR) at the i-th antenna of V_a and the j-th antenna of V_b can be expressed as

$$\gamma_{i,j,k}^{a,r} = \frac{\gamma_{i,k}^{a,r}\gamma_{j,k}^{b,r}}{2\gamma_{i,k}^{a,r} + \gamma_{j,k}^{b,r}} \quad \text{for } V_a, \tag{4.33a}$$

$$\gamma_{i,j,k}^{b,r} = \frac{\gamma_{i,k}^{a,r}\gamma_{j,k}^{b,r}}{2\gamma_{j,k}^{b,r} + \gamma_{i,k}^{a,r}} \quad \text{for } V_b \tag{4.33b}$$

where $\gamma_{i,k}^{a,r} \triangleq \gamma_0 (h_{i,k}^{a,r})^2$ is the instantaneous SNR of the channel between the i-th antenna of V_a and the k-th antenna of V_r with the expected value of $\bar{\gamma}_{i,k}^{a,r} = \gamma_0 \Omega_{i,k}^{a,r}$, and $\gamma_{j,k}^{b,r} \triangleq \gamma_0 (h_{j,k}^{b,r})^2$ is the instantaneous SNR of the channel between the j-th antenna of V_b and the k-th antenna of V_r with the expected value of $\bar{\gamma}_{j,k}^{b,r} = \gamma_0 \Omega_{j,k}^{b,r}$, for $\gamma_0 \triangleq \frac{P}{N_0}$.

With the help of (2.15) and (2.16), the pdf of the instantaneous SNR becomes

$$f_\chi(\gamma) = \frac{1}{\gamma \prod_{n=1}^{N} \Gamma(m_n)} G_{0,N}^{N,0}\left[\frac{\gamma}{\gamma_0}\prod_{n=1}^{N}\frac{m_n}{\Omega_n}\,\middle|\,{}^{-}_{m_1,\ldots,m_N}\right] \tag{4.34}$$

and the CDF of the instantaneous SNR becomes

$$F_\chi(\gamma) = \frac{1}{\prod_{n=1}^{N} \Gamma(m_n)} G_{1,N+1}^{N,1}\left[\frac{\gamma}{\gamma_0}\prod_{n=1}^{N}\frac{m_n}{\Omega_n}\,\middle|\,{}^{1}_{m_1,\ldots,m_N,0}\right] \tag{4.35}$$

where $\chi \in \{\gamma_{i,k}^{a,r}, \gamma_{j,k}^{b,r}\}$, $N \in \{N_{i,k}^{a,r}, N_{j,k}^{b,r}\}$, $m_n \in \{m_{i,k,n}^{a,r}, m_{j,k,n}^{b,r}\}$ and $\Omega_n \in \{\Omega_{i,k,n}^{a,r}, \Omega_{j,k,n}^{b,r}\}$. As it is mentioned before, by setting the fading parameter values in (4.34) and (4.35)

to unit, $m_{i,k,n}^{a,r} = m_{j,k,n}^{b,r} = 1$, the pdf and the CDF of the instantaneous SNR for the cascaded Rayleigh channels are obtained. Also by setting the cascading degrees to unit, $N_{i,k}^{a,r} = N_{j,k}^{b,r} = 1$, one can reach the non-cascaded channel conditions used in cellular communications.

4.2.2 Joint relay and antenna selection

In MIMO systems, the overall system performance may be stated in terms of the outage probability and it can be enhanced by performing relay and antenna selection. Therefore, maximization of the instantaneous E2E-SNR is aimed to decrease the outage probability of the system. For the systems having multiple sources like ours, target instantaneous E2E-SNR to be maximized is the minimum one among the instantaneous E2E-SNRs at all sources. Thus, by maximizing the performance of the weakest link, the performance enhancement of the whole system is achieved [132,133]. For this purpose, selection of the best relay and the best antennas at the nodes can be accomplished by using a $\max - \min$ criterion which is formulated as

$$\{I,J,L,K\} = \underset{\substack{1\leq i\leq M_a \\ 1\leq j\leq M_b \\ 1\leq r\leq R \\ 1\leq k\leq M_r}}{\arg\max}\{\min\left(\gamma_{i,j,k}^{a,r},\, \gamma_{i,j,k}^{b,r}\right)\} \tag{4.36}$$

where L is the index of the selected relay while I, J, and K are the indices of the selected antennas at V_a, V_b and the relay V_L, respectively. Then the overall instantaneous SNR of the system can be defined as

$$\gamma \overset{\triangle}{=} \max_{\substack{1\leq i\leq M_a \\ 1\leq j\leq M_b \\ 1\leq r\leq R \\ 1\leq k\leq M_r}} \left\{\min\left(\gamma_{i,j,k}^{a,r},\, \gamma_{i,j,k}^{b,r}\right)\right\} \tag{4.37}$$

and the statistical properties of γ determine the system performance.

4.2.3 Performance Analysis

In order to analyze the performance of a MIMO vehicular communication system employing AF PLNC with joint relay and antenna selection, the CDF of the overall instantaneous SNR, $F_\gamma(\gamma)$, should be known. Using this CDF, the outage probability, P_{out}, can be obtained as

$$P_{out} = P\left(\gamma \leq \gamma_{th}\right) = F_\gamma(\gamma_{th}) \tag{4.38}$$

where γ_{th} is the predefined threshold SNR value for γ. By substituting (4.37) in (4.38) and using order statistics in probability theory, P_{out} becomes

$$\begin{aligned} P_{out} &= P(\gamma \leq \gamma_{th}) \\ &= P(\max_{\substack{1\leq i\leq M_a \\ 1\leq j\leq M_b \\ 1\leq r\leq R \\ 1\leq k\leq M_r}} \left\{\min\left(\gamma_{i,j,k}^{a,r}, \gamma_{i,j,k}^{b,r}\right)\right\} \leq \gamma_{th}) \\ &= P(\max_{\substack{1\leq r\leq R \\ 1\leq k\leq M_r}} \left\{\min\left(\gamma_{I,J,k}^{a,r}, \gamma_{I,J,k}^{b,r}\right)\right\} \leq \gamma_{th}) \\ &= \prod_{k=1}^{M_r} P\left(\max_{1\leq r\leq R} \left\{\min\left(\gamma_{I,J,k}^{a,r}, \gamma_{I,J,k}^{b,r}\right)\right\} \leq \gamma_{th}\right) \end{aligned} \tag{4.39}$$

where $\gamma_{I,J,k}^{a,r}$ and $\gamma_{I,J,k}^{b,r}$ are the best E2E-SNRs of the sources for a given $\{r,k\}$ pair and determined as

$$\gamma_{I,J,k}^{a,r} = \max_{\substack{1\leq i\leq M_a \\ 1\leq j\leq M_b}} \left(\gamma_{i,j,k}^{a,r}\right) = \frac{\gamma_{I,k}^{a,r}\gamma_{J,k}^{b,r}}{2\gamma_{I,k}^{a,r} + \gamma_{J,k}^{b,r}}, \tag{4.40a}$$

$$\gamma_{I,J,k}^{b,r} = \max_{\substack{1\leq i\leq M_a \\ 1\leq j\leq M_b}} \left(\gamma_{i,j,k}^{b,r}\right) = \frac{\gamma_{I,k}^{a,r}\gamma_{J,k}^{b,r}}{\gamma_{I,k}^{a,r} + 2\gamma_{J,k}^{b,r}} \tag{4.40b}$$

where $\gamma_{I,k}^{a,r}$ and $\gamma_{J,k}^{b,r}$ are the maximum instantaneous SNRs belong to the best channels between V_a and V_r, and between V_b and V_r, respectively. Therefore, $\gamma_{I,k}^{a,r}$ and $\gamma_{J,k}^{b,r}$ are

$$\gamma_{I,k}^{a,r} = \max_{1\leq i\leq M_a} \left(\gamma_{i,k}^{a,r}\right), \tag{4.41a}$$

$$\gamma_{J,k}^{b,r} = \max_{1\leq j\leq M_b} \left(\gamma_{j,k}^{b,r}\right). \tag{4.41b}$$

With the help of the order statistics, the CDFs of $\gamma_{I,k}^{a,r}$ and $\gamma_{J,k}^{b,r}$ are given as

$$F_{\gamma_{I,k}^{a,r}}(\gamma) = \prod_{i=1}^{M_a} F_{\gamma_{i,k}^{a,r}}(\gamma), \tag{4.42a}$$

$$F_{\gamma_{J,k}^{b,r}}(\gamma) = \prod_{j=1}^{M_b} F_{\gamma_{j,k}^{b,r}}(\gamma). \tag{4.42b}$$

For the definition of $\gamma_{I,J,k}^{r} \stackrel{\triangle}{=} \min\left(\gamma_{I,J,k}^{a,r}, \gamma_{I,J,k}^{b,r}\right)$, the outage probability in (4.39) can be stated as

$$\begin{aligned} P_{out} &= F_{\gamma}(\gamma_{th}) \\ &= \prod_{k=1}^{M_r} P\left(\max_{1\leq r\leq R}(\gamma_{I,J,k}^{r}) \leq \gamma_{th}\right) \\ &= \prod_{r=1}^{R}\prod_{k=1}^{M_r} P\left(\gamma_{I,J,k}^{r} \leq \gamma_{th}\right). \end{aligned} \tag{4.43}$$

Thus, the overall outage probability of the system can be evaluated by calculating the probability of $P\left(\gamma^{r}_{I,J,k} \leq \gamma_{th}\right)$ which is

$$\begin{aligned} P\left(\gamma^{r}_{I,J,k} \leq \gamma_{th}\right) &= P\left(\min\left(\gamma^{a,r}_{I,J,k}, \gamma^{b,r}_{I,J,k}\right) \leq \gamma_{th}\right) \\ &= 1 - P\left(\min\left(\gamma^{a,r}_{I,J,k}, \gamma^{b,r}_{I,J,k}\right) \geq \gamma_{th}\right) \\ &= 1 - P^{*} \end{aligned} \tag{4.44}$$

where

$$\begin{aligned} P^{*} &= P\left(\min\left(\gamma^{a,r}_{I,J,k}, \gamma^{b,r}_{I,J,k}\right) \geq \gamma_{th}\right) \\ &= P\left(\gamma^{a,r}_{I,J,k} \geq \gamma_{th}, \gamma^{b,r}_{I,J,k} \geq \gamma_{th}\right) \\ &= P\left(\frac{\gamma^{a,r}_{I,k}\gamma^{b,r}_{J,k}}{2\gamma^{a,r}_{I,k} + \gamma^{b,r}_{J,k}} \geq \gamma_{th}, \frac{\gamma^{a,r}_{I,k}\gamma^{b,r}_{J,k}}{\gamma^{a,r}_{I,k} + 2\gamma^{b,r}_{J,k}} \geq \gamma_{th}\right) \\ &= P\left(\frac{2\gamma^{a,r}_{I,k} + \gamma^{b,r}_{J,k}}{\gamma^{a,r}_{I,k}\gamma^{b,r}_{J,k}} \leq \frac{1}{\gamma_{th}}, \frac{\gamma^{a,r}_{I,k} + 2\gamma^{b,r}_{J,k}}{\gamma^{a,r}_{I,k}\gamma^{b,r}_{J,k}} \leq \frac{1}{\gamma_{th}}\right) \\ &= P\left(\frac{2}{\gamma^{b,r}_{J,k}} + \frac{1}{\gamma^{a,r}_{I,k}} \leq \frac{1}{\gamma_{th}}, \frac{1}{\gamma^{b,r}_{J,k}} + \frac{2}{\gamma^{a,r}_{I,k}} \leq \frac{1}{\gamma_{th}}\right) \\ &= P\left(2Y + X \leq \beta, Y + 2X \leq \beta\right). \end{aligned} \tag{4.45}$$

Here, $X \triangleq \frac{1}{\gamma^{a,r}_{I,k}}$, $Y \triangleq \frac{1}{\gamma^{b,r}_{J,k}}$ and $\beta = \frac{1}{\gamma_{th}}$. We determine the joint probability in (4.45) by exploiting the graphical representation [109] shown in Figure 4.5.

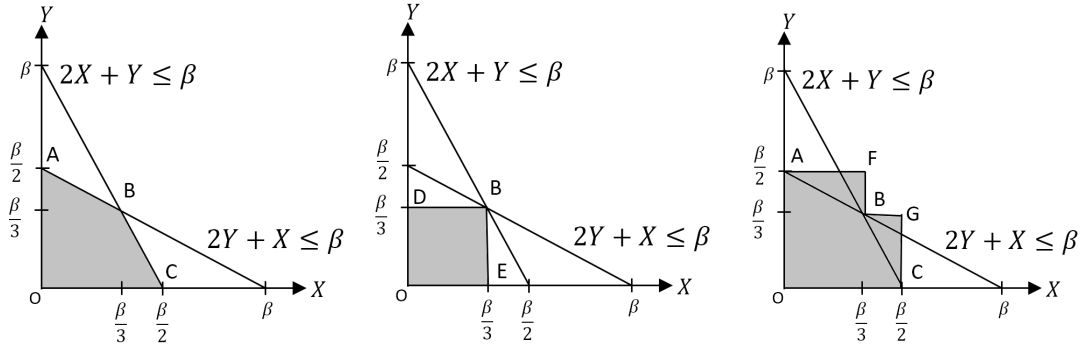

Figure 4.5 : Integral regions to evaluate the joint outage probability. (a) *OABC* for the exact expression, (b) *ODBE* for the upper bound and (c) *OAFBGC* for the lower bound.

4.2.3.1 Exact outage probability

Using integral region *OABC* in Figure 4.5(a), we find exact P^{*} as follows

$$P^{*} = \int_{0}^{\frac{\beta}{3}} \int_{0}^{\frac{\beta - x}{2}} f_Y(y) f_X(x) dy dx + \int_{\frac{\beta}{3}}^{\frac{\beta}{2}} \int_{0}^{\beta - 2x} f_Y(y) f_X(x) dy dx. \tag{4.46}$$

Using (4.42) and with the help of the basic probability theory, the CDF of X is $F_X(x/c) = 1 - F_{\gamma_{I,k}^{a,r}}(c/x) = 1 - \prod_{i=1}^{M_a} F_{\gamma_{i,k}^{a,r}}(c/x)$ for $c \in R^+$. Similarly, the CDF of Y is $F_Y(y/c) = 1 - F_{\gamma_{J,k}^{b,r}}(c/y) = 1 - \prod_{j=1}^{M_b} F_{\gamma_{j,k}^{b,r}}(c/y)$. Thus, (4.46) can be evolved as follows

$$\begin{aligned}
P^* &= \int_0^{\frac{\beta}{3}} F_Y(\frac{\beta - x}{2}) f_X(x)dx + \int_{\frac{\beta}{3}}^{\frac{\beta}{2}} F_Y(\beta - 2x) f_X(x)dx \\
&= \int_0^{\frac{\beta}{3}} \left[1 - F_{\gamma_{J,k}^{b,r}}(\frac{2}{\beta - x})\right] f_X(x)dx + \int_{\frac{\beta}{3}}^{\frac{\beta}{2}} \left[1 - F_{\gamma_{J,k}^{b,r}}(\frac{1}{\beta - 2x})\right] f_X(x)dx \\
&= F_X(\frac{\beta}{2}) - \int_0^{\frac{\beta}{3}} F_{\gamma_{J,k}^{b,r}}(\frac{2}{\beta - x}) \frac{1}{x^2} f_{\gamma_{I,k}^{a,r}}(1/x)dx - \int_{\frac{\beta}{2}}^{\frac{\beta}{3}} F_{\gamma_{J,k}^{b,r}}(\frac{1}{\beta - 2x}) \frac{1}{x^2} f_{\gamma_{I,k}^{a,r}}(1/x)dx \\
&= 1 - \prod_{i=1}^{M_a} F_{\gamma_{i,k}^{a,r}}(2\gamma_{th}) - \int_0^{\frac{\beta}{3}} \frac{1}{x^2} \prod_{j=1}^{M_b} F_{\gamma_{j,k}^{b,r}}(\frac{2}{\beta - x}) \sum_{i=1}^{M_a} f_{\gamma_{i,k}^{a,r}}(1/x) \prod_{\substack{t=1 \\ t \neq i}}^{M_a} F_{\gamma_{t,k}^{a,r}}(1/x)dx \\
&\quad - \int_{\frac{\beta}{2}}^{\frac{\beta}{3}} \frac{1}{x^2} \prod_{j=1}^{M_b} F_{\gamma_{j,k}^{b,r}}(\frac{1}{\beta - 2x}) \sum_{i=1}^{M_a} f_{\gamma_{i,k}^{a,r}}(1/x) \prod_{\substack{t=1 \\ t \neq i}}^{M_a} F_{\gamma_{t,k}^{a,r}}(1/x)dx.
\end{aligned} \tag{4.47}$$

Thus, using (4.43), the exact expression of P_{out} is found as

$$\begin{aligned}
P_{out}^{exact} &= \prod_{r=1}^{R} \prod_{k=1}^{M_r} [1 - P^*] \\
&= \prod_{r=1}^{R} \prod_{k=1}^{M_r} \left[\prod_{i=1}^{M_a} F_{\gamma_{i,k}^{a,r}}(2\gamma_{th}) + \int_0^{\frac{\beta}{3}} \frac{1}{x^2} \prod_{j=1}^{M_b} F_{\gamma_{j,k}^{b,r}}(\frac{2}{\beta - x}) \sum_{i=1}^{M_a} f_{\gamma_{i,k}^{a,r}}(1/x) \prod_{\substack{t=1 \\ t \neq i}}^{M_a} F_{\gamma_{t,k}^{a,r}}(1/x)dx \right. \\
&\quad \left. + \int_{\frac{\beta}{3}}^{\frac{\beta}{2}} \frac{1}{x^2} \prod_{j=1}^{M_b} F_{\gamma_{j,k}^{b,r}}(\frac{1}{\beta - 2x}) \sum_{i=1}^{M_a} f_{\gamma_{i,k}^{a,r}}(1/x) \prod_{\substack{t=1 \\ t \neq i}}^{M_a} F_{\gamma_{t,k}^{a,r}}(1/x)dx \right]
\end{aligned} \tag{4.48}$$

in terms of the pdf and the CDF expressions of the instantaneous SNRs at the channels. Then, by using (4.34) and (4.35), one can obtain the expression of the exact outage

probability of the system in terms of the Meijer's G-function as

$$
\begin{aligned}
P_{out}^{exact} &= \prod_{r=1}^{R}\prod_{k=1}^{M_r}\Bigg\{\prod_{i=1}^{M_a}\frac{G_{1,N_{i,k}^{a,r}+1}^{N_{i,k}^{a,r},1}\left[\frac{2\gamma_{th}}{\gamma_0}\prod_{n=1}^{N_{i,k}^{a,r}}\frac{m_{i,k,n}^{a,r}}{\Omega_{i,k,n}^{a,r}}\middle|\begin{matrix}1\\ \underline{m}_{i,k}^{a,r},0\end{matrix}\right]}{\prod_{n=1}^{N_{i,k}^{a,r}}\Gamma(m_{i,k,n}^{a,r})} \\
&\quad+\int_0^{\frac{\beta}{3}}\frac{1}{x^2}\prod_{j=1}^{M_b}\frac{G_{1,N_{j,k}^{b,r}+1}^{N_{j,k}^{b,r},1}\left[\frac{\frac{2}{\beta-x}}{\gamma_0}\prod_{n=1}^{N_{j,k}^{b,r}}\frac{m_{j,k,n}^{b,r}}{\Omega_{j,k,n}^{b,r}}\middle|\begin{matrix}1\\ \underline{m}_{j,k}^{b,r},0\end{matrix}\right]}{\prod_{n=1}^{N_{j,k}^{b,r}}\Gamma(m_{j,k,n}^{b,r})}\Upsilon(x)dx \\
&\quad+\int_{\frac{\beta}{3}}^{\frac{\beta}{2}}\frac{1}{x^2}\prod_{j=1}^{M_b}\frac{G_{1,N_{j,k}^{b,r}+1}^{N_{j,k}^{b,r},1}\left[\frac{\frac{1}{\beta-2x}}{\gamma_0}\prod_{n=1}^{N_{j,k}^{b,r}}\frac{m_{j,k,n}^{b,r}}{\Omega_{j,k,n}^{b,r}}\middle|\begin{matrix}1\\ \underline{m}_{j,k}^{b,r},0\end{matrix}\right]}{\prod_{n=1}^{N_{j,k}^{b,r}}\Gamma(m_{j,k,n}^{b,r})}\Upsilon(x)dx\Bigg\}
\end{aligned}
\tag{4.49}
$$

where the function $\Upsilon(x)$ is

$$
\begin{aligned}
\Upsilon(x) &= \sum_{i=1}^{M_a}x\left(\prod_{n=1}^{N_{i,k}^{a,r}}\Gamma(m_{i,k,n}^{a,r})\right)^{-1}G_{0,N_{i,k}^{a,r}}^{N_{i,k}^{a,r},0}\left[\frac{x^{-1}}{\gamma_0}\prod_{n=1}^{N_{i,k}^{a,r}}\frac{m_{i,k,n}^{a,r}}{\Omega_{i,k,n}^{a,r}}\middle|\begin{matrix}-\\ \underline{m}_{i,k}^{a,r}\end{matrix}\right] \\
&\quad\times\prod_{\substack{t=1\\ t\neq i}}^{M_a}\left(\prod_{n=1}^{N_{t,k}^{a,r}}\Gamma(m_{t,k,n}^{a,r})\right)^{-1}G_{1,N_{t,k}^{a,r}+1}^{N_{t,k}^{a,r},1}\left[\frac{x^{-1}}{\gamma_0}\prod_{n=1}^{N_{t,k}^{a,r}}\frac{m_{t,k,n}^{a,r}}{\Omega_{t,k,n}^{a,r}}\middle|\begin{matrix}1\\ \underline{m}_{t,k}^{a,r},0\end{matrix}\right].
\end{aligned}
\tag{4.50}
$$

P_{out}^{exact} is in a single integral form which is not available in a closed-form, even for the single antenna case where $M_a = M_b = 1$, due to the mathematical intractability of the integrals enclose the product of Meijer's G functions included by the pdfs and the CDFs seen in the expression. Thereby, (4.49) has to be solved numerically. This expression for the exact P_{out} is the most general form which covers any values of the cascading degrees and fading parameters for the channels. On the other hand, as a special case of the general cascaded Nakagami-*m* fading channel, the double Nakagami-*m* channel model is also studied in the literature. By setting the cascading degrees $N_{i,k}^{a,r}$ and $N_{j,k}^{b,r}$ to 2 in (4.49) and (4.50), one can easily obtain the exact outage probability expression for double Nakagami-*m* channels in terms of Meijer's G functions. Moreover, with the help of the equality of $G_{0,2}^{2,0}[z|b,c] = 2z^{\frac{b+c}{2}}K_{b-c}(2\sqrt{z})$ [131, 07.34.03.0605.01], the pdf

in (4.34) is written as

$$f_{\chi}(\gamma)=\frac{2\gamma^{-1}}{\Gamma(m_1)\Gamma(m_2)}\left(\frac{\gamma}{\bar{\chi}}m_1m_2\right)^{\frac{m_1+m_2}{2}}K_{m_1-m_2}\left(2\sqrt{\frac{\gamma}{\bar{\chi}}m_1m_2}\right). \tag{4.51}$$

Similarly, using the equality of $G_{1,3}^{2,1}\left[z|_{b_1,b_2,b_3}^{a}\right]=\pi csc(\pi(b_2-b_1))(\Gamma(1-a+b_1)z^{b_1}{}_1F_2(1-a+b_1;b_1-b_2+1,b_1-b_3+1;z)-\Gamma(1-a+b_2)z^{b_2}{}_1F_2(1-a+b_2;b_2-b_1+1,b_2-b_3+1;z))$ [131, 07.34.03.0727.01], the CDF given by (4.35) can be stated in terms of hypergeometric function ${}_1F_2(;;)$ as follows

$$\begin{aligned}F_{\chi}(\gamma)=\pi csc(\pi(m_2-m_1))&\\ \left(\frac{(\frac{\gamma}{\bar{\chi}}m_1m_2)^{m_1}}{\Gamma(m_2)}{}_1F_2(m_1;m_1-m_2+1,m_1+1;\frac{\gamma}{\bar{\chi}}m_1m_2)\right.&\\ \left.-\frac{(\frac{\gamma}{\bar{\chi}}m_1m_2)^{m_2}}{\Gamma(m_1)}{}_1F_2(m_2;m_2-m_1+1,m_2+1;\frac{\gamma}{\bar{\chi}}m_1m_2)\right)&\end{aligned} \tag{4.52}$$

for $\chi\in\{\gamma_{i,k}^{a,r},\,\gamma_{j,k}^{b,r}\}$, $\bar{\chi}\in\{\bar{\gamma}_{i,k}^{a,r},\,\bar{\gamma}_{j,k}^{b,r}\}=\{\gamma_0\Omega_{i,k,1}^{a,r}\Omega_{i,k,2}^{a,r},\,\gamma_0\Omega_{j,k,1}^{b,r}\Omega_{j,k,2}^{b,r}\}$ and $m_n\in\{m_{i,k,n}^{a,r},\,m_{j,k,n}^{b,r}\}$, $n=1,2$. Therefore, substituting (4.51) and (4.52) into (4.48), the exact P_{out} expression can be found as

$$\begin{aligned}P_{out}^{exact}=\prod_{r=1}^{R}\prod_{k=1}^{M_r}\left[\prod_{i=1}^{M_a}\pi csc(\pi(m_{i,k,2}^{a,r}-m_{i,k,1}^{a,r}))\right.&\\ \left(\frac{\left(2\gamma_{th}Z_{i,k}^{a,r}\right)^{m_{i,k,1}^{a,r}}}{\Gamma(m_{i,k,2}^{a,r})}{}_1F_2\left(m_{i,k,1}^{a,r};m_{i,k,1}^{a,r}-m_{i,k,2}^{a,r}+1,m_{i,k,1}^{a,r}+1;\frac{2\gamma_{th}}{\gamma_0}Z_{i,k}^{a,r}\right)\right.&\\ \left.\left.-\frac{\left(2\gamma_{th}Z_{i,k}^{a,r}\right)^{m_{i,k,2}^{a,r}}}{\Gamma(m_{i,k,1}^{a,r})}{}_1F_2\left(m_{i,k,2}^{a,r};m_{i,k,2}^{a,r}-m_{i,k,1}^{a,r}+1,m_{i,k,2}^{a,r}+1;\frac{2\gamma_{th}}{\gamma_0}Z_{i,k}^{a,r}\right)\right)\right.&\\ +\int_0^{\frac{\beta}{3}}\prod_{j=1}^{M_b}\left(\frac{\left(2Z_{j,k}^{b,r}\right)^{m_{j,k,1}^{b,r}}{}_1F_2\left(m_{j,k,1}^{b,r};m_{j,k,1}^{b,r}-m_{j,k,2}^{b,r}+1,m_{j,k,1}^{b,r}+1;\frac{2Z_{j,k}^{b,r}}{\gamma_0(\beta-x)}\right)}{(\beta-x)^{m_{j,k,1}^{b,r}}\Gamma(m_{j,k,2}^{b,r})}\right.&\\ \left.\left.-\frac{\left(2Z_{j,k}^{b,r}\right)^{m_{j,k,2}^{b,r}}{}_1F_2\left(m_{j,k,2}^{b,r};m_{j,k,2}^{b,r}-m_{j,k,1}^{b,r}+1,m_{j,k,2}^{b,r}+1;\frac{2Z_{j,k}^{b,r}}{\gamma_0(\beta-x)}\right)}{(\beta-x)^{m_{j,k,2}^{b,r}}\Gamma(m_{j,k,1}^{b,r})}\right)\Psi(x)dx\right.&\end{aligned}$$

$$+\int_{\frac{\beta}{3}}^{\frac{\beta}{2}}\prod_{j=1}^{M_b}\left(\frac{\left(Z_{j,k}^{b,r}\right)^{m_{j,k,1}^{b,r}}{}_1F_2\left(m_{j,k,1}^{b,r};m_{j,k,1}^{b,r}-m_{j,k,2}^{b,r}+1,m_{j,k,1}^{b,r}+1;\frac{Z_{j,k}^{b,r}}{\gamma_0(\beta-2x)}\right)}{(\beta-2x)^{m_{j,k,1}^{b,r}}\Gamma(m_{j,k,2}^{b,r})}\right.$$
$$\left.-\frac{\left(Z_{j,k}^{b,r}\right)^{m_{j,k,2}^{b,r}}{}_1F_2\left(m_{j,k,2}^{b,r};m_{j,k,2}^{b,r}-m_{j,k,1}^{b,r}+1,m_{j,k,2}^{b,r}+1;\frac{Z_{j,k}^{b,r}}{\gamma_0(\beta-2x)}\right)}{(\beta-2x)^{m_{j,k,2}^{b,r}}\Gamma(m_{j,k,1}^{b,r})}\right)\Psi(x)dx\Bigg] \tag{4.53}$$

for the double Nakagami-m channel model in terms of the modified Bessel and hypergeometric functions. Here, $Z_{i,k}^{a,r}=\frac{m_{i,k,1}^{a,r}m_{i,k,2}^{a,r}}{\Omega_{i,k,1}^{a,r}\Omega_{i,k,2}^{a,r}}$, $Z_{j,k}^{b,r}=\frac{m_{j,k,1}^{b,r}m_{j,k,2}^{b,r}}{\Omega_{j,k,1}^{b,r}\Omega_{j,k,2}^{b,r}}$ and

$$\begin{aligned}\Psi(x) &= \frac{1}{x^2}\sum_{i=1}^{M_a}\frac{2x}{\Gamma(m_{i,k,1}^{a,r})\Gamma(m_{i,k,2}^{a,r})}\left(x^{-1}Z_{i,k}^{a,r}\right)^{\frac{m_{i,k,1}^{a,r}+m_{i,k,2}^{a,r}}{2}}\\
&\quad\times K_{m_{i,k,1}^{a,r}-m_{i,k,2}^{a,r}}\left(2\sqrt{x^{-1}Z_{i,k}^{a,r}}\right)\prod_{\substack{t=1\\t\neq j}}^{M_a}\pi csc(\pi(m_{t,k,2}^{a,r}-m_{t,k,1}^{a,r}))\\
&\quad\times\left(\frac{\left(x^{-1}Z_{t,k}^{a,r}\right)^{m_{t,k,1}^{a,r}}}{\Gamma(m_{t,k,2}^{a,r})}{}_1F_2\left(m_{t,k,1}^{a,r};m_{t,k,1}^{a,r}-m_{t,k,2}^{a,r}+1,m_{t,k,1}^{a,r}+1;\frac{Z_{t,k}^{a,r}}{x\gamma_0}\right)\right.\\
&\quad\left.-\frac{\left(x^{-1}Z_{t,k}^{a,r}\right)^{m_{t,k,1}^{a,r}}}{\Gamma(m_{t,k,1}^{a,r})}{}_1F_2\left(m_{t,k,2}^{a,r};m_{t,k,2}^{a,r}-m_{t,k,1}^{a,r}+1,m_{t,k,2}^{a,r}+1;\frac{Z_{t,k}^{a,r}}{x\gamma_0}\right)\right).\end{aligned} \tag{4.54}$$

For the case of the single Nakagami-m fading, as it is said in the introduction section, this channel model is insufficient to model the fading phenomenon observed in the vehicular environments. But, it is noted for the interested reader that, by using $N_{i,k}^{a,r}=N_{j,k}^{b,r}=1$ in (4.34) and (4.35) and the equalities $G_{0,1}^{1,0}[z|b]=e^{-z}z^b$ [131, 07.34.03.0228.01] and $G_{1,2}^{1,1}\left[z|_{b,a-1}^{a}\right]=z^{a-1}\Gamma(b-a+1;0,z)$ [131, 07.34.03.0275.01], (4.34) and (4.35) simplify to

$$f_\chi(\gamma)=\frac{m^m\gamma^{m-1}}{\Gamma(m)\bar{\chi}^m}e^{-\frac{m}{\bar{\chi}}\gamma}, \tag{4.55a}$$

$$F_\chi(\gamma)=\frac{\Gamma\left(m,\frac{m}{\bar{\chi}}\gamma\right)}{\Gamma(m)} \tag{4.55b}$$

which are the well-known pdf and the CDF expressions of the instantaneous SNR for the single Nakagami-m channel. Then substituting (4.55a) and (4.55b) into (4.48), the

exact P_{out} can be found as

$$P_{out}^{exact} = \prod_{r=1}^{R}\prod_{k=1}^{M_r} \left[\prod_{i=1}^{M_a} \frac{\Gamma\left(m_{i,k}^{a,r}, \frac{mi,k^{a,r}}{\gamma_0 \Omega_{i,k}^{a,r}} 2\gamma_{th}\right)}{\Gamma\left(m_{i,k}^{a,r}\right)} + \int_0^{\frac{\beta}{3}} \frac{1}{x^2} \prod_{j=1}^{M_b} \frac{\Gamma\left(m_{j,k}^{b,r}, \frac{mj,k^{b,r}}{\gamma_0 \Omega_{j,k}^{b,r}} \frac{2}{\beta - x}\right)}{\Gamma\left(m_{j,k}^{b,r}\right)} \Phi(x) dx \right.$$
$$\left. + \int_{\frac{\beta}{3}}^{\frac{\beta}{2}} \frac{1}{x^2} \prod_{j=1}^{M_b} \frac{\Gamma\left(m_{j,k}^{b,r}, \frac{mj,k^{b,r}}{\gamma_0 \Omega_{j,k}^{b,r}} \frac{1}{\beta - 2x}\right)}{\Gamma\left(m_{j,k}^{b,r}\right)} \Phi(x) dx \right] \tag{4.56}$$

in terms of the exponential and Gamma functions for the single Nakagami-*m* channel. Here, the function $\Phi(x)$ is

$$\Phi(x) = \sum_{i=1}^{M_a} \frac{\left(m_{i,k}^{a,r}\right)^{m_{i,k}^{a,r}} (1/x)^{m_{i,k}^{a,r}-1}}{\Gamma(m_{i,k}^{a,r}) \left(\Omega_{i,k}^{a,r}\right)^{m_{i,k}^{a,r}}} e^{-\frac{m_{i,k}^{a,r}}{\gamma_0 \Omega_{i,k}^{a,r}}(1/x)} \prod_{\substack{t=1 \\ t \neq j}}^{M_a} \frac{\Gamma\left(m_{t,k}^{a,r}, \frac{m_{t,k}^{a,r}}{\gamma_0 \Omega_{t,k}^{a,r}}(1/x)\right)}{\Gamma(m_{t,k}^{a,r})}. \tag{4.57}$$

4.2.3.2 Lower and upper bounds for the outage probability

Although the closed-form solution of the exact outage probability for the considered system is not available, a lower and an upper bound for P_{out} will give us an insight about the performance limits of the system. Therefore, by bounding the integral region with *ODBE* in Figure 4.5(b), we obtain a lower bound for P^* as

$$\begin{aligned} P_{lower}^{*} &= \int_0^{\frac{\beta}{3}} \int_0^{\frac{\beta}{3}} f_Y(y) f_X(x) dy dx \\ &= F_X(\frac{\beta}{3}) F_Y(\frac{\beta}{3}) \\ &= 1 - F_{\gamma_{I,k}^{a,r}}(3\gamma_{th}) - F_{\gamma_{J,k}^{b,r}}(3\gamma_{th}) + F_{\gamma_{I,k}^{a,r}}(3\gamma_{th}) F_{\gamma_{J,k}^{b,r}}(3\gamma_{th}). \end{aligned} \tag{4.58}$$

Then using (4.58), an upper bound for P_{out} is derived as

$$\begin{aligned} P_{out}^{upper} &= \prod_{r=1}^{R}\prod_{k=1}^{M_r} [1 - P_{lower}^{*}] \\ &= \prod_{r=1}^{R}\prod_{k=1}^{M_r} \left[\prod_{i=1}^{M_a} F_{\gamma_{i,k}^{a,r}}(3\gamma_{th}) + \prod_{j=1}^{M_b} F_{\gamma_{j,k}^{b,r}}(3\gamma_{th}) \left(1 - \prod_{i=1}^{M_a} F_{\gamma_{i,k}^{a,r}}(3\gamma_{th})\right) \right] \end{aligned} \tag{4.59}$$

in the closed-form. When we expand the integral region to $OAFBGC$ in Figure 4.5(c), an upper bound for P^* is found as

$$\begin{aligned} P^*_{upper} &= \int_0^{\frac{\beta}{3}}\int_0^{\frac{\beta}{3}} f_Y(y)f_X(x)dydx + \int_{\frac{\beta}{3}}^{\frac{\beta}{2}}\int_0^{\frac{\beta}{3}} f_Y(y)f_X(x)dydx + \int_0^{\frac{\beta}{3}}\int_{\frac{\beta}{3}}^{\frac{\beta}{2}} f_Y(y)f_X(x)dydx \\ &= F_X(\frac{\beta}{3})F_Y(\frac{\beta}{3}) + \left(F_X(\frac{\beta}{2}) - F_X(\frac{\beta}{3})\right)F_Y(\frac{\beta}{3}) + F_X(\frac{\beta}{3})\left(F_Y(\frac{\beta}{2}) - F_Y(\frac{\beta}{3})\right) \\ &= 1 - F_{\gamma^{a,r}_{I,k}}(2\gamma_{th}) - F_{\gamma^{b,r}_{J,k}}(2\gamma_{th}) + F_{\gamma^{a,r}_{I,k}}(2\gamma_{th})F_{\gamma^{b,r}_{J,k}}(3\gamma_{th}) + F_{\gamma^{a,r}_{I,k}}(3\gamma_{th})F_{\gamma^{b,r}_{J,k}}(2\gamma_{th}) \\ &\quad - F_{\gamma^{a,r}_{I,k}}(3\gamma_{th})F_{\gamma^{b,r}_{J,k}}(3\gamma_{th}). \end{aligned} \tag{4.60}$$

By using (4.60), we find a lower bound for P_{out} as

$$\begin{aligned} P^{lower}_{out} &= \prod_{r=1}^{R}\prod_{k=1}^{M_r}\left[1 - P^*_{upper}\right] \\ &= \prod_{r=1}^{R}\prod_{k=1}^{M_r}\left[\prod_{i=1}^{M_a} F_{\gamma^{a,r}_{i,k}}(2\gamma_{th})\left(1 - \prod_{j=1}^{M_b} F_{\gamma^{b,r}_{j,k}}(3\gamma_{th})\right)\right. \\ &\quad \left. + \prod_{j=1}^{M_b} F_{\gamma^{b,r}_{j,k}}(2\gamma_{th})\left(1 - \prod_{i=1}^{M_a} F_{\gamma^{a,r}_{i,k}}(3\gamma_{th})\right) + \prod_{i=1}^{M_a} F_{\gamma^{a,r}_{i,k}}(3\gamma_{th})\prod_{j=1}^{M_b} F_{\gamma^{b,r}_{j,k}}(3\gamma_{th})\right] \end{aligned} \tag{4.61}$$

in the closed-form. Here again, using (4.35), (4.52), and (4.55b) in (4.59) and (4.61), one can obtain the explicit forms of the lower and the upper bound expressions for cascaded Nakagami-m fading, double Nakagami-m fading and single Nakagami-m fading conditions, respectively.

4.2.3.3 Asymptotic diversity order

Asymptotic diversity order can be obtained by examining the behavior of the system in high SNR regime. The outage probability in high SNR is given by

$$P^{\infty}_{out} = \alpha\zeta^{d_o} + O\left(\zeta^{d_o+1}\right) \tag{4.62}$$

which is a function of $\zeta \triangleq \gamma_{th}/\bar{\gamma}$, and for $\zeta \to 0^+$, the asymptotic diversity order becomes d_o. With the help of the series representation property [131, 07.34.06.0006.01] of the Meijer's G-function for $\zeta \to 0^+$, the CDF in (4.35) becomes

$$F_{\chi}(c\zeta) \cong \prod_{n=1}^{N}\Gamma(m_n)^{-1}\sum_{t=1}^{N} c^{m_t}\frac{\Gamma(m_t)}{\Gamma(1+m_t)}\prod_{n=1}^{N} m_n^{m_t}\prod_{\substack{s=1\\ s\neq t}}^{N}\Gamma(m_s - m_t)\,\zeta^{m_t} \tag{4.63}$$

where $c \in R^{+}$, $\chi \in \{\gamma_{i,k}^{a,r}, \gamma_{j,k}^{b,r}\}$, $N \in \{N_{i,k}^{a,r}, N_{j,k}^{b,r}\}$, $m_u \in \{m_{i,k,u}^{a,r}, m_{j,k,u}^{b,r}\}$, for $u \in \{n,t,s\}$. By assuming equal average SNR for all channels, i.e., $\bar{\gamma}_{i,k}^{a,r} = \bar{\gamma}_{j,k}^{b,r} = \bar{\gamma}$ and substituting (4.63) into (4.59) and (4.61), then rearranging the expressions in the form of (4.62), we obtain the asymptotic diversity order for both lower and upper bounds as

$$d_o = \sum_{r=1}^{R} \sum_{k=1}^{M_r} \min \left(\sum_{i=1}^{M_a} \min\{m_{i,k,1}^{a,r}, ..., m_{i,k,N_{i,k}^{a,r}}^{a,r}\}, \sum_{j=1}^{M_b} \min\{m_{j,k,1}^{b,r}, ..., m_{j,k,N_{j,k}^{b,r}}^{b,r}\} \right) \quad (4.64)$$

as a function of the number of the relay, the number of the antennas installed on all the vehicles and the channel parameters which are the cascading degrees and the m parameter values.

4.2.4 Numerical Results

In order to verify the derived analytical results, we present computer simulations in this section. Considering the multi-antenna multi-relay vehicular communication system employing AF PLNC with joint relay and antenna selection over cascaded Nakagami-m channel, Monte-Carlo simulations have been executed with the assumptions such that the average powers at the channels are equal as $\Omega_{i,k}^{a,r} = \Omega_a$ and $\Omega_{j,k}^{b,r} = \Omega_b$ for all values of i, j, r and k. All vehicles transmit with the unit power, $P_a = P_b = P_r = 1$. We assume that the channels from sources to relays and relays to sources are symmetrical. For simplicity, the cascading degrees are also assumed as equal for all channels between a particular source (V_a or V_b), and all intermediate vehicles, i.e., $N_{i,k}^{a,r} = N_a$ for all values of i, r and k, and $N_{j,k}^{b,r} = N_b$ for all values of j, r and k. Finally we assume that the values of the m parameters of Nakagami-m distributed random variables composing the cascading fading coefficient are equal for all channels between a given source (V_a or V_b) and all relays, i.e., $m_{i,k,n}^{a,r} = m_a$ for all values of i, r, k and n, and $m_{j,k,n}^{b,r} = m_b$ for all values of j, r, k and n. In Figure 4.6, we represent the impact of the channels' cascading degrees on the outage probability. Here, threshold SNR is $\gamma_{th} = 5$ dB and values of the m parameters for all channels are chosen equal as $m_a = m_b = 1.5$. The number of relays is $R = 2$, and all sources and relays are equipped with double antennas, i.e., $M_a = M_b = M_r = 2$. The simulations are executed for the cascading degrees of $N_a = N_b = 4$, 5 and 6. It is shown that the outage probability increases when the cascading degrees of the channels increase, which means increasing the cascading degree worsens the performance of the vehicular

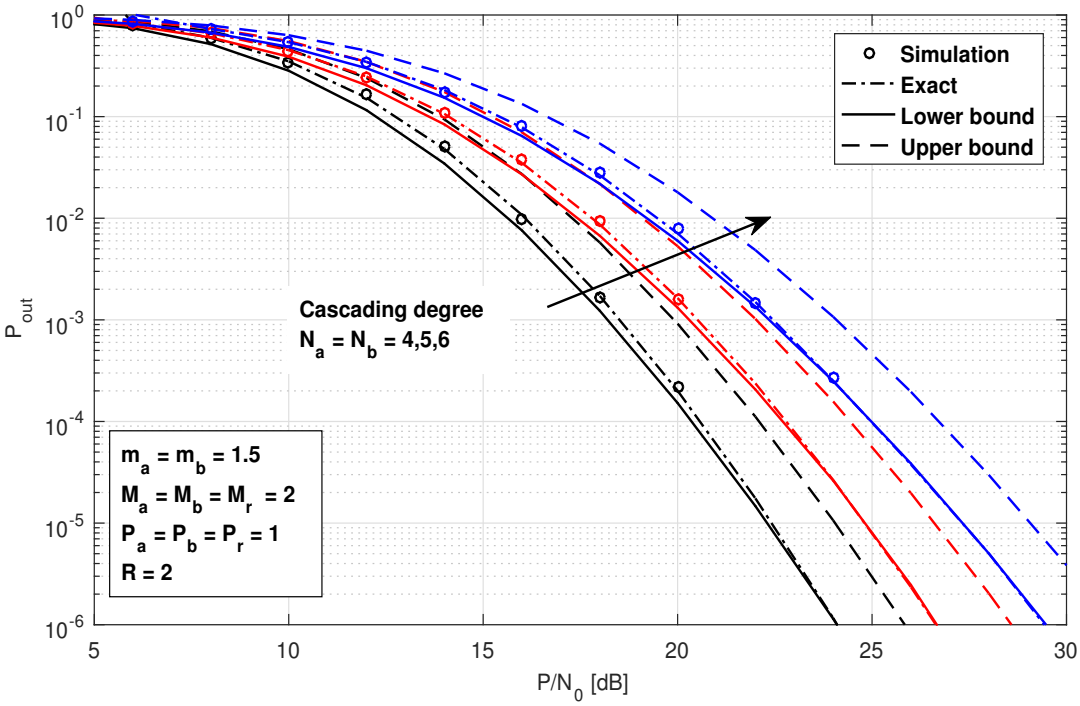

Figure 4.6 : Impact of the channel's cascading degrees on the outage probability for threshold SNR $\gamma_{th} = 5$ dB.

communication system because the higher the cascading degree is, the worse the fading effects are.

Figure 4.7 reveals the effect of the relays' number on the system performance. The number of the installed antennas on the sources is $M_a = M_b = 3$ while the relays are equipped with $M_r = 4$ antennas. Threshold SNR is chosen as $\gamma_{th} = 5$ dB. The values of the fading parameter m and the cascading degrees for all channels are chosen as $m_a = m_b = 1.2$ and $N_a = N_b = 5$, respectively. During the simulations and the analytic calculations, the number of the relay vehicles is set to $R = 1$, 3 and 5. As seen from the plots, increasing relays' number leads to higher diversity gain, thus the outage probability becomes lower. Thereby, the increasing number of the relays in the system with the relay selection scheme enhances the performance of the system over cascaded fading channels.

Relation between the number of the antennas on the source and the relay vehicles and the outage probability of MIMO AF PLNC vehicular communication system performing the antenna selection scheme is considered in Figure 4.8 and Figure 4.9 for threshold SNR $\gamma_{th} = 7$ dB. The values of the fading parameter m for all channels are assumed as $m_a = m_b = 1.5$, and their cascading degrees are set as $N_a = N_b = 4$. In order to obtain a clear view, we omit the upper bound plots on these graphs.

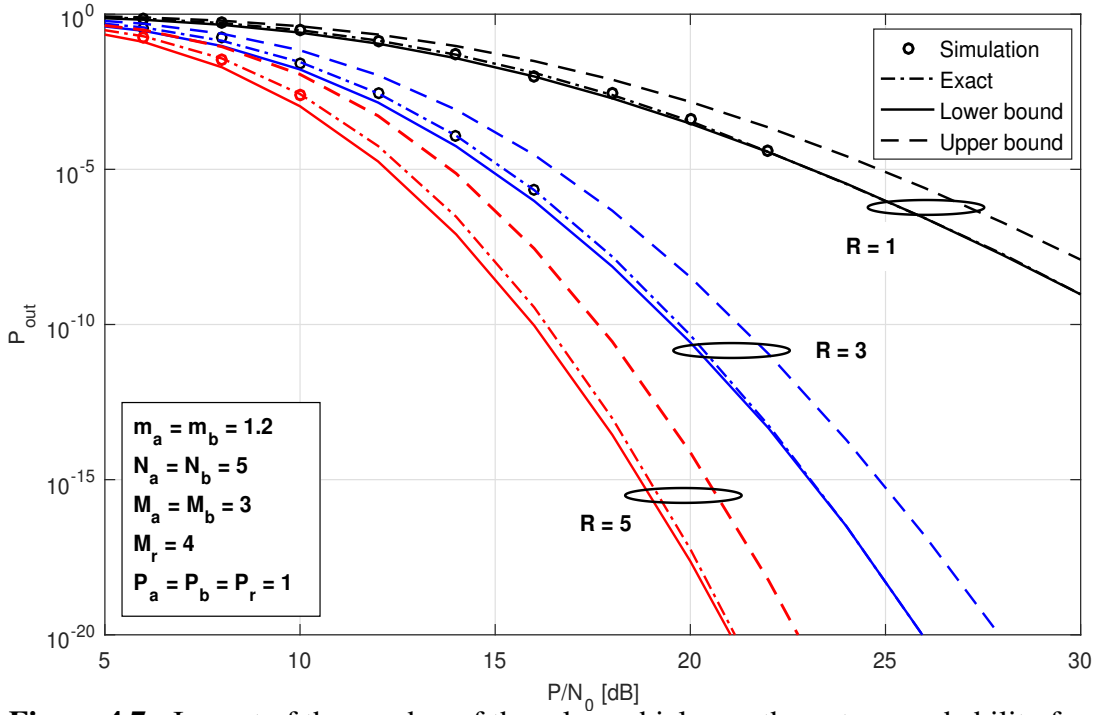

Figure 4.7 : Impact of the number of the relay vehicles on the outage probability for threshold SNR $\gamma_{th} = 5$ dB.

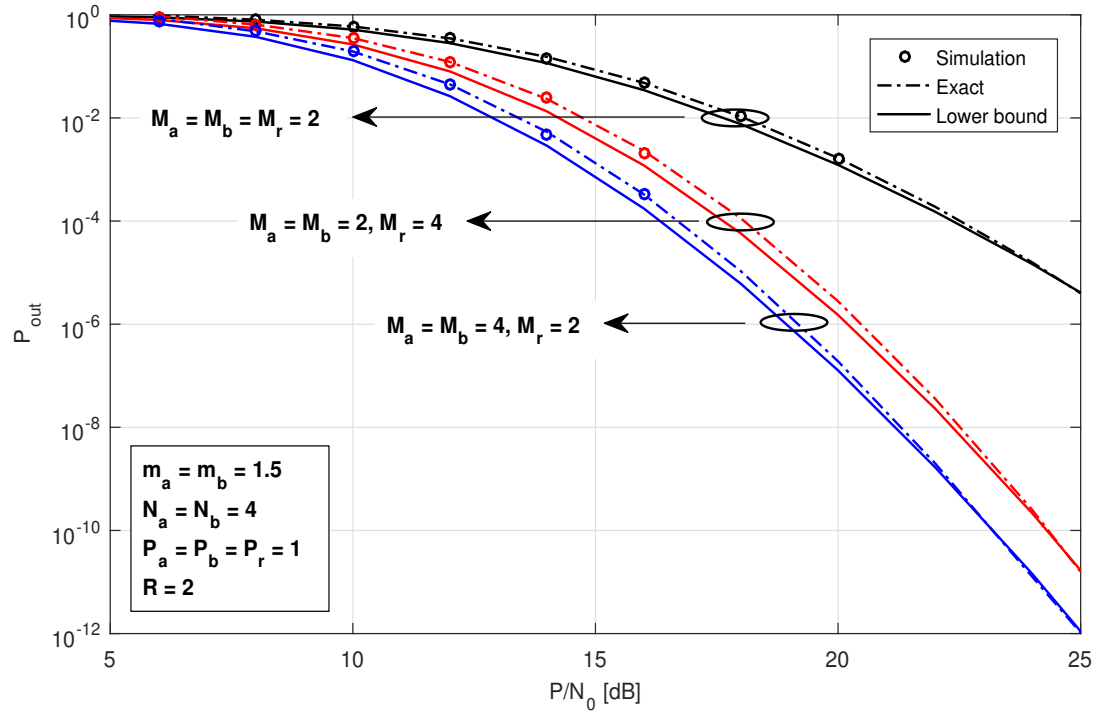

Figure 4.8 : Impact of the antenna numbers on the vehicles to the outage probability for threshold SNR $\gamma_{th} = 7$ dB.

In Figure 4.8, the number of the relay vehicles are $R = 3$. Here, we present three different combinations for the number of the antennas on the sources and the relays which are $M_a = M_b = M_r = 2$, $M_a = M_b = 2$, $M_r = 4$, and $M_a = M_b = 4$, $M_r = 2$. The figure reveals that the increasing number of the antennas on vehicles performing the

antenna selection enhances the system performance in general by reducing the outage probability. On the other hand, we present via the plots that the number of the antennas on the source vehicles is more effective than those on the relays in terms of improving the performance. In Figure 4.9, to enhance the value of the simulations and point out the merits of the different relay and antenna numbers, we compare the SISO (single input single output) PLNC and MIMO PLNC systems. The scenarios in this figure are selected as $(M_a = M_b = M_r = R = 1)$, $(M_a = M_b = M_r = 1, R = 2)$, $(M_a = M_b = M_r = 2, R = 1)$, $(M_a = M_b = M_r = 2, R = 2)$, $(M_a = M_b = 2, M_r = 1, R = 1)$, and $(M_a = M_b = 1, M_r = 2, R = 1)$. This figure shows that the MIMO systems give better outage performance in comparison with the SISO systems. It is also seen that the cases of $(M_a = M_b = M_r = 1, R = 2)$ and $(M_a = M_b = M_r = 2, R = 1)$ have exactly the same performance as expected from the analytic results.

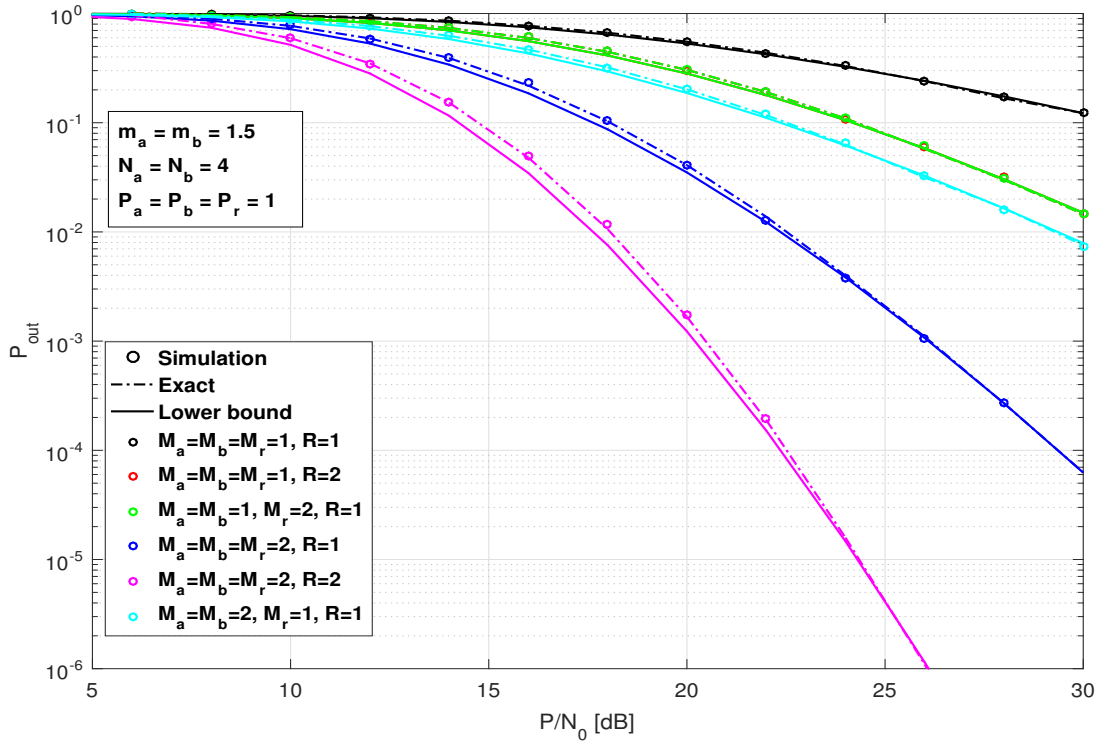

Figure 4.9 : Comparison of the SISO PLNC and MIMO PLNC systems over cascaded fading channels.

Figure 4.10 presents the impact of the fading parameter m values on the outage probability. Here, we assume the system parameters as threshold SNR $\gamma_{th} = 7$ dB, the cascading degree of the channels as $N_a = N_b = 7$, the number of the relay vehicles as $R = 3$ and the number of the antennas on all vehicles as $M_a = M_b = M_r = 3$. The simulations and the analytic calculations are implemented for the values of

$m_a = m_b = 1$, 1.5 and 2. The results present that the increasing m parameter value in cascaded fading channels decreases the outage probability of the system.

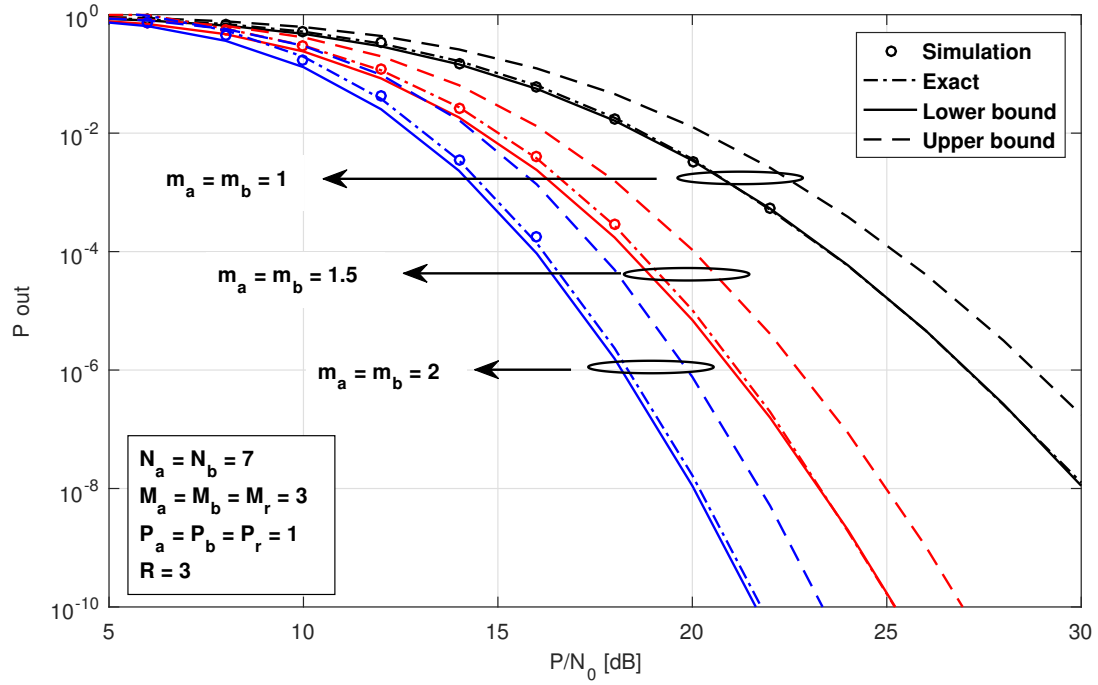

Figure 4.10 : Impact of the fading parameters on the outage probability for threshold SNR $\gamma_{th} = 7$ dB.

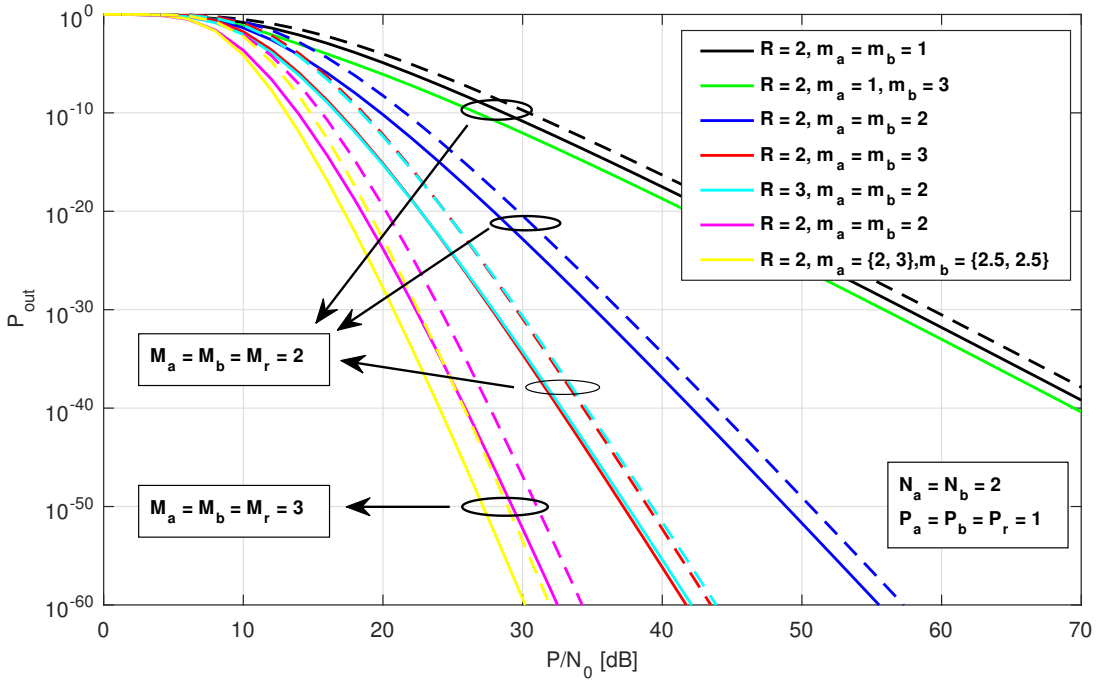

Figure 4.11 : The outage probability behavior in high SNR region for threshold SNR $\gamma_{th} = 5$ dB.

Finally, we present the outage probability behavior of the system in high SNR region in Figure 4.11. The threshold SNR is chosen as $\gamma_{th} = 5$ dB. The channels

between the sources and the relays are assumed as double Nakagami-m fading channels where the cascading degrees are set as $N_a = N_b = 2$. As it is seen from the plots, the diversity orders obtained for the upper and the lower bounds are consistent with those obtained by the analytical expression given in (4.64). For example, the diversity order of the system with the number of the relays as $R = 2$, the number of the antennas on the vehicles as $M_a = M_b = M_r = 3$, and the fading parameters of the channels as $\underline{m}_a = \{m_{a,1}, m_{a,2}\} = \{2, 3\}$ and $\underline{m}_b = \{m_{b,1}, m_{b,2}\} = \{2.5, 2.5\}$ is almost 36. This is consistent with the analytic derivation $d_o = \sum_{r=1}^{2} \sum_{k=1}^{3} \min(\sum_{i=1}^{3} \min\{2, 3\}, \sum_{j=1}^{3} \min\{2.5, 2.5\}) = 36$. Also the relations between the asymptotic diversity order and the system parameters, the number of the relays, the number of the antennas on the vehicles and the channels' fading parameters, are seen clearly from the plots. It is shown that the increasing number of the relays and/or the antennas on the vehicles can improve the asymptotic diversity order of the system significantly.

As it is seen from the figures, the plots of exact analytic and simulation results match perfectly. Furthermore, the plots of the lower bound and the exact analytic results overlap for high SNR region. Thus, the lower bound of the outage probability is quite tight and can be used as a benchmark for MIMO vehicular communication systems employing AF PLNC with joint relay and antenna selection over cascaded fading channels.

5. STTC DESIGN FOR MIMO AF PLNC SYSTEMS FOR V2V COMMUNICATIONS

Space-time coding techniques are used to improve the performance of MIMO systems. These techniques are grouped under two main categories which are STBC and STTC. STTCs provide both diversity and coding gain, therefore, they outperform STBCs which offer only the maximum possible diversity without any coding gain.

In this chapter, we combine PLNC and STTC techniques to improve the error performance of V2V systems. To this end, we first show that the mixture gamma distribution model can be used to examine the pdf of instantaneous SNR in double Rayleigh fading channels. Then, we evaluate the pdf expression for the summation of i.i.d. double Rayleigh distributed random variables. Then, the PEP analysis is performed for a fixed-gain AF PLNC V2V system employing STTC over double Rayleigh fading channels, and an upper bound for PEP is obtained. By examining the behavior of the upper bound expression in high SNR region, we derive a new design criterion for STTCs using two transmit antennas. Finally, using this criterion we propose novel STTCs for MIMO V2V systems employing PLNC over double cascaded Rayleigh fading channels.

5.1 System Model

In a V2V system pictured in Figure 5.1, V_a and V_b are source vehicles having M_a and M_b antennas, respectively. The system includes R single antenna relays, $\{V_r\}_{r=1}^{R}$, employing fixed-gain AF PLNC. For $i \in \{a,b\}$ and $j = 1, ..., M_i$, the gain of the channel between the j-th antenna of the i-th source and the r-th relay is denoted by $h_{i,r}^{j}$ which is assumed to be double Rayleigh distributed. Therefore, channel gain vectors can be given as $\mathbf{h}_{i,r} = \left[h_{i,r}^{1}, h_{i,r}^{2}, ..., h_{i,r}^{M_i}\right]$.

When the sources are communicating, they send their $M_i \times 1$ signal vectors $\mathbf{x}_i = \left[x_i^1, x_i^2, ..., x_i^{M_i}\right]^T$ to the relay in the first time slot of the PLNC scheme. Here $(.)^T$

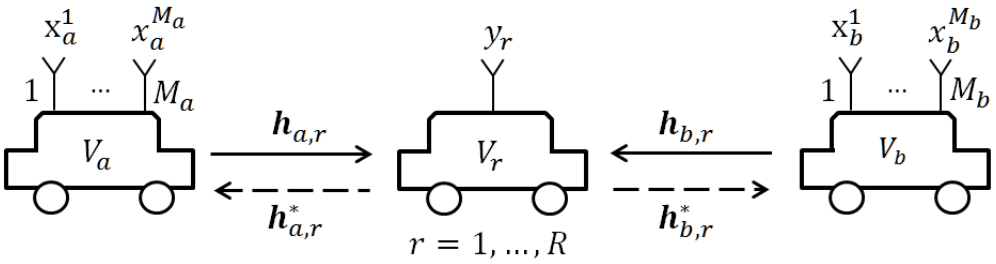

Figure 5.1 : A MIMO V2V system including the r-th single antenna relay performing fixed-gain AF PLNC.

denotes the matrix transpose operator. Hence, the r-th relay receives the signal

$$y_r = \mathbf{h}_{a,r}\mathbf{x}_a + \mathbf{h}_{b,r}\mathbf{x}_b + n_r \tag{5.1}$$

where n_r is the Gaussian noise with the distribution of $N(0,\sigma^2)$. Then the relay scales the signal y_r by the fixed power scaling factor given as

$$G = \sqrt{\frac{P_r}{P_a + P_b + \sigma^2}} \tag{5.2}$$

and forwards it towards the sources in the second time slot. Here P_a, P_b and P_r are transmission powers of V_a, V_b and V_r, respectively. We assume that all of the channels are the reciprocal channels whose gains in consecutive time slots are complex-conjugate of each other. Therefore the signals received at the sources are

$$\mathbf{y}_a = \sum_{r=1}^{R} \mathbf{h}_{a,r}^* G\mathbf{h}_{a,r}\mathbf{x}_a + \sum_{r=1}^{R} \mathbf{h}_{a,r}^* G\mathbf{h}_{b,r}\mathbf{x}_b + \sum_{r=1}^{R} \mathbf{h}_{a,r}^* G n_r + \mathbf{n}_a \tag{5.3a}$$

$$\mathbf{y}_b = \sum_{r=1}^{R} \mathbf{h}_{b,r}^* G\mathbf{h}_{a,r}\mathbf{x}_a + \sum_{r=1}^{R} \mathbf{h}_{b,r}^* G\mathbf{h}_{b,r}\mathbf{x}_b + \sum_{r=1}^{R} \mathbf{h}_{b,r}^* G n_r + \mathbf{n}_b \tag{5.3b}$$

where $(.)^*$ represents complex-conjugate transpose operator and $\mathbf{n}_i \sim N(0,\sigma^2\mathbf{I})$ denote $M_i \times 1$ Gaussian noise vectors at the sources. It is assumed that the sources have perfect CSI and therefore they cancel self-interference, and then obtain the signals

$$\tilde{\mathbf{y}}_a = \sum_{r=1}^{R} G\mathbf{h}_{a,r}^* \mathbf{h}_{b,r}\mathbf{x}_b + \sum_{r=1}^{R} G\mathbf{h}_{a,r}^* n_r + \mathbf{n}_a \tag{5.4a}$$

$$\tilde{\mathbf{y}}_b = \sum_{r=1}^{R} G\mathbf{h}_b^* \mathbf{h}_a\mathbf{x}_a + \sum_{r=1}^{R} G\mathbf{h}_b^* n_r + \mathbf{n}_b \tag{5.4b}$$

at the end of the second time slot of the PLNC signaling scheme.

5.2 Statistical Analysis of the SNR for Double Rayleigh Fading Channels

In the double Rayleigh channels channels, pdf for the power of the channel gain, $z = |h|^2/2$ where $|h|$ is the channel gain's envelope which is the double Rayleigh distributed with unit mean power, is given by

$$f_z(z) = 2K_0\left(2\sqrt{z}\right) \tag{5.5}$$

where $K_0(.)$ is the modified second-type Bessel function with zero-order. As mentioned in Section 2.1.6, it is proposed to express any pdf in terms of a weighted sum of the gamma distributions to simplify the analysis associated with the complicated or intractable performance expressions involving the special functions [35]. By using the definition of Bessel function [125, 8.432.7[7]] given as

$$K_\nu(xy) = \frac{1}{2}\left(\frac{y}{2}\right)^\nu \int_0^\infty e^{-\frac{x}{2}\left(t+\frac{y^2}{t}\right)} t^{-\nu-1} dt \tag{5.6}$$

and setting the parameter values as $\nu = 0$, $x = 2$ and $y = \sqrt{z}$, the pdf in (5.5) can be expressed in Gauss-Laguerre integral form [125] as follows

$$f_z(z) = \int_0^\infty e^{-t} g(t) dt \tag{5.7}$$

where $g(t) = 4t^{-1}e^{-\frac{z}{t}}$. In that case, we can model the double Rayleigh fading channels by using the mixture gamma model, and write the pdf in (5.5) in the form of

$$f_z(z) = \sum_{k=1}^{K} \alpha_k z^{\beta_k - 1} e^{-\zeta_k z} \tag{5.8}$$

with the parameter values of $\beta_k = 1$, $\zeta_k = \frac{1}{t_k}$ and $\alpha_k = \psi\left(\frac{w_k}{t_k}, \beta_k, \zeta_k\right)$, where $\psi(\theta_k, \beta_k, \zeta_k) = \frac{\theta_k}{\sum_{j=1}^{K} \theta_j \Gamma(\beta_j) \zeta_j^{-\beta_j}}$. Here $w_k = \frac{\alpha_k \Gamma(\beta_k)}{\zeta_k^{\beta_k}}$ is the weighting coefficient of the k-th gamma component satisfying $\sum_{k=1}^{K} w_k = 1$. In that case, the MGF of z becomes as given in (2.24). At this point, let $\Xi = \sum_{l=1}^{L} z_l$, where $\{z_l\}_{l=1}^{L}$ denote the powers of channels' gains with the equal mean value as $E[z_l] = \Omega$, in the double Rayleigh channels. Thus, the MGF of Ξ becomes

$$M_\Xi(s) = \prod_{l=1}^{L} M_{z_l}(s) = \left(M_{z_l}(s)\right)^L. \tag{5.9}$$

Substituting (2.24) in (5.10) and using multinomial theorem given as

$$\left(\sum_{k=1}^{K} x_i\right)^L = \sum_{n_1+\ldots+n_K=L} \frac{L!}{n_1!\ldots n_K!} \prod_{k=1}^{K} x_k^{n_k}, \tag{5.10}$$

and then by following the approach in [136], $M_\Xi(s)$ is written as

$$M_\Xi(s) = \sum_{n_1+\ldots+n_K=L} \frac{L!}{n_1!\ldots n_K!} \prod_{k=1}^{K} \alpha_k^{n_k} \prod_{k=1}^{K} \left(\frac{1}{\zeta_k+s}\right)^{n_k}. \tag{5.11}$$

Then using the property $\mathscr{L}^{-1}\{\frac{1}{(s+\zeta)^n}\} = \frac{x^{n-1}}{(n-1)!}e^{-\zeta x}$ of the inverse Laplace transform, the pdf of Ξ is obtained as

$$\begin{aligned} f_\Xi(\xi) &= \mathscr{L}^{-1}\{M_\Xi(s)\} \\ &= \sum_{n_1+\ldots+n_K=L} \frac{L!}{n_1!\ldots n_K!} \prod_{k=1}^{K} \alpha_k^{n_k} \sum_{k=1}^{K} \sum_{l=0}^{n_k} \phi_{kl} \xi^l e^{-\zeta_k \xi}, \end{aligned} \tag{5.12}$$

where ϕ_{kl} denotes the coefficient of the l-th term. On the other hand, to examine the case of unequal mean value, we define Ξ as $\Xi = \sum_{l=1}^{L} \eta_l$, where $\eta_l \stackrel{\triangle}{=} \lambda_l z_l$ is the power of channel gain with the mean value of $\Omega_l = \lambda_l \Omega$. In this case, MGF of Ξ becomes

$$M_\Xi(s) = \prod_{l=1}^{L} M_{\lambda_l z_l}(\lambda_l s) = \prod_{l=1}^{L} \sum_{k=1}^{K} \frac{\alpha_k}{\zeta_k + s\lambda_l}. \tag{5.13}$$

The pdf in (5.12) and MGF in (5.13) are used to analysis of the PEP in the following section.

5.3 Analysis of the Pairwise Error Probability

Let an STTC is used in the considered system. The conditional PEP, which is probability of the erroneous decoding of a code-word $\mathbf{X}$ transmitted by V_a as another code-word $\hat{\mathbf{X}}$ at V_b, is given as

$$P(\mathbf{X} \to \hat{\mathbf{X}} | \mathbf{H}_1, \ldots, \mathbf{H}_R) = Q\left(G\sqrt{\frac{E_s}{2N_0} \sum_{r=1}^{R} \| \mathbf{H}_r \left(\mathbf{X} - \hat{\mathbf{X}}\right) \|^2}\right) \tag{5.14}$$

[73, 76] where E_s is the energy per symbol, N_0 is the noise power, $\mathbf{H}_r = \mathbf{h}_{b,r}^* \mathbf{h}_{a,r}$ is the channel matrix between V_a and V_b through V_r, and $Q(x)$ is the Gauss Q-function defined as [127]

$$Q(x) = \frac{1}{\pi} \int_0^{\pi/2} e^{-\frac{x^2}{2\sin^2\alpha}} d\alpha. \tag{5.15}$$

Using the inequality property of $Q(x) \leq e^{-x^2/2}$ and taking the average of (5.14) over all realizations of $\{\mathbf{H}_r\}_{r=1}^R$, an upper bound for PEP, $P(\mathbf{X} \to \hat{\mathbf{X}})$, is obtained as

$$P(\mathbf{X} \to \hat{\mathbf{X}}) \leq \int_0^\infty e^{-sx} f_X(x) dx = E\left[e^{-sx}\right] = M_X(s)\Big|_{s=\frac{G^2 E_s}{4N_0}} \tag{5.16}$$

where $X \stackrel{\triangle}{=} \| \sum_{r=1}^{R} \mathbf{H}_r \left(\mathbf{X}-\hat{\mathbf{X}}\right) \|^2$, $f_X(.)$ is the pdf of X and $M_X(.)$ is the MGF of X [73, 76]. For the random variable X, by using the triangle inequality, we can introduce an upper bound as

$$X = \| \sum_{r=1}^{R} \mathbf{H}_r \left(\mathbf{X}-\hat{\mathbf{X}}\right) \|^2 \leq \sum_{r=1}^{R} \| \mathbf{H}_r \left(\mathbf{X}-\hat{\mathbf{X}}\right) \|^2 = \sum_{r=1}^{R} X_r \tag{5.17}$$

where $X_r = \| \mathbf{H}_r \left(\mathbf{X}-\hat{\mathbf{X}}\right) \|^2$ and thus following relationship between the MGFs of X and $\sum_{r=1}^{R} X_r$ holds

$$M_X(s) \leq M_{\sum_{r=1}^{R} X_r}(s) = \prod_{r=1}^{R} M_{X_r}(s). \tag{5.18}$$

since the cahnnels' gains are i.i.d., $\{X_r\}_{r=1}^{R}$ become i.i.d., therefore by substituting (5.18) in (5.16), the PEP can be upper-bounded as

$$P\left(\mathbf{X} \to \hat{\mathbf{X}}\right) \leq \left(M_{X_r}(s)\right)^R. \tag{5.19}$$

At this point, in order to evaluate $M_{X_r}(s)$, we can drive

$$\begin{aligned} X_r = \| \mathbf{H}_r \left(\mathbf{X}-\hat{\mathbf{X}}\right) \|^2 &= \| \mathbf{h}_{b,r}^* \mathbf{h}_{a,r} \left(\mathbf{X}-\hat{\mathbf{X}}\right) \|^2 \\ &= Tr\left(\mathbf{h}_{b,r}^* \mathbf{h}_{a,r} \left(\mathbf{X}-\hat{\mathbf{X}}\right) \left(\mathbf{X}-\hat{\mathbf{X}}\right)^* \mathbf{h}_{a,r}^* \mathbf{h}_{b,r}\right) \\ &= \| \mathbf{h}_{a,r} \left(\mathbf{X}-\hat{\mathbf{X}}\right) \|^2 \| \mathbf{h}_{b,r} \|^2 \\ &= \sum_{j=1}^{M_a} \lambda_j |h_{a,r}^j|^2 \sum_{j=1}^{M_b} |h_{b,r}^j|^2 \\ &= \sum_{j=1}^{M_a} \lambda_j z_a^j \sum_{j=1}^{M_b} z_b^j \end{aligned} \tag{5.20}$$

where $Tr(.)$ is the trace operator, $z_a^j = |h_{a,r}^j|^2$, $z_b^j = |h_{b,r}^j|^2$ and the λ_j coeffients are the eigen-values of the matrix $\left(\mathbf{X}-\hat{\mathbf{X}}\right)\left(\mathbf{X}-\hat{\mathbf{X}}\right)^*$, which is a symmetric positive definite matrix making all λ_j non-negative. If z_a, z_b and X_r are defined as

$$z_a \stackrel{\triangle}{=} \sum_{j=1}^{M_a} \lambda_j z_a^j \tag{5.21a}$$

$$z_b \stackrel{\triangle}{=} \sum_{j=1}^{M_b} z_b^j \tag{5.21b}$$

$$X_r \stackrel{\triangle}{=} z_a z_b, \tag{5.21c}$$

the pdf of X_r becomes $f_{X_r}(x) = \int_0^\infty \rho^{-1} f_{z_b}(\rho) f_{z_a}(\frac{x}{\rho}) d\rho$. Therefore $M_{X_r}(s)$ is obtained as

$$M_{X_r}(s) = \int_0^\infty e^{-sx} f_{X_r}(x) dx = \int_0^\infty f_{z_b}(x) M_{z_a}(sx) dx \tag{5.22}$$

where $M_{z_a}(.)$ is the MGF of z_a in (5.21a), and $f_{z_b}(.)$ is the pdf of z_b in (5.21b). Using (5.12), the pdf of z_b becomes

$$f_{z_b}(x) = \sum_{n_1+\ldots+n_K=M_b} \frac{M_b!}{n_1!\ldots n_K!} \prod_{k=1}^{K} \alpha_k^{n_k} \sum_{k=1}^{K} \sum_{l=0}^{n_k} \phi_{kl} x^l e^{-\zeta_k x}. \tag{5.23}$$

The MGF of z_a is obtained as

$$M_{z_a}(s) = \prod_{j=1}^{M_a} M_{\lambda_j z_a^j}(s) = \prod_{j=1}^{M_a} M_{z_a^j}(\lambda_j s) = \prod_{j=1}^{M_a} \sum_{k=1}^{K} \frac{\alpha_k}{\zeta_k + s\lambda_j} \tag{5.24}$$

with the help of (5.13). Since $\lambda_j > 0$ and $0 < x \leq \infty$, we can write that

$$M_{z_a}(sx) \leq \prod_{j=1}^{M_a} \sum_{k=1}^{K} \frac{\alpha}{\zeta + s\lambda_j x} \tag{5.25}$$

where $\alpha \stackrel{\triangle}{=} \max(\alpha_k)$ and $\zeta \stackrel{\triangle}{=} \min(\zeta_k)$. Therefore, by substituting (5.25) in (5.22), we have

$$M_{X_r}(s) \leq \int_0^{\infty} f_{z_b}(x) \left(\frac{K\alpha}{\zeta}\right)^{M_a} \prod_{j=1}^{M_a} \frac{1}{1+\frac{s\lambda_j}{\zeta}x} dx. \tag{5.26}$$

On the other hand, it can be shown

$$\prod_{j=1}^{M} \frac{1}{(c_1 + c_2 x_j)} = \sum_{j=1}^{M} \frac{(-c_1)^{M-1}}{(c_1 + c_2 x_j)} \prod_{\substack{t=1 \\ t\neq j}}^{M} \frac{x_j}{x_t - x_j}, \qquad x_t \neq x_j \tag{5.27}$$

in a straightforward manner, where c_1 and c_2 are constants. Therefore, using (5.23) and (5.25) with (5.27), (5.26) can be re-expressed as

$$M_{X_r}(s) \leq \sum_{n_1+\ldots+n_K=M_b} \frac{M_b!}{n_1!\ldots n_K!} \prod_{k=1}^{K} \alpha_k^{n_k} \sum_{k=1}^{K} \sum_{l=0}^{n_k} \phi_{kl} \left(\frac{K\alpha}{\zeta}\right)^{M_a} \sum_{j=1}^{M_a} \left(\prod_{\substack{t=1 \\ t\neq j}}^{M_a} \frac{\lambda_j}{\lambda_j - \lambda_t} \right) I \tag{5.28}$$

where the integral I is defined as

$$I = \int_0^{\infty} \frac{x^l e^{-\zeta_k x}}{1+\frac{s}{\zeta}\lambda_j x} dx. \tag{5.29}$$

Using the integral property [125, 3.353-5.[7]] of exponentials and rational functions, which is given as

$$\int_0^{\infty} \frac{x^n e^{-\mu x}}{\beta + x} dx = (-1)^{n-1} \beta^n e^{\beta\mu} Ei[-\beta\mu] + \sum_{k=1}^{n} (k-1)! (-\beta)^{l-k} \mu^{-k}$$
$$|\arg(\beta)| < \pi, Re(\mu) > 0, \tag{5.30}$$

the integral in (5.29) is solved as

$$I = (-1)^{l-1}\beta^{l+1}e^{\beta\zeta_i}Ei[-\beta\zeta_i] + \sum_{k=1}^{l}(-1)^{l-k}(k-1)!\beta^{l-k+1}\zeta_i^{-k} \tag{5.31}$$

where $\beta \triangleq \frac{\zeta}{s\lambda_j}$. As $\beta \to 0$, namely $s \to \infty$, the second term of (5.31) satisfies that

$$\lim_{\substack{\beta\to 0 \\ (s\to\infty)}} \quad \sum_{k=1}^{l}(-1)^{l-k}(k-1)!\beta^{l-k+1}\zeta_i^{-k} = 0, \tag{5.32}$$

thus, I is approximately equal to the following expression

$$I \simeq (-1)^{l-1}\beta^{l+1}e^{\beta\zeta_i}Ei[-\beta\zeta_i]. \tag{5.33}$$

Furthermore, by using the definition of the exponential integral function given in [125, 8.212-1.[8]] as

$$Ei(-x) = C + e^{-x}\ln x + \int_0^x e^{-t}\ln t dt \qquad [x > 0], \tag{5.34}$$

the approximated expression of I in (5.33) is expanded as

$$I \simeq (-1)^{l-1}\beta^{l+1}\left(\ln(\beta\zeta_i) + e^{\beta\zeta_i}\left(C + \int_0^{\beta\zeta_i} e^{-t}\ln t dt\right)\right). \tag{5.35}$$

Since

$$\lim_{\substack{\beta\to 0 \\ (\beta\zeta_i\to 0)}} \quad e^{\beta\zeta_i}\left(C + \int_0^{\beta\zeta_i} e^{-t}\ln t dt\right) = C \tag{5.36}$$

holds, we can simplify the expression of I as

$$I \simeq (-1)^{l-1}\left(\frac{\zeta}{s\lambda_j}\right)^{l+1}\left(\ln\zeta + \ln\zeta_i - \ln s - \ln\lambda_j + C\right), \tag{5.37}$$

and therefore, an an asymptotic solution for the integral I can be obtained as

$$I \simeq (-1)^{l}\left(\frac{\zeta}{\lambda_j}\right)^{l+1}\frac{\ln\left(s\lambda_j\right)}{s^{l+1}}. \tag{5.38}$$

Substituting (5.38) in (5.28), an upper bound for PEP is found as

$$P(\mathbf{X}\to\hat{\mathbf{X}}) \leq \left(\sum_{n_1+\ldots+n_K=M_b}\frac{M_b!}{n_1!\ldots n_K!}\prod_{k=1}^{K}\alpha_k^{n_k}\right. \\ \left.\sum_{k=1}^{K}\sum_{l=0}^{n_k}\phi_{kl}\left(\frac{K\alpha}{\zeta}\right)^{M_a}\left(\frac{\zeta}{s}\right)^{l+1}g(l,\lambda_j,s)\right)^{R} \tag{5.39}$$

where the function $g(l,\lambda_j,\gamma)$ is defined as

$$g(l,\lambda_j,s) \triangleq (-1)^l \sum_{j=1}^{M_a} \left(\prod_{\substack{t=1 \\ t\neq j}}^{M_a} \frac{\lambda_j}{\lambda_j-\lambda_t} \right) \frac{\ln s + \ln \lambda_j}{\lambda_j^{l+1}}. \tag{5.40}$$

As it is seen from this upper bound, when $s \to \infty$, $P(\mathbf{X} \to \hat{\mathbf{X}}) \to 0$. At this stage, if the SNR is high enough in the summation over l of (5.39), the first term corresponding to $l = 0$ becomes dominant and the remaining terms can be discarded because the coefficient $\phi_{kl} \left(\frac{K\alpha}{\zeta}\right)^{M_a} \left(\frac{\zeta}{s}\right)^{l+1}$ goes to zero as $l \geq 1$, i.e.,

$$\sum_{l=0}^{n_k} \phi_{kl} \left(\frac{K\alpha}{\zeta}\right)^{M_a} \left(\frac{\zeta}{s}\right)^{l+1} g(l,\lambda_j,s) \approx \phi_{k0} \left(\frac{K\alpha}{\zeta}\right)^{M_a} \frac{\zeta}{s} g(0,\lambda_j,s). \tag{5.41}$$

At this stage, the derived upper bound expression of the PEP can be used to evaluate a design rule for the STTCs to be used in MIMO V2V PLNC systems.

5.4 A Design Criterion for STTCs for Double Rayleigh Fading Channels

By substituting (5.40) in the approximation given in (5.41), the upper bound for $M_{X_r}(s)$ becomes

$$M_{X_r}(s) \leq \sum_{n_1+\ldots+n_K=M_b} \frac{M_b!}{n_1!\ldots n_K!} \prod_{k=1}^{K} \alpha_k^{n_k} \sum_{k=1}^{K} \phi_{k0} \left(\frac{K\alpha}{\zeta}\right)^{M_a} \zeta \left(\frac{\ln s}{s} \sum_{j=1}^{M_a} \left(\prod_{\substack{t=1 \\ t\neq j}}^{M_a} \frac{\lambda_j}{\lambda_j-\lambda_t} \right) \lambda_j^{-(l+1)} + \frac{1}{s} \sum_{j=1}^{M_a} \left(\prod_{\substack{t=1 \\ t\neq j}}^{M_a} \frac{\lambda_j}{\lambda_j-\lambda_t} \right) \frac{\ln \lambda_j}{\lambda_j^{l+1}} \right) \tag{5.42}$$

At this point, we consider an STTC whose encoder has two transmit antennas corresponding to the case of $M_a = 2$. In this case, the term $\prod_{\substack{t=1 \\ t\neq j}}^{M_a} \frac{\lambda_j}{\lambda_j-\lambda_t}$ becomes zero and (5.42) reduces to

$$M_{X_r}(s) \leq \sum_{n_1+\ldots+n_K=M_b} \frac{M_b!}{n_1!\ldots n_K!} \prod_{k=1}^{K} \alpha_k^{n_k} \sum_{k=1}^{K} \phi_{k0} \frac{K^{M_a}\alpha^{M_a}}{s\zeta^{M_a-1}} \sum_{j=1}^{M_a} \left(\prod_{\substack{t=1 \\ t\neq j}}^{M_a} \frac{\lambda_j}{\lambda_j-\lambda_t} \right) \frac{\ln \lambda_j}{\lambda_j} \tag{5.43}$$

Since $P(\mathbf{X} \to \hat{\mathbf{X}}) \leq (M_{X_r}(s))^R$, by replacing $s = \frac{G^2 E_s}{4N_0}$ and omitting the terms that are independent of the eigen-values, we obtain a design criterion for an STTC to be used in the MIMO PLNC V2V systems over double Rayleigh fading channels as

$$d = \sum_{j=1}^{M_a} \left(\prod_{\substack{k=1 \\ k\neq j}}^{M_a} \frac{\lambda_j}{\lambda_j-\lambda_k} \right) \frac{\ln \lambda_j}{\lambda_j} \tag{5.44}$$

in case of the encoder with two transmit antennas.

5.5 Code Search and Numerical Results

The code searches have been performed at two stages. At the first stage, we execute an exhaustive search algorithm evaluating the eigen-values and calculate the criterion value given above over all possible 4 and 8 states STTCs with QPSK modulation to find trellises which have the lowest values according to (5.44). After determining the set of trellises having the minimum d, we perform Monte-Carlo simulations for each trellis in this set to find the best one achieving the best SER performance in moderate and high SNR regions for the MIMO V2V systems employing fixed-gain AF PLNC over the double Rayleigh fading channels.

In the simulations, two transmit and one receive antennas are assumed. The simulations have been performed under the block fading assumption, and the average power of the fading coefficients was set to unity. It is also assumed that 50000 frames are transmitted out of each antenna of the space-time trellis encoder and each frame consists of 10 QPSK symbols. We place the QPSK symbols $\{0,1,2,3\}$ to the points $\{1,1i,-1,-1i\}$ on the constellation. For a given node (V_1, V_2 or $\{V_r\}_{r=1}^{R}$), it is assumed that all the antennas of the node transmit with equal power as $P_a = P_b = P_r = 1$, and SNR at this node was defined as the ratio of the total transmit power to the noise power,

Table 5.1 : Search result for the 4 and 8 states STTCs with QPSK modulation.

	States / Modulation	d_E^2	d	Generator matrix
Proposed	4 / QPSK	10	1.281	$G = \begin{bmatrix} 3 & 2 & 0 & 2 \\ 2 & 0 & 2 & 3 \end{bmatrix}$
Firmanto	4 / QPSK	10	1.756	$G = \begin{bmatrix} 3 & 2 & 2 & 0 \\ 1 & 2 & 1 & 2 \end{bmatrix}$
Canpolat	4 / QPSK	10	1.756	$G = \begin{bmatrix} 3 & 2 & 3 & 2 \\ 3 & 2 & 2 & 0 \end{bmatrix}$
Ilhan	4 / QPSK	10	1.756	$G = \begin{bmatrix} 2 & 3 & 2 & 1 \\ 2 & 3 & 0 & 2 \end{bmatrix}$
Proposed	8 / QPSK	14	2.15	$G = \begin{bmatrix} 2 & 3 & 2 & 1 & 2 \\ 0 & 2 & 2 & 3 & 0 \end{bmatrix}$
Firmanto	8 / QPSK	10	2.31	$G = \begin{bmatrix} 0 & 2 & 1 & 1 & 2 \\ 2 & 2 & 3 & 2 & 0 \end{bmatrix}$
Canpolat	8 / QPSK	12	3.06	$G = \begin{bmatrix} 2 & 3 & 2 & 3 & 1 \\ 2 & 3 & 1 & 2 & 0 \end{bmatrix}$
Ilhan	8 / QPSK	12	3.06	$G = \begin{bmatrix} 1 & 2 & 1 & 0 & 1 \\ 2 & 1 & 3 & 2 & 1 \end{bmatrix}$

N_0. Table 5.1 presents the search results for the 4 and 8 states STTCs with QPSK modulation. The proposed codes have the value of $d = 1.281$ and $d = 2.15$ for the case of 4 and 8 states, respectively. We also present values of d for the codes proposed by Firmanto *et al.* [77], Canpolat *et al.* [78] and Ilhan *et al.* [79] for the comparison purpose. It is seen from the table that the proposed codes have the lowest d values.

Figure 5.2 presents the SER performance of the MIMO V2V system employing the fixed-gain AF PLNC with 4-state STTCs over the double Rayleigh fading channels. The performance of the proposed 4-state code is compared with STTCs of the same memory order proposed in [77] for non-cooperative communication systems over the fast Rayleigh fading channels and proposed in [78] and [79] for classical cooperative communication systems over the quasi-static Rayleigh and double Rayleigh fading channels, respectively. It is shown that (5.44) offers a better STTC design criterion for the MIMO V2V systems employing fixed-gain AF PLNC over the double Rayleigh fading channels, and the proposed 4-state code has approximately 1–2 dB advantage against the existing codes in the high SNR region.

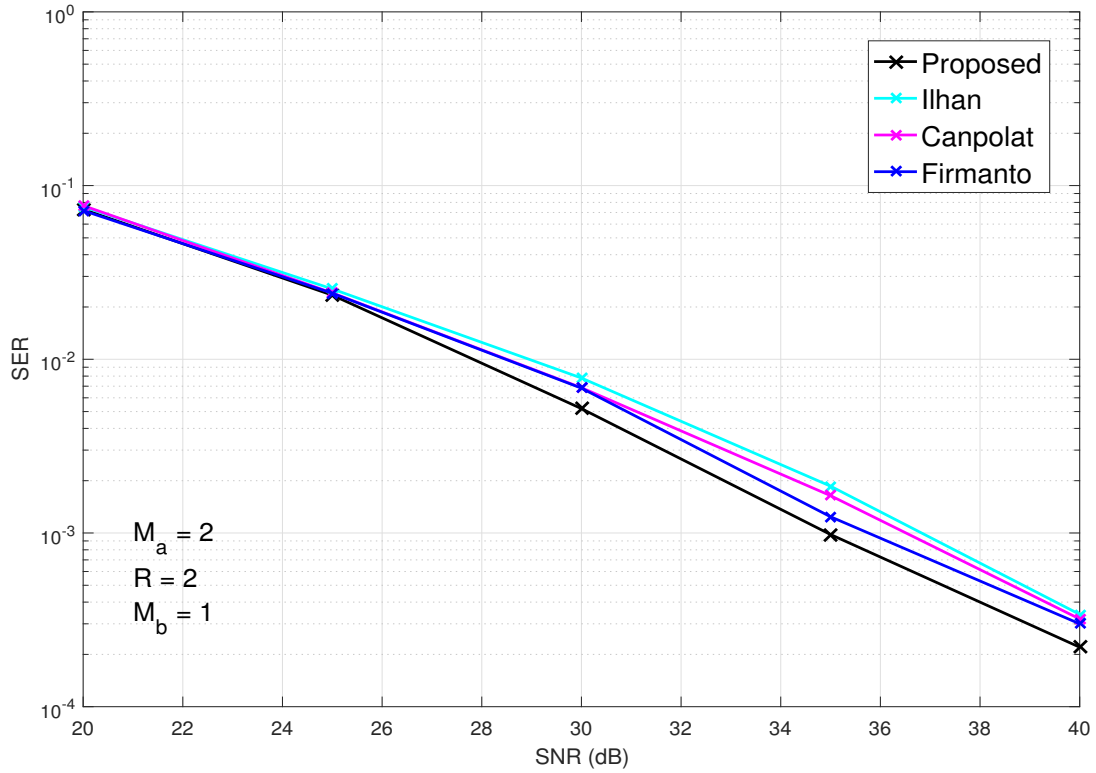

Figure 5.2 : SER comparison between Firmanto's, Canpolat's, Ilhan's and the proposed 4-state STTC for fixed-gain AF PLNC V2V systems over cascaded fading channels.

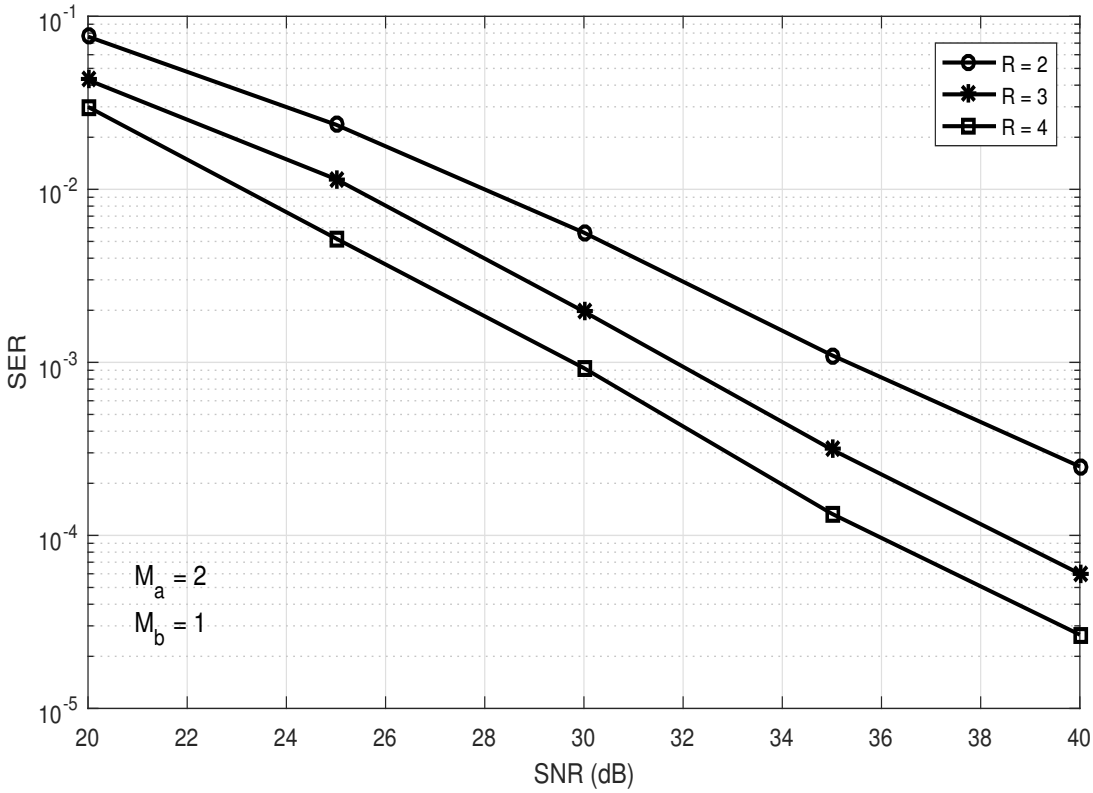

Figure 5.3 : SER performance of the proposed 4-state STTC for various relay numbers.

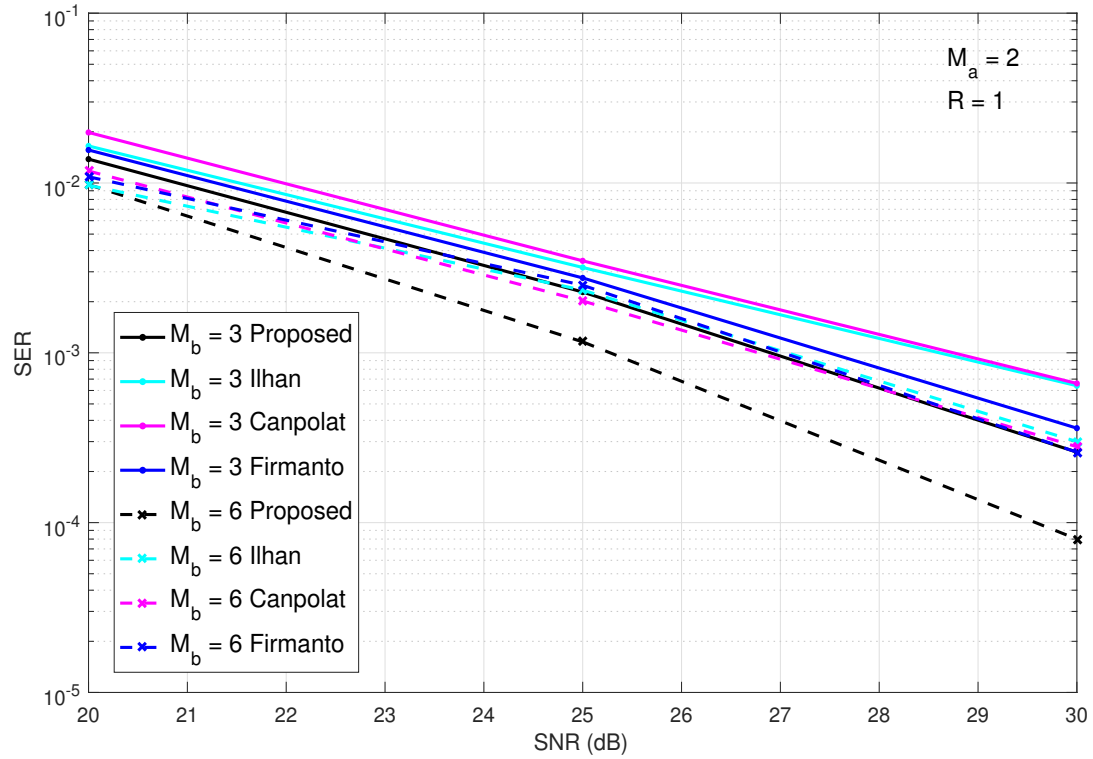

Figure 5.4 : SER performance of the proposed 4-state STTC for various receiver antenna numbers.

In Figure 5.3, we present the SER performance of the proposed 4-state STTC for various relay numbers. As it is expected, the increasing number of relays enhances the SER performance. For example, 35 dB SNR is required to achieve a SER value of 10^{-3} when $R = 2$, whereas the same SER value can be obtained at 32 dB in case of $R = 3$. Furthermore, increasing the number of relays from 3 to 4 provides an additional 2 dB SNR gain.

Figure 5.4 reveals the SER performance of the proposed 4-state STTC in the single-relay PLNC system for various receiver antenna numbers. It is shown that the increasing number of receiver antennas improves the SER performance. For example, 2 dB SNR gain can be obtained by increasing the number of receiver antennas from 3 to 6 at a SER value of 10^{-3}. The proposed code provides significant amount of SNR with respect to the existing 4-state codes.

We present the SER performances of the novel and previously proposed 8-state STTCs in Figure 5.5. Here we assume a single-relay system, $R = 1$, where the source vehicles have 2 antennas as $M_b = 2$. It is shown that the novel 8-state STTC provides approximately 0.5–1.5 dB advantage against the existing 8-state codes.

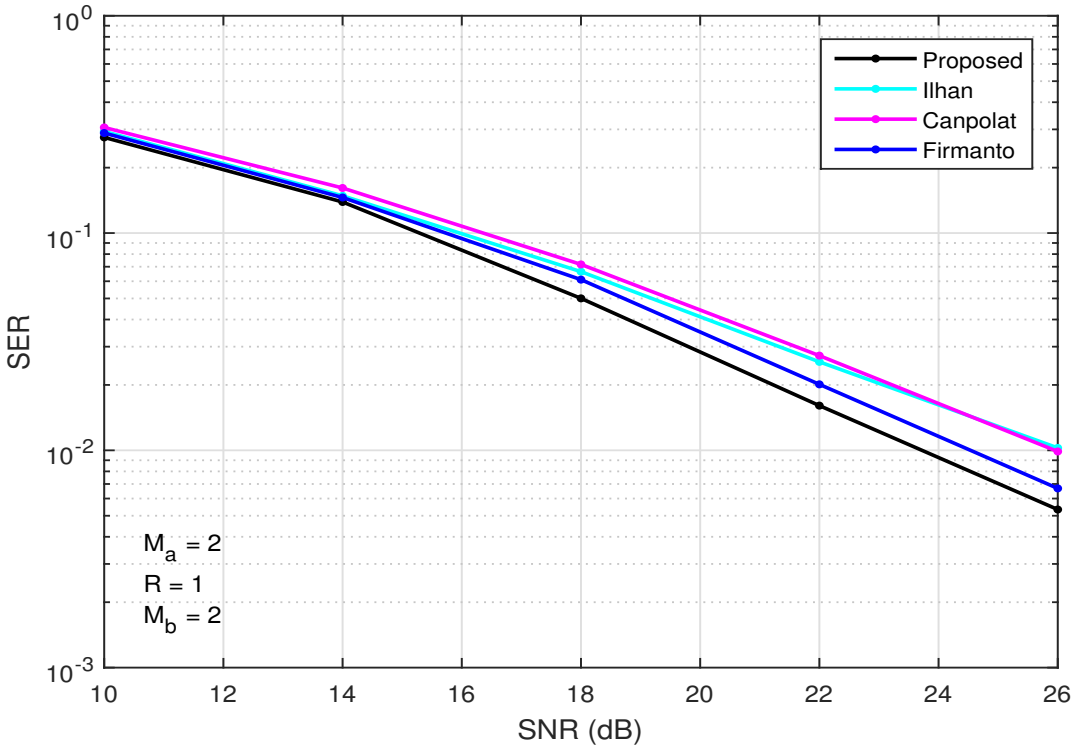

Figure 5.5 : SER performance of the Firmanto's, Canpolat's, Ilhan's and the proposed 8-state STTC for fixed-gain AF PLNC V2V systems over cascaded fading channels.

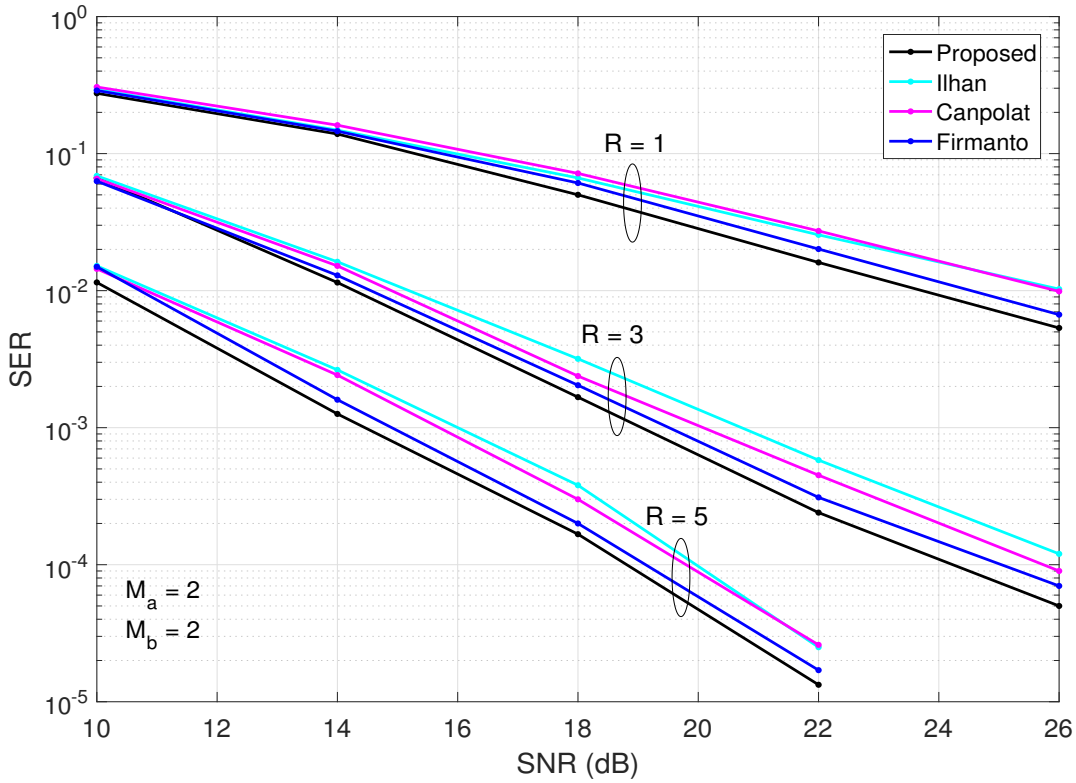

Figure 5.6 : SER performance comparison between the existing and the proposed 8-state STTCs for the various relay numbers.

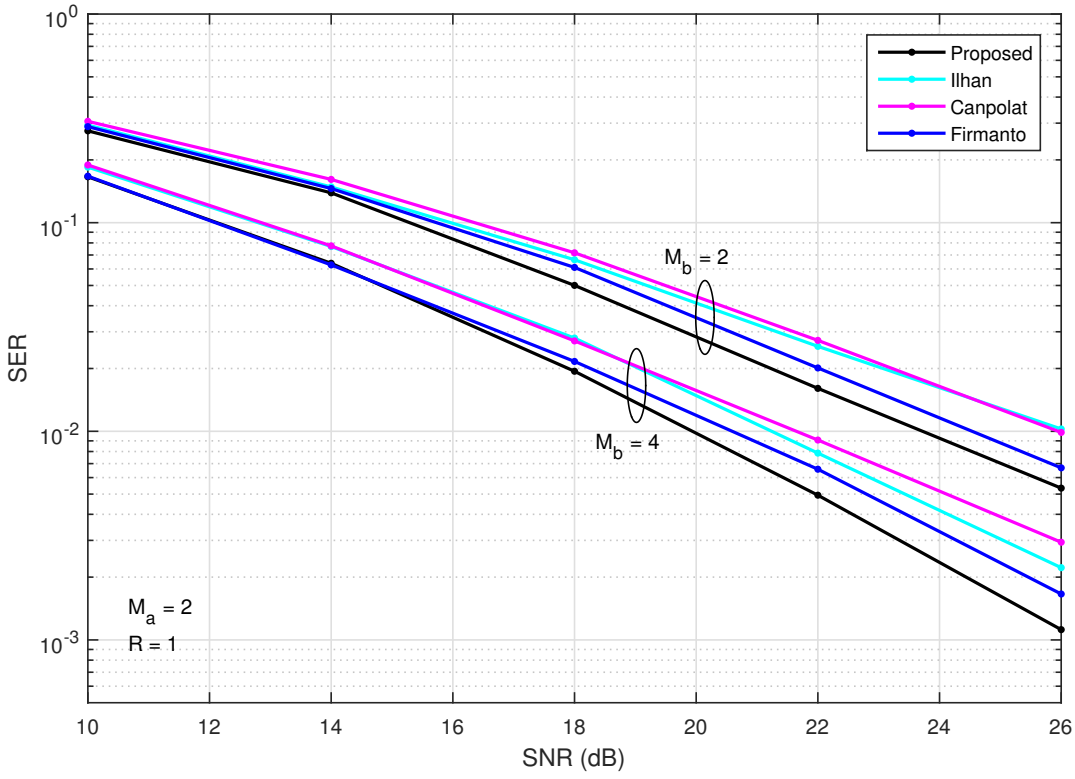

Figure 5.7 : SER performances of the proposed and the existing 8-state STTCs for the various receiver antenna numbers.

Figure 5.6 represents the SER performance of the proposed 8-state STTC for various relay numbers. It is shown that the SER performance of the system can be improved by increasing the number of the relays. For example, the novel code provides approximately 4 dB SNR gain at the 10^{-3} SER value by increasing the relay number from $R = 3$ to $R = 5$.

We present the SER performance comparison of the proposed 8-state STTC and the existing codes for various receiver antenna numbers in Figure 5.7. The figure that the SER performance can be enhanced with the increasing number of receiver antennas. For example, 3.5 dB SNR gain can be obtained at a SER value of 10^{-3} by increasing the receiver antenna number from 2 to 4. It is also shown that the proposed 8-state STTC provides significant amount of SNR with respect to the existing codes.

6. CONCLUSIONS AND FUTURE DIRECTIONS

In this thesis, we first propose an inter-vehicle communication system employing PLNC with fixed gain AF method at the relay over cascaded Nakagami-*m* channels. We investigate the performance of the system in terms of outage probability and SER performance. The results for various cascaded (or non-cascaded conventional) fading models are obtained as special cases of our results. We derive the CDF of E2E-SNR, then obtain the closed-form expression of the outage probability. Also we derive general closed-form SER expressions for various modulation types. The analytic results are verified by computer simulations. We show that the increasing cascading degrees of channels worsens the outage probability and SER performance of the system.

As a continuation of this work, we propose an M2M communication system employing PLNC with fixed gain AF method on the relay, and investigate the performance of the system for the case of imperfect self-interference cancellation at the receiver. For this purpose, we find the expression of E2E-SINR at the receiver. Then, we derive the closed-form expression of the CDF of E2E-SINR for fast fading cascaded Rayleigh channels. Using this CDF, we obtain the closed-form expression of the outage probability. We verify the analytic results by comparing with computer simulations. Our results show that the outage probability increases when the performance of the self-interference cancellation of the receiver decreases. Furthermore it is shown that the self-interference may cause an error floor in the performance of the network coded communication systems. Also we show that the increasing cascading degree of the channels decreases the outage performance of the system.

As a second research topic in the thesis, we focus on the antenna and/or relay selection techniques to improve the performance of MIMO V2V systems employing PLNC over cascaded fading channels. In this context, we first investigate the relay antenna selection problem in a multi-antenna single-relay V2V PLNC system. We derive upper and lower bounds for E2E-SNR and obtain their corresponding CDFs

for double-Nakagami-*m* channels. Using the derived CDFs, we find closed-form expressions of the upper and lower bounds of the outage probability. We show that increasing the number of antennas on the relay improves the outage probability in the V2V PLNC system with antenna selection. We also show that the derived lower bound is very close to the exact outage probability for all SNR values. Moreover, we determine the asymptotic diversity order in terms of the number of relay antennas and the channel parameters. Theoretical results are verified by computer simulations.

In the next part of our studies on antenna/relay selection techniques, we investigate the performance of a MIMO V2V communication system employing a joint relay and antenna selection scheme based on the maximization of the instantaneous E2E-SNR of the weakest link in the system where the variable gain AF PLNC is used. All derivations are performed in case of cascaded Nakagami-*m* fading channel conditions, covering cascaded Rayleigh and conventional cellular channel models. We express overall instantaneous SNR of the system in terms of instantaneous SNRs at the channels, then evaluate the performance of the system in terms of joint outage probability of the sources. Lower and upper bounds for the joint outage probability are derived in closed-form expressions while exact expression is found as a single integral form due to mathematical intractability of the integrals including the product of Meijer's G-functions. Using high SNR approximation, we analyze asymptotic diversity order and quantify it as a function of numbers of relays and antennas on the source and relay vehicles, and channel parameters of cascading degree and fading parameter values. Analytic results are verified by computer simulations. We show through the comparative graphics that the cascading degree has a negative effect on the system performance, and the outage probability increases by the increasing cascading degrees of the channels. On the other hand, we present that the outage probability can be reduced by using multiple antennas and relays and performing relay and antenna selection in a V2V system using PLNC, thus the system performance can be enhanced. It is also observed that the lower bound we have found is quite tight and can be used as a benchmark while analyzing the performance of the MIMO vehicular communication systems employing AF PLNC with joint relay and antenna selection over cascaded fading channels.

As the last part of the thesis, we employ the space-time trellis coding technique to a multi-antenna multi-relay V2V PLNC system to further improve the error performance over cascaded fading channels. To this end, we first show that the mixture gamma distribution model can be used to examine the pdf of instantaneous SNR in double Rayleigh fading channels. Then, we evaluate the pdf expression for the summation of i.i.d. double Rayleigh distributed random variables. Then, the PEP analysis is performed for a fixed-gain AF PLNC V2V system employing STTC over double Rayleigh fading channels, and we obtain an upper bound for PEP. By examining the behavior of the upper bound expression in high SNR region, we derive a novel design criterion for STTCs. By using this criterion we propose novel STTCs with 4 and 8 states for MIMO V2V systems employing PLNC over double cascaded Rayleigh fading channels. In the simulations, we compare the performance of the proposed codes with STTCs proposed for fast fading channels and for cooperative communication systems over Rayleigh and double Rayleigh fading channels. The simulations shows that the proposed design criterion offers a better design measure for the MIMO V2V systems employing fixed gain AF PLNC over double Rayleigh fading channels. We also show that the proposed 4-state code has approximately 1–2 dB advantage against the competing codes in the high SNR region. Furthermore, it is shown that the SER performance of the proposed 4-state code can be enhanced by increasing the number of relays. For example, by increasing the number of relays from 2 to 3, 5 dB gain can be obtained to achieve a SER value of 10^{-3}. Furthermore, increasing the number of relays from 3 to 4 provides an additional 2 dB performance gain. Similarly, the simulation results confirm that novel 8-state STTC outperforms the existing codes in the literature. For example, our proposed STTC provides approximately 0.5–1.5 dB advantage against the existing 8-state codes. Also, by increasing the number of relays from 3 to 5, 4 dB SNR gain can be obtained for the 10^{-3} SER value by using the novel 8-state STTC. Furthermore we show that the proposed 8-state code provides significant amount of SNR with respect to the existing codes when the number of receiver antennas is increased.

Throughout this thesis, we assume that the proposed V2V PLNC systems employ AF method on the relays. As a future work, performance analysis of DF method for V2V PLNC systems can be studied in case of cascaded fading channels. Also all relay

nodes are assumed to operate in half-duplex mode. On the other hand, if full-duplex relays are employed, data transmission rates of the PLNC systems can be doubled. But, in literature, very few number of studies addresses this subject. Therefore, design and performance analysis of the V2V communication systems employing PLNC via full-duplex relays is considered as a productive research area for the future work.

REFERENCES

[1] **U.S. Federal Communications Commission** (1999). http://transition.fcc.gov/Bureaus/Engineering_Technology/News_Releases/1999/nret9006.html, date retrieved 2016.

[2] **European Telecommunications Standards Institute** (2008). http://www.etsi.org/index.php/news-events/news/226-press-release-30th-september-2008, date retrieved 2016.

[3] **U.S. Federal Communications Commission** (2003). http://wireless.fcc.gov/services/index.htm?job=about&id=dedicated_src, date retrieved 2016.

[4] **Stüber, G.L.** (2002). *Principles Of Mobile Communication, 2nd Ed.*, Kluwer Academic.

[5] **Akki, A. and Haber, F.** (1986). A statistical model of mobile-to-mobile land communication channel, *IEEE Trans. Vehicular Tech.*, *35*, 2–5.

[6] **Ergec, V.**, **Fortune, S.**, **Ling, J.**, **Rustako, A. and Valenzuela, R.** (1997). Vehicle-to-vehicle channel modeling and measurements: Recent advances and future challenges, *IEEE J. Sel. Areas Commun.*, *15*, 677–684.

[7] **Sen, I. and Matolak, D.** (2008). Vehicle-vehicle channel models for the 5 GHz band, *IEEE Trans. Intelligent Transportation Sys.*, *9*, 235–245.

[8] **Molish, A.**, **Tufvesson, F.**, **Karedal, J. and Mecklenbrauker, C.** (2009). A survey on vehicle-to-vehicle propagation channels, *IEEE Wireless Communication*, *38*, 12–22.

[9] **Wang, C.**, **Cheng, X. and Laurenson, D.** (2009). Vehicle-to-vehicle channel modeling and measurements: Recent advances and future challenges, *IEEE Commun. Mag.*, 96–103.

[10] **Matolak, D. and Frolik, J.** (2011). Worse-than-Rayleigh fading: Experimental results and theoretical models, *IEEE Trans. Antennas Propag.*, 140–146.

[11] **Mecklenbrauker, C.**, **Molisch, A.**, **Karedal, J.**, **Tufvesson, F.**, **Paier, A.**, **Bernado, L.**, **Zemen, T.**, **Klemp, O. and Czink, N.** (2011). Vehicular channel characterization and its implications for wireless system design and performance, *IEEE Proceedings*, 1189–1212.

[12] **Talha, B. and Patzold, M.** (2011). Channel models for mobile-to-mobile cooperative communication systems, *IEEE Vehicular Tech. Mag.*, 33–43.

[13] **Andersen, J.** (2002). Statistical distributions in mobile communications using multiple scattering, *URSI General Assembly, The Netherlands*.

[14] **Andersen, J. and Kovacs, I.** (2002). Power distributions revisited, *COST 273 TD(02) 004*.

[15] **Salo, J.**, **El-Sallabi, H. and Vainikainen, P.** (2006). Statistical analysis of the multiple scattering radio channel, *IEEE Trans. Antennas Propag.*, *54*, 3114–3124.

[16] **Shankar, P.** (2004). Error rates in generalized shadowed fading channels, *Wireless Personal Commun.*, *28*, 222–238.

[17] **Uysal, M.** (2005). Maximum achievable diversity order for cascaded Rayleigh fading channels, *IET Electronic Lett.*, *41*, 1289–1290.

[18] **Salo, J.**, **El-Sallabi, H. and Vainikainen, P.** (2006). The distribution of the product of independent Rayleigh random variables, *IEEE Trans. Antennas Propag.*, *54*, 639–643.

[19] **Karagiannidis, G.**, **Sagias, N. and Mathiopoulos, P.** (2007). N*Nakagami: A novel stochastic model for cascaded fading channels, *IEEE Trans. Commun.*, *55*, 1453–1458.

[20] **Sagias, N. and Tombras, G.** (2007). On the cascaded Weibull fading channel model, *J.Franklin Inst.*, *344*, 1–11.

[21] **Shin, H. and Win, M.** (2008). MIMO diversity in the presence of double scattering, *IEEE Trans. Inf. Theory*, *54*, 2976–2996.

[22] **Zlatanov, N.**, **Hadzi-Velkov, Z. and Karagiannidis, G.** (2008). Level crossing rate and average fade duration of the double Nakagami-m random process and application in MIMO keyhole fading channels, *IEEE Commun. Lett.*, *12*, 822–824.

[23] **Trigui, I.**, **Laourine, A.**, **Affes, S. and Stephenne, A.** (2009). On the performance of cascaded generalized-K fading channels, *IEEE GLOBECOM*, *Spring*, 1–5.

[24] **Talha, B.**, **Patzold, M. and Primak, S.** (2010). Performance analysis of M-ary PSK modulation schemes over multiple double Rayleigh fading channels with EGC in cooperative networks, *Proc. IEEE ICC*, 1–6.

[25] **Talha, B. and Patzold, M.** (2010). On the statistical analysis of the channel capacity of double Rayleigh channels with equal gain combining in V2V communication systems, *IEEE Vehicular Tech. Conf.*, *Spring*, 1–6.

[26] **Peppas, K.**, **Lazarakis, F.**, **Alexandridis, A. and Dangakis, K.** (2010). Cascaded generalised-K fading channel, *IET Communications*, *4*, 116–124.

[27] **Shankar, P.** (2011). Statistical models for fading and shadowed fading channels in wireless systems: A pedagogical perspectives, *Wireless Personal Commun.*, *60*, 191–213.

[28] **Van der Meulen, E.** (1971). Three-terminal communication channels, *Adv. Appl. Prob.*, *3*, 120–154.

[29] **Cover, T. and Gamal, A.** (1979). Capacity theorems for the relay channel, *IEEE Trans. Inf. Theory*, *25*, 572–584.

[30] **Ahlswede, R.**, **Cai, N.**, **Li, S. and Yeung, R.** (2000). Network information flow, , *IEEE Trans. Inform. Theory*, *46*, 1204–1216.

[31] **Li, S.**, **Yeung, R. and Cai, N.** (2003). Linear network coding, *IEEE Trans. Inform. Theory*, *49*, 371–381.

[32] **Katti, S.**, **Rahul, H.**, **Hu, W.**, **Katabi, D.**, **Medard, M. and Crowcroft, J.** (2008). XORs in the air: Practical wireless network coding, *IEEE Trans. Networking*, *16*, 497–510.

[33] **Zhang, S.**, **Liew, S. and P., L.** (2006). Hot topic: Physical layer network coding, *Proc. Annual Int. Conf. on Inf., Commun. Signal Proc.*

[34] **Liew, S.**, **S., Z. and L., L.** (2013). Physical-layer network coding: Tutorial, survey, and beyond, *Physical Commun.*, *6*, 4–42.

[35] **Atapattu, S.**, **Tellambura, C. and Jiang, H.** (2011). A mixture gamma distribution to model the SNR of wireless channels, *IEEE Trans. Wireless Commun.*, *10*, 4193–4203.

[36] **Foschini, G. and Gans, M.** (1998). On limits of wireless communication in a fading environment when using multiple antennas, *Wireless Pers. Commun.*, *6*, 311–335.

[37] **Telatar, I.** (1999). Capacity of multi-antenna Gaussian channels, *Eur. Trans. Telecommun.*, *10*, 585–595.

[38] **Rentapalli, V. and Khan, Z.** (2011). MIMO and smart antenna technologies for 3G and 4G, *Commun. in Computer and Inf. Sci.*, *147*, 493–498.

[39] **El-Mashed, M. and El-Rabaie, S.** (2015). Service enhancement for user equipments in LTE-A downlink physical layer network, *Wireless Personal Commun.*, *83*, 149–161.

[40] **Agustin, A. and Vidal, J.** (2008). Amplify-and-forward cooperation under interference-limited spatial reuse of the relay slots, *IEEE Trans. Wireless Commun.*, *7*, 1952–1962.

[41] **Gorokhov, A.** (2003). Receive antenna selection for MIMO spatial multiplexing, theory and algorithms, *IEEE Trans. Sig. Proc.*, *51*, 2796–2807.

[42] **Bahçeci, I.**, **Duman, T. and Y., A.** (2003). Antenna selection for multiple-antenna transmission systems: Performance analysis and code construction, *IEEE Trans. Inform. Theory*, *49*, 2669–2681.

[43] **Ghrayeb, A.**, **Sanei, A. and Shayan, Y.** (2004). Space-time trellis codes with receive antenna selection in fast fading, *IET Electronics Lett.*, *40*.

[44] **Chen, Z.**, **Yuan, J. and Vucetic, B.** (2005). Analysis of transmit antenna selection/maximal-ratio combining in Rayleigh fading channels, *IEEE Trans. Vehicular Tech.*, *54*, 1312–1321.

[45] **Peters, S. and Heath, R.** (2008). Nongenerative MIMO relaying with optimal transmit antenna selection, *IEEE Signal Proc. Lett.*, *15*, 421–424.

[46] **Ju, M.**, **Song, H.K. and Kim, I.M.** (2010). Joint relay-and-antenna selection in multi-antenna relay networks, *IEEE Trans. on Commun.*, *58*, 3417–3422.

[47] **Ozdemir, O.**, **Altunbas, I. and Bayrak, M.** (2010). Performance of super-orthogonal space-time trellis codes with transmit antenna selection, *IET Commun.*, *4*, 1942–1951.

[48] **Amarasuriya, G.**, **Tellambura, C. and Ardakani, M.** (2012). Joint relay and antenna selection for dual-hop amplify-and-forward MIMO relay networks, *IEEE Trans. Wireless Commun.*, *11*, 493–499.

[49] **Coskun, A.**, **Kucur, O. and Altunbas, I.** (2013). Performance analysis of Alamouti scheme with transmit antenna selection in non-identical Nakagami-m fading channel, *Wireless Communications and Mobile Computing*, *13*, 671–680.

[50] **Cai, X. and Giannakis, G.** (2004). Performance analysis of combined transmit selection diversity and receive generalized selection combining in Rayleigh fading channels, *IEEE Trans. Wireless Commun.*, *3*, 1980–1983.

[51] **Güçlüoğlu, T. and T.M., D.** (2008). Performance analysis of transmit and receive antenna selection over flat fading channels, *IEEE Trans. Wireless Commun.*, *7*, 3056–3065.

[52] **Hammerschmidt, J.**, **Hutter, A. and C., D.** (1999). Comparison of single antenna, selection combining, and optimum combining reception at the vehicle, *IEEE Vehicular Tech. Conf.*

[53] **Ito, K.**, **Itoh, N.**, **Sanda, K. and Karasawa, Y.** (2006). A novel MIMO-STBC scheme for inter-vehicle communications at intersection, *IEEE Vehicular Tech. Conf.*, *Spring*, 2937–2941.

[54] **Renaudin, O.**, **Kolmonen, V.**, **Vainikainen, P. and Oestges, C.** (2010). Non-stationary narrowband MIMO intervehicle channel characterization in the 5-GHz band, *IEEE Trans. Vehicular Tech.*, *59*, 2007–2015.

[55] **Nuckelt, J. and T., K.** (2011). MRC performance benefit in V2V communication systems in urban traffic scenarios, *6th European Conf. on Antennas and Propagation (EUCAP)*, 2311–2315.

[56] **Maier, G.**, **Paier, A. and Mecklenbrauker, C.** (2012). Performance evaluation of IEEE 802.11p infrastructure-tovehicle real-world measurements with receive diversity, *IEEE Int. Wire. Commun. Mob. Comp. Conf.*, 1113–1118.

[57] **Abbas, T.**, **Karedal, J. and Tufvesson, F.** (2013). Measurement-based analysis: The effect of complementary antennas and diversity on vehicle-to-vehicle communication, *IEEE Antennas and Wireless Propagation Lett.*, 309–312.

[58] **Mousavi, H.**, **Khalighinejad, B. and Khalaj, B.** (2013). Capacity maximization in MIMO vehicular communication using a novel antenna selection algorithm, *IEEE Int. Wire. Commun. Mob. Comp. Conf.*, 1246–1251.

[59] **Jedari, E.**, **Atlasbaf, Z.**, **Noghanian, S. and Shahrrava, B.** (2013). Effects of antenna selection on vehicle to vehicle communication in highways, *Proc. Antennas and Propagation Society Int. Symposium (APSURSI)*, 2109–2110.

[60] **Sendonaris, A.**, **Erkip, E. and Aazhang, B.** (1998). Increasing uplink capacity via user cooperation diversity, *Proc. IEEE ISIT*.

[61] **Leneman, J. and Wornell, G.** (2003). Distributed space-time coded protocols for exploiting cooperative diversity in wireless networks, *IEEE Trans. Inform. Theory*, *49*, 2415–2425.

[62] **Chen, D. and Laneman, J.** (2006). Modulation and demodulation for cooperative diversity in wireless systems, *IEEE Trans. Wireless Commun.*, *5*, 1785–1794.

[63] **Laneman, J.**, **Tse, D. and Wornell, G.** (2004). Cooperative diversity in wireless networks: efficient protocols and outage behavior, *IEEE Trans. Inform. Theory*, *50*, 3062–3080.

[64] **Hasna, M. and Alouini, M.** (2003). End-to-end performance of transmission systems with relays over Rayleigh fading channels, *IEEE Trans. Wireless Commun.*, *2*, 1126–1131.

[65] **Hasna, M. and Alouini, M.** (2004). A Performance study of dual-hop transmissions with fixed gain relays, *IEEE Trans. Wireless Commun.*, *3*, 1963–1968.

[66] **Blestas, A.**, **Khisti, A.**, **Reed, D. and Lippman, A.** (2006). A simple cooperative diversity method based on network path selection, *IEEE Journal on Selected Areas Commun.*, *24*, 659–672.

[67] **Zhao, Y.**, **Adve, R. and Lim, T.** (2006). Symbol error rate of selection amplify-and-forward relay system, *IEEE Commun. Lett.*, *10*, 757–759.

[68] **Jing, Y. and Jafarkhani, H.** (2009). Single and multiple relay selection schemes and their achiecable diversity orders, *IEEE Trans. Wireless Commun.*, *8*, 1414–1423.

[69] **Ikki, S. and Ahmed, M.** (2010). On the performance of cooperative-diversity networks with the Nth best-relay selection scheme, *IEEE Trans. Commun.*, *58*, 3062–3069.

[70] **Vhu, S.** (2011). Performance of amplify-and-forward cooperative communications with the N-th best-relay selection scheme over Nakagami-m fading channels, *IEEE Commun. Lett.*, *15*, 172–174.

[71] **Chen, Y.**, **Wang, C.**, **Xiao, H. and Yuan, D.** (2011). Novel partial selection schemes for AF relaying in Nakagami-m fading channels, *IEEE Trans. Vehicular Tech.*, *60*, 3497–3503.

[72] **Hussain, S.**, **Alouini, M. and Hasna, M.** (2013). Performance analysis of selective cooperation in amplify-and-forward relay networks over identical Nakagami-m channels, *Wireless Communications and Mobile Computing*, *13*, 790–797.

[73] **Tarokh, V.**, **Seshadri, N. and Calderbank, A.** (1998). Space-time codes for high data rate wireless communication: Performance criteria and code construction, *IEEE Trans. Inform. Theory*, *44*, 744–765.

[74] **Alamouti, S.** (1998). A simple transmit diversity technique for wireless communications, *IEEE Journal on Selected Areas Commun.*, *16*, 1451–145.

[75] **Chen, Z.**, **Vucetic, B.**, **Yuan, J. and Lo, K.** (2001). Improved space-time trellis coded modulation scheme on slow Rayleigh fading channels, *IEE Electronics Lett.*, *37*, 440–441.

[76] **Vucetic, B. and Yuan, J.** (2003). *Space-Time Coding, 7th Ed.*, John Wiley and Sons Ltd.

[77] **Firmanto, W.**, **Vucetic, B. and Yuan, J.** (2001). Space–Time TCM with improved performance on fast fading channels, *IEEE Commun. Lett.*, *5*, 154–156.

[78] **Canpolat, O. and Uysal M., F.M.** (2007). Analysis and design of distributed space-time trellis codes with amplify-and-forward relaying, *IEEE Trans. Vehicular Tech.*, *56*, 1649–1660.

[79] **Ilhan, H.**, **I., A.**, **and Uysal, M.** (2010). Novel distributed space-time trellis codes for relay systems over cascaded Rayleigh fading, *IEEE Commun. Lett.*, *14*, 1140–1142.

[80] **Li, Z.**, **Hu, H.**, **Zhao, Y. and Jia, L.** (2009). Power allocation methods in relay-assisted network with mobile-to-mobile channels, *Proc. ICCTA*, 1–6.

[81] **Hadizadeh, H.**, **Muhaidat, S. and Bajic, I.** (2010). Impact of imperfect channel estimation on the performance of inter-vehicular cooperative networks, *25th Biennial Symposium on Commun.*, 373–376.

[82] **Li, Z.**, **Hu, H.**, **Jia, L.**, **Li, F. and Wang, H.** (2010). Outage bound analysis in relay-assisted inter-vehicular communications, *Proc. IEEE VTC*, *Spring*.

[83] **Li, Z.**, **Zhao, Y.**, **Chen, H. and Hu, H.** (2010). Outage probability bound analysis in vehicle-assisted inter-vehicular communications, *Proc. CSCWD*.

[84] **Talha, B. and Patzold, M.** (2010). On the statistical analysis of equal gain combining over multiple double Rice fading channels in cooperative networks, *Proc. IEEE VTC*, *Fall*.

[85] **Han, C.** (2010). Performance of distributed GLD codes over mobile-to-mobile fading channels, *Int. Conf. on Sig. Proc. Sys.*, *5*, 1–5.

[86] **Lee, K.**, **Kwon, H.**, **Sawan, E.**, **Shim, Y.**, **Park, H. and Lee, Y.** (2013). Selection of amplify-and-forward mobile relay under cascaded Rayleigh fading, *Proc. IEEE VTC*, *Spring*, 1–5.

[87] **Seyfi, M.**, **Muhaidat, S.**, **Liang, J. and Uysal, M.** (2011). Relay selection in dual-hop vehicular networks, *IEEE Signal Processing Lett.*, *18*, 134–137.

[88] **Akın, A. and Ilhan, H.** (2012). Performance analysis of AF relaying cooperative systems with relay selection over double Rayleigh fading channels, *Proc. ICSPCS*.

[89] **Alghorani, Y.**, **Kaddoum, G.**, **Muhaidat, S.**, **Pierre, S. and Al-Dhahir, N.** (2016). On the performance of multihop-intervehicular communications systems Over N*Rayleigh Fading Channels, *IEEE Wireless Commun. Lett.*, *5*, 116–119.

[90] **Ilhan, H.**, **Uysal, M. and I., A.** (2009). Cooperative diversity for inter-vehicular communication: Performance analysis and optimization, *IEEE Trans. Vehicular Tech.*, *58*, 3301–3310.

[91] **Gong, F.**, **Ge, J. and Zhang, N.** (2011). SER analysis of the mobile-relay-based M2M communication over double Nakagami-m fading channels, *IEEE Commun. Lett.*, *15*, 34–36.

[92] **Ilhan, H.**, **I., A.**, **and Uysal, M.** (2010). MGF-based performance evaluation of amplify-and-forward relaying in N*Nakagami-m fading channels, *IET Commun.*, *5*, 253–263.

[93] **Bissias, N.**, **Efthymoglou, G. and Aalo, V.** (2012). Performance analysis of dual-hop relay systems with single relay selection in composite fading channels, *AEÜ - Int. Journal of Electronics and Communications*, *66*, 39–44.

[94] **Cao, J.**, **Yang, L. and Zhong, Z.** (2012). Performance analysis of multihop wireless links over generalized-K fading channels, *IEEE Trans. Vehicular Tech.*, *61*, 1590–1598.

[95] **Lateef, H.**, **Ghogho, M. and McLemon, D.** (2011). On the performance analysis of multi-hop cooperative relay networks over generalized-K fading channels, *IEEE Commun. Lett.*, *15*, 968–970.

[96] **Karademir, A. and Altunbas, I.** (2013). SER of multiple-relay cooperative systems with selection combining in generalized-K channels, *Proc. ISWCS*.

[97] **Rankov, B. and Wittneben, A.** (2007). Spectral efficient protocols for half-duplex fading relay channels, *IEEE Journal on Selected Areas Commun.*, *25*, 379–389.

[98] **Koike-Akino, T.**, **Popovski, P. and Tarokh, V.** (2009). Optimized constellations for two-way wireless relaying with physical network coding, *IEEE Journal on Selected Areas Commun.*, *27*, 773–787.

[99] **Han, Y.**, **Ting, S.**, **Ho, C. and Chin, W.** (2009). Performance bounds for two-way amplify-and-forward relaying, *IEEE Trans. Wireless Commun.*, *8*, 432–439.

[100] **Louie, R.**, **Yonghui, L. and Vucetic, B.** (2010). Practical physical layer network coding for two-way relay channels: performance analysis and comparison, *IEEE Trans. Wireless Commun.*, *9*, 764–777.

[101] **Zhang, Y.**, **Yi, M. and Tafazolli, R.** (2010). Power allocation for bidirectional AF relaying over Rayleigh fading channels, *IEEE Commun. Lett.*, *14*, 145–147.

[102] **Yang, J.**, **Fan, P.**, **Duong, T. and Lei, X.** (2011). Exact performance of two-way AF relaying in Nakagami-m fading environment, *IEEE Trans. Wireless Commun.*, *10*, 980–987.

[103] **Xia, M. and Aissa, A.** (2012). Moments based framework for performance analysis of one-way/two-way CSI-assisted AF relaying, *IEEE Journal on Selected Areas Commun*, *30*, 1464–1476.

[104] **Sahin, S. and Aygolu, U.** (2012). Physical-layer network coding with limited feedback in two-way relay channels, *IET Commun.*, *6*, 548–556.

[105] **Yang, T. and Collings, I.** (2014). On the optimal design and performance of linear physical-layer network coding for fading two-way relay channels, *IEEE Trans. Wireless Commun.*, *13*, 956–967.

[106] **Amarasuriya, G.**, **Tellambura, C. and Ardakani, M.** (2012). Two-way amplify-and-forward multiple-input multiple output relay networks with antenna selection, *IEEE Journal on Selected Areas*, *30*, 1513–1529.

[107] **Huang, M. and Yuan, J.** (2014). Error performance of physical-layer network coding in multiple-antenna TWRC, *IEEE Trans. Vehicular Tech.*, *63*, 3750–3761.

[108] **Yang, K.**, **Yang, N.**, **Xing, C. and Wu, J.** (2014). Relay antenna selection in MIMO two-way relay networks over Nakagami-m fading channels, *IEEE Trans. Vehicular Tech.*, *63*, 2349–2362.

[109] **Guo, H. and J., G.** (2011). Performance analysis of two-way opportunistic relaying over Nakagami-m fading channels, *IET Electronics Lett.*, *47*.

[110] **Song, L.** (2011). Relay selection for two-way relaying with amplify-and-forward protocols, *IEEE Trans. Vehicular Tech.*, *60*, 1954–1959.

[111] **Upadhyay, P. and Prakriya, S.** (2011). Performance of two-way opportunistic relaying with analog network coding over Nakagami-m fading, *IEEE Trans. Vehicular Tech.*, *60*, 1965–1971.

[112] **Atapattu, S.**, **Jing, Y.**, **Jiang, H. and Tellambura, C.** (2013). Relay selection schemes and performance analysis approximations for two-way networks, *IEEE Trans. Commun.*, *61*, 987–998.

[113] **Cui, T.**, **Gao, F.**, **Ho, T. and Nallanathan, A.** (2009). Distributed space-time coding for two-way wireless relay networks, *IEEE Trans. Signal Processing*, *57*, 658–671.

[114] **Gong, F.**, **Zhang, J. and Ge, J.** (2013). Novel distributed quasi-orthogonal space-time block codes for two-way two-antenna relay networks, *IEEE Trans. Wireless Commun.*, *12*, 4338–4349.

[115] **Sahin, S. and Aygolu, U.** (2012). Physical-layer network coding with limited feedback using orthogonal space-time block codes, *Int. Journal of Communication Systems*, *27*, 2577–2592.

[116] **Beygi, S.**, **Kafashan, M.**, **Bahrami, H.**, **Le-Ngoc, T. and Maleki, M.** (2013). Space-time trellis codes for two-way relay MIMO channels with single-antenna relay nodes, *IEEE Trans. Vehicular Tech.*, *62*, 4040–4045.

[117] **Ilhan, H.** (2012). Performance analysis of two-way AF relaying systems over cascaded Nakagami-m fading channels, *IEEE Signal Processing Lett.*, *19*, 332–335.

[118] **Zhang, C.**, **Ge, J.**, **Li, J. and Hu, Y.** (2013). Performance analysis for mobile-relay-based M2M two-way AF relaying in N*Nakagami-m fading, *IET Electron Lett.*, *49*.

[119] **Yadav, S. and Upadhyay, P.** (2013). Performance analysis of two-way AF relaying systems over cascaded generalized-K fading channels, *Proc. Nat. Commun. Conf.*, 1–5.

[120] **Wang, X.**, **Zhang, H.**, **Gulliver, T.**, **Shi, W. and Zhang, H.** (2013). Performance Analysis of Two-Way AF cooperative relay networks over Weibull fading channels, *Journal of Communications*, *8*, 372–377.

[121] **Shakeri, R.**, **Khakzad, H.**, **Taherpour, A. and Gazor, S.** (2014). Performance of two-way multi-relay inter-vehicular cooperative networks, *IEEE Wireless Commun. and Network Coding Conf.*

[122] **Shirkhani, M.**, **Tirkan, Z. and Taherpour, A.** (2012). Performance analysis and optimization of two-way cooperative communications in inter-vehicular networks, *Wireless Commun. and Signal Proc. Conf.*, 1–6.

[123] **Ilhan, H.** (2014). Relay-selection in two-way cooperative systems, *Wireless Personal Commun.*, *77*, 1329–1341.

[124] **Hu, Y.**, **Li, H.**, **Zhang, C. and Li, J.** (2014). Partial relay selection for a roadside-based two-way amplify-and-forward relaying system in mixed Nakagami-m and double Nakagami-m fading, *IET Commun.*, *8*, 571–577.

[125] **Gradshteyn, I. and Ryzhik, I.** (2007). *Table of Integrals, Series, and Products, 7th Ed.*, Elsevier Inc.

[126] **Chen, Y. and Tellambura, C.** (2004). Distribution functions of selection output in equally correlated Rayleigh, Rician, and Nakagami-m fading channels, *IEEE Trans. Commun.*, *52*, 1948–195.

[127] **Simon, M. and Alouini, M.** (2004). *Digital Communication over Fading Channels, 2nd Ed.*, Wiley-IEEE Press.

[128] **Ikki, S. and Ahmed, M.** (2007). Performance analysis of cooperative diversity wireless networks over Nakagami-m fading channel, *IEEE Commun. Lett.*, *11*, 334–336.

[129] **Yang, L. and Chen, H.** (2008). Error probability of digital communications using relay diversity over Nakagami-m fading channels, *IEEE Trans. Wireless Commun.*, *7*, 1806–1811.

[130] **Nabar, R.**, **Bolchskei, H. and F.W., K.** (2004). Fading relay channels: Performance limits and space-time signal design, *IEEE Journal on Selected Areas Commun.*, *22*, 1099–1109.

[131] **Wolfram Research, I.**, `http://functions.wolfram.com`, 2016.

[132] **Tse, D.**, **Viswanath, P. and Zheng, L.** (2004). Diversity-multiplexing trade-off in multiple-access channels, *IEEE Trans. Inf. Theory*, *50*, 1859–1874.

[133] **Eslamifar, M.**, **Yuen, C.**, **Chin, W. and Guan, Y.** (2010). Max-Min antenna selection for bi-directional multi-antenna relaying, *IEEE VTC*.

[134] **Soleimani-Nasab, E. and Ardebilipour, M.** (2013). Multi-antenna AF two-way relaying over Nakagami-m fading channels, *Wireless Pers. Commun.*, *73*, 717–729.

[135] **Wang, Z. and Giannakis, G.** (2003). A simple and general parameterization quantifying performance in fadind channels, *IEEE Trans. on Commun.*, *51*, 1389–1398.

[136] **Jung, J.**, **Lee, S.**, **Park, H.**, **Lee, S. and Lee, I.** (2014). Capacity and error probability analysis of diversity reception schemes over generalized-K fading channels using a mixture gamma distribution, *IEEE Trans. Wireless Commun*, *13*, 4721–4730.

APPENDICES

APPENDIX A : Meijer's G-function
Following properties of Meijer's G-function are taken from the web site *http://functions.wolfram.com* as part of the official website of Wolfram Research, Inc.

Traditional name

Meijer's G-function

Traditional notation

$$G_{p,q}^{m,n}\left[z\left|\begin{matrix}a_1,a_2,...,a_n,a_{n+1},...,a_p\\ \\ b_1,b_2,...,b_m,b_{m+1},...,b_q\end{matrix}\right.\right]$$

Primary definition
A general definition of the Meijer's G-function is defined as a contour integral in the complex plane. The primary definition of the function is given by

(07.34.02.0001.01)

$$G_{p,q}^{m,n}\left[z\left|\begin{matrix}a_1,a_2,...,a_n,a_{n+1},...,a_p\\ \\ b_1,b_2,...,b_m,b_{m+1},...,b_q\end{matrix}\right.\right]=\frac{1}{2\pi i}\int_{\mathscr{L}}\frac{\prod_{k=1}^{m}\Gamma(s+b_k)\prod_{k=1}^{n}\Gamma(1-a_k-s)}{\prod_{k=n+1}^{p}\Gamma(s+a_k)\prod_{k=m+1}^{q}\Gamma(1-b_k-s)}z^{-s}ds$$

where $m,n,p,q\in\mathscr{N}$, $m\leq q$ and $n\leq p$

Series Representation
The series representation of the Meijer's G-function is given by

(07.34.06.0006.01)

$$G_{p,q}^{m,n}\left[z\left|\begin{matrix}a_1,...,a_n,...,a_p\\ \\ b_1,...,b_m,...,b_p\end{matrix}\right.\right]=\sum_{k=1}^{m}\frac{\prod_{\substack{j=1\\ j\neq k}}^{m}\Gamma(b_j-b_k)\prod_{j=1}^{n}\Gamma(1-a_j+b_k)}{\prod_{j=n+1}^{p}\Gamma(a_j-b_k)\prod_{j=m+1}^{q}\Gamma(1-b_j+b_k)}z^{b_k}(1+O(z))$$

for $z\to 0$ and $p<q$

Transformations and argument simplifications

The transformations and argument simplifications properties of the Meijer's G-function are given by

(07.34.16.0001.01)

$$G_{p,q}^{m,n}\left[z\left|\begin{matrix}\alpha+a_1,\alpha+a_2,...,\alpha+a_n,\alpha+a_{n+1},...,\alpha+a_p\\ \\ \alpha+b_1,\alpha+b_2,...,\alpha+b_m,\alpha+b_{m+1},...,\alpha+b_q\end{matrix}\right.\right]=z^{\alpha}G_{p,q}^{m,n}\left[z\left|\begin{matrix}a_1,a_2,...,a_n,a_{n+1},...,a_p\\ \\ b_1,b_2,...,b_m,b_{m+1},...,b_q\end{matrix}\right.\right]$$

(07.34.16.0002.01)

$$G_{p,q}^{m,n}\left[\frac{1}{z}\left|\begin{matrix}a_1,a_2,...,a_n,a_{n+1},...,a_p\\ \\ b_1,b_2,...,b_m,b_{m+1},...,b_q\end{matrix}\right.\right]=G_{q,p}^{n,m}\left[z\left|\begin{matrix}1-b_1,1-b_2,...,1-b_m,1-b_{m+1},...,1-b_q\\ \\ 1-a_1,1-a_2,...,1-a_n,1-a_{n+1},...,1-a_p\end{matrix}\right.\right]$$

Definite integrations

Some of the integral properties of the Meijer's G-function are given as follows

(07.34.21.0009.01)

$$\int_0^{\infty}\tau^{\alpha-1}G_{p,q}^{m,n}\left[z\tau\left|\begin{matrix}a_1,a_2,...,a_n,a_{n+1},...,a_p\\ \\ b_1,b_2,...,b_m,b_{m+1},...,b_q\end{matrix}\right.\right]d\tau=\frac{\prod_{k=1}^{m}\Gamma(\alpha+b_k)\prod_{k=1}^{n}\Gamma(1-a_k-\alpha)}{\prod_{k=n+1}^{p}\Gamma(\alpha+a_k)\prod_{k=m+1}^{q}\Gamma(1-b_k-\alpha)}z^{-\alpha}$$

(07.34.21.0011.01)

$$\int_0^{\infty}\tau^{\alpha-1}G_{u,v}^{s,t}\left[\omega\tau\left|\begin{matrix}c_1,c_2,...,c_s,c_{s+1},...,c_u\\ \\ d_1,d_2,...,d_s,d_{s+1},...,d_v\end{matrix}\right.\right]G_{p,q}^{m,n}\left[z\tau\left|\begin{matrix}a_1,a_2,...,a_n,a_{n+1},...,a_p\\ \\ b_1,b_2,...,b_m,b_{m+1},...,b_q\end{matrix}\right.\right]d\tau=$$
$$\omega^{-\alpha}G_{v+p,u+q}^{m+t,n+s}\left[\frac{z}{\omega}\left|\begin{matrix}a_1,...,a_n,1-\alpha-d_1,...,1-\alpha-d_v,a_{n+1},...,a_p\\ \\ b_1,...,b_m,1-\alpha-c_1,...,1-\alpha-c_u,b_{m+1},...,b_q\end{matrix}\right.\right]$$

(07.34.21.0082.01)

$$\int_0^{\infty}\tau^{\alpha-1}G_{u,v}^{s,t}\left[\sigma+\tau\left|\begin{matrix}c_1,c_2,...,c_s,c_{s+1},...,c_u\\ \\ d_1,d_2,...,d_s,d_{s+1},...,d_v\end{matrix}\right.\right]G_{p,q}^{m,n}\left[\omega\tau\left|\begin{matrix}a_1,a_2,...,a_n,a_{n+1},...,a_p\\ \\ b_1,b_2,...,b_m,b_{m+1},...,b_q\end{matrix}\right.\right]d\tau=$$
$$\sum_{k=0}^{\infty}\frac{(-\sigma)^k}{k!}G_{v+p+1,u+q+1}^{m+t,n+s+1}\left[\omega\left|\begin{matrix}1-\alpha,a_1,...,a_n,k-\alpha-d_1+1,...,k-\alpha-d_v+1,a_{n+1},...,a_p\\ \\ b_1,...,b_m,k-\alpha-c_1+1,...,k-\alpha-c_u+1,k-\alpha+1,b_{m+1},...,b_q\end{matrix}\right.\right]$$

(07.34.21.0088.01)

$$\int_0^\infty \tau^{\alpha-1} e^{-\sigma\tau} G_{p,q}^{m,n}\left[\omega\tau^{l/k}\middle|\begin{matrix}a_1,a_2,...,a_n,a_{n+1},...,a_p\\ \\ b_1,b_2,...,b_m,b_{m+1},...,b_q\end{matrix}\right] d\tau =$$

$$\frac{k^\mu l^{\alpha-1/2}\sigma^{-\alpha}}{(2\pi)^{(k-1)c^*+\left(\frac{l-1}{2}\right)}} G_{kp+l,kq}^{km,kn+l}\left[\frac{\omega^k l^l}{\sigma^l k^{k(q-p)}}\middle|\begin{matrix}\frac{1-\alpha}{l},...,\frac{l-\alpha}{l},\frac{a_1}{k},...,\frac{a_1+k-1}{k},...,\frac{a_p}{k},...,\frac{a_p+k-1}{k}\\ \\ \frac{b_1}{k},...,\frac{b_1+k-1}{k},...,\frac{b_q}{k},...,\frac{b_q+k-1}{k}\end{matrix}\right]$$

where $c^* = m+n-\frac{p+q}{2}$ and $\mu = \sum_{j=1}^{q} b_j - \sum_{j=1}^{p} a_j + \frac{p-q}{2} + 1$

CURRICULUM VITAE

Name Surname: Serdar Özgür ATA

Place and Date of Birth: Sivas -Turkey, 20.04.1973

E-Mail: serdar.ata@tubitak.gov.tr

EDUCATION:

- **B.Sc.:** 1996, Istanbul Technical University, Faculty of Electrical and Electronics Engineering, Electronics and Communication Engineering Department.
- **M.Sc.:** 2010, Istanbul Technical University, Graduate School of Science Engineering and Technology, Telecommunication Engineering Programme.

PROFESSIONAL EXPERIENCE AND REWARDS:

- May 1996 - Sep. 1996 Istanbul Technical University Center of Defense Research (İTÜ-SAM), Research Engineer.
- Mayıs 1998 - Feb. 2001 NETAŞ, R/D, Software Design Engineer.
- Feb. 2001 - July 2001 Nitec/NorthelNetworks, R/D, Software Design Engineer.
- Nov. 2002 - ... Turkish Scientific and Technological Research Institute-Electronics ve Cryptology Research Institute (TÜBİTAK-UEKAE), Department of Voice, Avionic and Space Crypto Systems, Chief Research Engineer.

PUBLICATIONS AND PRESENTATIONS ON THE THESIS:

- **Serdar Özgür Ata**, İbrahim Altunbaş (2016). Fixed-gain AF PLNC over cascaded Nakagami-m fading channels for vehicular communications, *AEU - International Journal of Electronics and Communications,* 70(4), 510-516. http://dx.doi.org/doi:10.1016/j.aeue.2016.01.003
- **Serdar Özgür Ata**, İbrahim Altunbaş (2017). Joint relay and antenna selection in MIMO PLNC inter-vehicular communication systems over cascaded fading channels, *Wireless Personal Communication* 90(2), 901-923, 2017. http://dx.doi.org/10.1007/s11277-016-3584-2
- **Serdar Özgür Ata**, İbrahim Altunbaş (2015). Relay antenna selection for V2V communications using PLNC over cascaded fading channels, *IEEE Int. Wireless Commun. and Mobile Computing Conf.*, 1336-1340, Dubrovnik, Croatia. http://dx.doi.org/doi:10.1109/IWCMC.2015.7289276

- **Serdar Özgür Ata**, İbrahim Altunbaş (2015). Relay antenna selection for V2V PLNC system, *IEEE 23rd Signal Proc. and Commun. App. Conf.*, Malatya, Turkey. http://dx.doi.org/doi:10.1109/SIU.2015.7129958

- **Serdar Özgür Ata**, İbrahim Altunbaş (2016). Analog network coding over cascaded fast fading Rayleigh channels in the presence of self-interference, *IEEE 24th Signal Proc. and Commun. App. Conf.*, Zonguldak, Turkey. http://dx.doi.org/doi:10.1109/SIU.2016.7495725

- **Serdar Özgür Ata**, İbrahim Altunbaş (2016). STTC design for MIMO V2V PLNC systems over cascaded fading channels. Submitted to journal of Transaction on Emerging Telecommunication Technologies.

OTHER PUBLICATIONS AND PRESENTATIONS:

- **Serdar Özgür Ata**, Cevdet Işık (2013). High-resolution direction-of-arrival estimation via concentric circular arrays, *ISRN Signal Processing*, *Vol. 2013*, *Article ID 859590*, 1-8. http://dx.doi.org/10.1155/2013/859590

- **Serdar Özgür Ata**, Hakan Çırpan (2011). Signal detection based on linear trend in the noise-originated eigenvalues of the correlation matrix for cognitive radio, *IEEE 19th Signal Proc. and Commun. App. Conf.*, Antalya, Turkey. http://dx.doi.org/doi:10.1109/SIU.2011.5929695

- **Serdar Özgür Ata**, Cevdet Işık (2010). Direction-of-arrival estimation via concentric circular antenna arrays, *IEEE 18th Signal Proc. and Commun. App. Conf.*, Diyarbakır, Turkey. http://dx.doi.org/doi:10.1109/SIU.2010.5650429